T.R.
VAN YUZUNCU YIL UNIVERSITY
INSTITUTE OF NATURAL AND APPLIED SCIENCES
DEPARTMENT OF CHEMISTRY

DETERMINATION OF C-REACTIVE PROTEIN WITH MOLECULARLY IMPRINTED POLYMERS

M.Sc. THESIS

PREPARED BY: Abdulqader Taher TAWFEEQ
SUPERVISOR: Asst. Prof. Dr. Çiğdem ÖTER

VAN-2023

T.R.
VAN YUZUNCU YIL UNIVERSITY
INSTITUTE OF NATURAL AND APPLIED SCIENCES
DEPARTMENT OF CHEMISTRY

DETERMINATION OF C-REACTIVE PROTEIN WITH MOLECULARLY IMPRINTED POLYMERS

M.Sc. THESIS

PREPARED BY: Abdulqader Taher TAWFEEQ

This project was supported by Scientific Research Projects Coordination Unit of Van Yuzuncu Yil University with project no: FYL-2022-10092

VAN-2023

ACCEPTANCE and APPROVAL PAGE

This thesis entitled ‘Determination of C-Reactive Protein with Molecularly Imprinted Polymers’ presented by Abdulqader Taher TAWFEEQ under supervision of Assist. Assoc. Dr. Çiğdem ÖTER in the department of Chemistry has been accepted as a M. Sc. thesis according to Legislations of Graduate Higher Education on 27/01/2023 with unanimity members of jury.

Chair: Doç. Dr. Leyla MİS	Signature:
Member: Dr. Öğr. Üyesi Özgül GÖK	Signature:
Member: Dr. Öğr. Üyesi Çiğdem ÖTER	Signature:

This thesis has been approved by the committee of The Institute of Natural and Applied Science on ..……../……../…..….... with decision number .....

Director of Institute

THESIS STATEMENT

All information presented in the thesis obtained in the frame of ethical behavior and academic rules. In addition, all kinds of information that does not belong to me have been cited appropriately in the thesis prepared by the thesis writing rules.

Abdulqader Taher TAWFEEQ

ABSTRACT

DETERMINATION OF C-REACTIVE PROTEIN WITH MOLECULAR PRINTED POLYMERS

TAWFEEQ, Abdulqader Taher
M.Sc. Thesis, Department of Chemistry
Supervisor: Asst. Prof. Dr. Çiğdem ÖTER
February 2023, 101 pages

C-Reactive protein (CRP) is a member of the pentraxin protein group. CRP is considered an acute phase protein produced by the liver during inflammation in various medical conditions limited to pathogenic infection. It is very important that the serum CRP concentration can be measured quickly, reliably, and easily. Therefore, three-dimensional cross-linked molecular imprinted polymer with selective recognition sites for CRP was synthesized and characterization analyzes (SEM, FT-IR, and TGA) were performed.

The binding abilities of the synthesized polymers via the adsorption of CRP in aqueous solution were evaluated in detail and compared with the capabilities of an unprinted polymer (CRP-NIP) used as a reference. It was observed that the MIP prepared by the printing effect selectively adsorbed the template molecule CRP. This effect was evaluated by testing their adsorption abilities against different positive acute phase reactants such as α1-antitrypsin and α1-acid glycoprotein. Adsorption process of CRP from aqueous solutions onto polymer adsorbents; Equilibrium was evaluated in terms of kinetic and thermodynamic conditions and the necessary parameters to describe the process were calculated under these conditions. Adsorption data: Langmuir, Freundlich, Dubinin-Radushkevich and Temkin isotherm models, Pseudo first order kinetic model, Pseudo second order kinetic model, Elovich kinetic model and intraparticle diffusion model were investigated, and thermodynamic parameters ΔG°, ΔH° and ΔS° were calculated.

Keywords: Adsorption c-reactive protein, Isotherm, Kinetics, MIP, Thermodynamics.

ÖZET

MOLEKÜLER BASKILI POLİMERLER İLE C-REAKTİF PROTEİNİN BELİRLENMESİ

TAWFEEQ, Abdulqader Taher
Yüksek Lisans Tezi, Kimya Anabilim Dalı
Danışman: Dr. Öğr. Üyesi Çiğdem ÖTER
Şubat 2023, 101 sayfa

C-Reaktif protein (CRP), pentraksin protein grubunun bir üyesidir. CRP, patojenik enfeksiyonla sınırlı çeşitli tıbbi durumlarda iltihaplanma sırasında karaciğer tarafından üretilen bir akut faz proteini olarak kabul edilir. Serum CRP konsantrasyonunun hızlı, güvenilir ve kolay bir şekilde ölçülebilmesi çok önemlidir. Bu nedenle, CRP için seçici tanıma bölgelerine sahip üç boyutlu çapraz bağlı moleküler baskılı polimer sentezlendi ve karakterizasyon analizleri (SEM, FT-IR ve TGA) yapıldı.

Sentezlenen polimerlerin CRP'nin sulu çözeltide adsorpsiyonu yoluyla bağlanma yetenekleri detaylı olarak değerlendirilmiş ve referans olarak kullanılan baskısız bir polimerin (CRP-NIP) yetenekleri ile karşılaştırıldı. Baskı etkisi sayesinde hazırlanan MIP, kalıp molekül CRP'yi seçici olarak adsorbe ettiği gözlendi. Bu etki, α1-antitripsin ve α1-asit glikoprotein gibi farklı pozitif akut faz reaktanlarına karşı adsorpsiyon yetenekleri test edilerek değerlendirildi.

CRP'nin sulu çözeltilerden polimer adsorbanlar üzerine adsorpsiyon işlemi; denge, kinetik ve termodinamik koşullar açısından değerlendirildi ve bu koşullar altında süreci açıklamak için gerekli parametreler hesaplandı. Adsorpsiyon verileri: Langmuir, Freundlich, Dubinin-Radushkevich ve Temkin izoterm modelleri, Pseudo birinci dereceden kinetik model, Pseudo ikinci dereceden kinetik model, Elovich kinetik modeli ve partikül içi difüzyon modeli incelenmiş ve termodinamik parametreler ΔG°, ΔH° ve ΔS° hesaplanmıştır.

Anahtar kelimeler: Adsorpsiyon, C-reactive protein, İzoterm, Kinetik, MIP, Termodinamik.

ACKNOWLEDGMENTS

This MSc thesis would have been impossible to perform without a group of people who encouraged me, helped, and advised me throughout its development.

I would like to express my deep gratitude to Asst. Prof. Dr. Çiğdem ÖTER, my MSc thesis supervisors, for her patient guidance, enthusiastic encouragement, and useful critiques of this research work. I would also like to thank the Head of the Institute of Natural and Applied Sciences for their advice and assistance in keeping my progress on schedule. My grateful thanks are also extended to the staff and instructors of the Department of Chemistry for enabling me to visit them any times to get information. I also wish to thank my parents for their support and encouragement throughout my study. Finally, I would like to thank everyone who helped me directly or indirectly to complete my studies and finish my project.

2023

Abdulqader Taher TAWEEQ

TABLE OF CONTENTS

Page

ABSTRACT i
ÖZET iii
ACKNOWLEDGMENTS xv
TABLE OF CONTENTS vii
LIST OF TABLES xi
LIST OF FIGURES xiii
SYMBOLS AND ABBREVIATIONS xv
1. INTRODUCTION 1
1.1. Clinical Use of C-reactive Protein (CRP) 1
1.2. Structure of CRP 2
1.3. Functions of Human CRP 4
1.4. Synthesis of CRP 4
1.5. Molecular Imprinting Technology 5
1.5.1. Main components of molecular ımprinting 7
1.5.1.1. Template (target) molecule 7
1.5.1.2. Functional monomers 9
1.5.1.3. Crosslinkers 10
1.5.1.4. Solvents 12
1.5.1.5. Initiators 13
1.5.2. Classification of methods MIPs 14
1.5.2.1. Covalent imprinting 14
1.5.2.2. Non-covalent imprinting 15
1.5.2.3. Semi-covalent imprinting 17
1.5.3. Applications of imprinted polymers 18
1.5.3.1. Environmental monitoring 18
1.5.3.2. Food analysis 18
1.5.3.3. Biomedical diagnostic 19
1.5.3.4. Drug delivery systems (DDS) 19
1.5.3.5. Molecularly imprinted polymers (MIPs) as biomimetic ligands . 19

Page

1.5.4. Adsorption 20
1.5.5. Types of adsorptions 21
1.5.5.1. Physical adsorption 21
1.5.5.2. Chemical adsorption 22
1.5.5.3. Displacement adsorption 23
1.5.5.4. Ionic adsorption 23
1.5.6. Factors effecting adsorption 24
1.5.6.1. Effect of pH on adsorption 24
1.5.6.2. Effects of mixing speed 25
1.5.6.3. Effects of temperature on adsorption 25
1.5.6.4. Contact time 26
1.5.6.5. Surface area 26
1.5.6.6. Surface tension 26
1.5.6.7. Effect of structural features 27
1.5.7. Adsorption isoterms 27
1.5.7.1. Langmuir isotherm model 29
1.5.7.2. Freundlich isotherm model 31
1.5.7.3. Temkin isotherm model 32
1.5.7.4. Dubinin-Radushkevich model 33
1.5.8. Adsorption kinetics 34
1.5.8.1. Pseudo-first-order kinetic model 36
1.5.8.2. Pseudo-second-order kinetic model 36
1.5.8.3. Elovich kinetic model 37
1.5.8.4. Intraparticle diffusion model 37
1.5.9. Adsorption thermodynamics 38
1.5.10. The aim of the study 39
2. LITERATURE REVIEW 41
3. MATERIALS AND METHODS 47
3.1. Materials 47
3.2. Synthesis of CRP-MIP 47
3.3. Synthesis of NIP 48

Page

3.4. Removal of the Template CRP from CRP-MIP 49
3.5. Characterization of Polymers 49
3.5.1. SEM (scanning electron microscope) analysis 49
3.5.2. FT-IR (fourier transform-infrared) spectrum analysis 50
3.5.3. Thermogravimetric analysisi (TGA)…. 51
4. RESULTS 55
4.1. Adsorption Studies 55
4.2. Adsorption of C-reactive protein by CRP-MIP 56
4.2.1. Contact time effect and kinetic studies 56
4.2.2. pH effect 60
4.2.3. Initial concentration effect and isotherm studies 61
4.2.4. Temperature effect and thermodynamic studies 64
4.3. Adsorption of C-Reactive Protein by CRP-NIP 66
4.3.1. Contact time effect and kinetic studies 66
4.3.2. pH effect 70
4.3.3. Initial concentration effect and isotherm studies 71
4.3.4. Temperature effect and thermodynamic studies 74
4.4. Selectivity Studies 77
4.5. Rebinding of CRP to Imprinted Polymer in Human Serum 78
5. DISCUSSION AND CONCLUSION 79
REFERENCES 81
EXTENDED TURKISH SUMMARY (GENİŞLETİLMİŞ TÜRKÇE ÖZET) 89
CURRICULUM VITAE 101

LIST OF TABLES

Table **Page**

Table 1.1. Comparison between covalent and non-covalent ımprinting techniques 8

Table 1.2. Advantages and disadvantages of covalent and non-covalent imprinting..... 16

Table 4.1. Kinetic parameters of CRP adsorption onto CRP-MIP 59

Table 4.2. Isotherm parameters of CRP adsorption onto CRP-MIP 63

Table 4.3. Thermodynamics parameters of CRP adsorption on CRP-MIP 66

Table 4.4. Kinetic parameters of CRP adsorption on CRP-NIP 69

Table 4.5. Isotherm parameters of CRP adsorption onto CRP-NIP 73

Table 4.6. Thermodynamics parameters of CRP adsorption on CRP-MIP 76

LIST OF FIGURES

Figure **Page**

Figure 1.1. Three-dimensional X-ray crystal structure of the human C-reactive protein (CRP) molecule 3

Figure 1.2. Schematic representation of the molecular imprinting process 6

Figure 1.3. Structures of commercially available functional monomers used for imprinting optimization 10

Figure 1.4. Common cross-linkers used in MIP preparation..... 11

Figure 1.5. Chemical structure of common initiators..... 14

Figure 1.6. Principle of molecular imprinting 16

Figure 1.7. Semi-covalent molecular imprinting of cholesterol using the sacrificial spacer approach 17

Figure 1.8. Schematic representation of MIPs 20

Figure 1.9. Adsorption isotherm models 28

Figure 1.10. Illustration of diffusion steps of the adsorbate for liquid–solid adsorption 35

Figure 3.1. Schematic illustration for the synthesis of a molecularly imprinted polymer.48

Figure 3.2. SEM of polymers; (a, b) MIP and (c, d) NIP…….50

Figure 3.3. FTIR spectra of (a) uneluted CRP-MIP (b) eluted MIP and (c) NIP…….51

Figure 3.4. TG and dTG curves (a) CRP-MIP (b) CRP-NIP……52

Figure 4.1. Calibration plot for CRP determination……56

Figure 4.2. Effects of contact time on CRP adsorption……57

Figure 4.3. Kinetic studies for CRP adsorption on CRP-MIP; (a) pseudo-first order, (b) pseudo-second order, (c) Intraparticle-diffusion, (d) Elovich kinetic models……..….58

Figure 4.4. Effects of pH on CRP adsorption……60

Figure 4.5. Effects of initial concentration on CRP adsorption……61

Figure 4.6. Isotherm plots for CRP adsorption on CRP-MIP……62

Figure **Page**

Figure 4.7. Effects of temperature on CRP adsorption…….64

Figure 4.8. The Van't Hoff plots for the CRP adsorption on CRP-MIP……..65

Figure 4.9. Effects of contact time on CRP adsorption…….67

Figure 4.10. Kinetic studies for CRP adsorption on CRP-NIP; (a) pseudo-first order, (b) pseudo-second order, (c) Intraparticle-diffusion, (d) Elovich kinetic models……....68

Figure 4.11. Effects of pH on CRP adsorption……70

Figure 4.12. Effects of initial concentration on CRP adsorption…….71

Figure 4.13. Isotherm plots for CRP adsorption on CRP-NIP……..72

Figure 4.14. Effects of temperature on CRP adsorption…….…….…….75

Figure 4.15. The Van't Hoff plots for the CRP adsorption on CRP-MIP……..76

Figure 4.16. Formula structures of the compounds used……..77

Figure 4.17. Adsorption yield of MIP and NIP for CRP, α1-asiglikoprotein and α1-antitripsin compounds……...…….78

SYMBOLS AND ABBREVIATIONS

Some symbols and abbreviations used in this thesis are presented below, along with their descriptions.

Symbols	Description
α	Alpha (μmol/g.min)
β	Beta (g/μmol)
C^{o}	Temperature (Celsius)
cm^{-1}	Wavenumber
Hz	Hertz
Kd	Dispersion coefficient
μg	Microgram
μl	Microliter
μm	Micrometer
M	Molar
mg	Milligram
min	Minute
mL	Mililiter
mM	Milimolar
nm	Nanometer
R^{2}	Correlation coefficient
R%	Removal efficiency
T	Temperature
U/L	Unit/liter
UV	Ultraviolet
V	Volume of the solution

Abbreviations	Description
AIBN	2,2’-azobis (2-methylpropionitrile)
CLRP	Controlled/Living Radical Polymerization
CRP	C-Reactive Protein
D-R	Dubinin- Radushkevich
EGDMA	Ethylene Glycol Dimethacrylate
IPD	Intra-Particle Diffusion Model
LOD	Limit of Detection
MAA	Methacrylic Acid
MIP	Molecular Imprinting Polymers
MIP	Molecular Imprinting Technology
NIP	Non- Imprinting Polymers
SEM	Scanning Electron Microscope

1. INTRODUCTION

1.1. Clinical Use of C-Reactive Protein (CRP)

CRP is an acute-phase inflammatory protein that is enhanced in inflammatory, pathogenic, coronary heart disease, rheumatoid arthritis, and a wide range of other metabolic diseases. As a matter of fact, CRP may be considered not only a principal marker of inflammatory disease, but also an important regulator of inflammatory processes. Many researchers have studied the role of CRP in vascular tissue biology and realized that more research is needed to recognize the specific role of this intermediary in peripheral tissues. Many strategies have been implemented in bio-sensing arrangement for CRP detection in recent years; notwithstanding, some restrictions such as ion concentration and temperature influence the performance of these biosensors. As a result, more effort is required to create appropriate and easy-to-use CRP biosensors for in-situ diagnosis. Besides that, the interaction of CRP biomarkers with other protein markers presents significant difficulties that need to be overcome (Sohrabi et al., 2020).

The erythrocyte sedimentation rate (ESR) and serum C-reactive protein (CRP) accumulation are prospective laboratory surrogate signifiers (biomarkers) for clinical symptoms in Crohn's disease (CD) and ulcerative colitis (UC). Other inflammatory biomarkers in inflammatory bowel disease (IBD) involve hemoglobin, platelet count, leukocyte count, serum albumin, and serum orosomucoid concentrations. Whereas ESR evaluates inflammation implicitly, CRP development by hepatocytes is stimulated by pro-inflammatory cytokines such like interleukins 1 and 6. Moreover, some studies have examined the connection between CRP, and another quantify of disease activity, such as clinical, endoscopic, or radiologic activity, in IBD patients. A comprehensive study comparing all these parameters in patients with IBD is needed. The importance of clearly defining the relationship between serum CRP concentrations and IBD activity is highlighted by the outcome of several recent randomized, controlled trials of biologic agents in Crohn’s disease (Solem et al., 2005).

Post-hoc analysis results of these experiments (where the primary endpoints were not met) revealed that the subset of CD people who had high CRP concentrations had

reduced rates of placebo response, whilst those who had normal CRP concentrations had increased rates of placebo response, increasing the likelihood that patients with symptoms and low CRP did not have endoscopic and/or radiologic indication of inflammation. A better understanding of the relationship between serum CRP concentrations and endoscopic and radiologic outcomes in IBD patients may help with both patient therapy and clinical trial design. We wanted to examine the link between CRP and clinical, endoscopic, histologic, and radiographic activity in IBD patients in this retrospective analysis (Hanauer and Sandborn, 2001).

The association between demographics or baseline medical appearances and a response to etanercept in patients with ankylosing spondylitis (AS) was reconnoitered in a pooled investigation of different randomized trials. In that study, baseline CRP above the maximum bound of normal (CRP >ULN) was correlated with overall improving the quality of care than baseline CRP ULN, with the variation in clinical responses between the two CRP classifications being the lowest in patients with duration of illness of 0-2 years at benchmark and the greatest in patients with disease duration >10 years. Other post-hoc studies have revealed similar results (Baraliakos et al., 2019).

Furthermore, a post hoc review of two randomized clinical trials in patients with AS medicated with etanercept (ETN) or adalimumab for one year found a link between modifications in patient-reported consequences and objective inflammation-related symptoms (including CRP) in patients with shorter symptom period (four years), but not in those who have longer symptom duration (four years). Ultimately, these results indicate that CRP may play a crucial role in the management of AS, particularly since the 12-week response to anti-TNF treatment in patients with AS is thought to anticipate both long-term clinical results and drug preservation (Braun et al., 2002).

1.2. Structure of CRP

C-reactive protein is a non-glycosylated circulating plasma protein that, along with the distinguishable but closely connected protein serum amyloid P component (SAP), forms the pentraxin family of proteins, which is a subfamily of the lectin fold superfamily. Each pentraxin is made up of five equivalent non-covalently linked subunits that are organized in a disc-like arrangement with cyclic pentameric symmetry and exhibit

calcium-dependent binding to specific ligands (Fig. 1). Each CRP protomer has the pancaked -jellyroll lectin fold and possesses a pocket on one face, the B or binding face, containing two calcium ions bound just 4 apart by synchronization with protein carboxylate and amide side chains deduced from loops that gather on one face of the protomer core. These calcium atoms are required for all neurobiological ligand binding by CRP and significantly regulate both the protomer framework and the native pentamer integrity. Furthermore, calcium is always prevalent in the extracellular medium in vivo where CRP exists and omitting calcium when handling CRP for in vitro assays results in misleading results (Srinivasan et al., 1996).

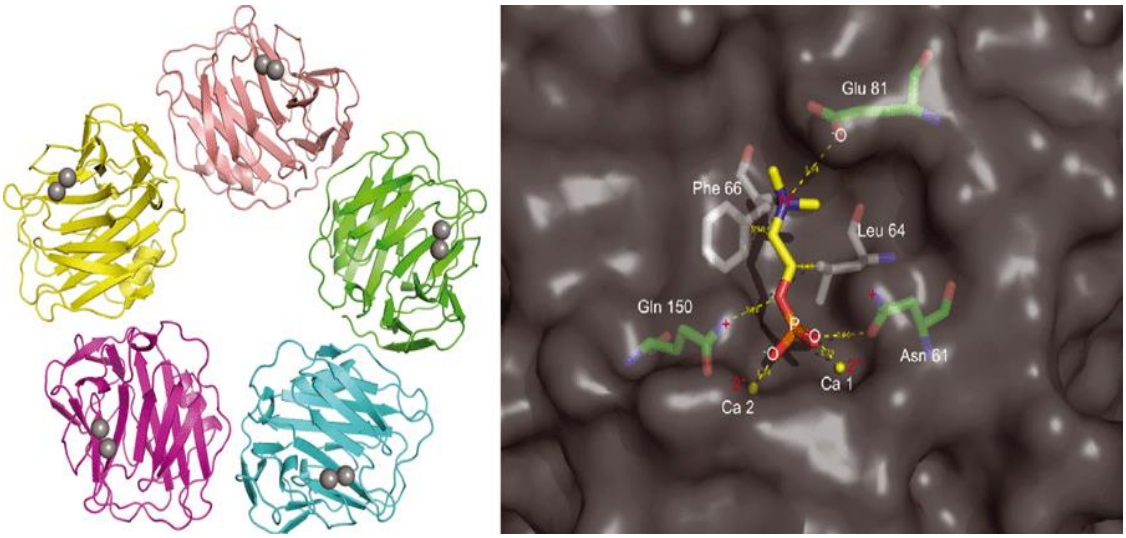

Figure 1.1. Three-dimensional X-ray crystal structure of the human C-reactive protein (CRP) molecule (Thompson et al., 1999).

In the absence of calcium, even if pH and ionic intensity are purely physical, CRP easily and frequently aggregates, starts losing its physiological ligand binding and the regular indirect impacts thereof, dissolved into protomers, which then quickly misfold and become vulnerable to proteolytic processing. Native CRP, on the other hand, is phenomenally stable in the presence of physiological conditions such as calcium, pH, and ionic strength. Although isolation of pure CRP can aggregate when exposed to violent turbulence, it is otherwise too constant, unchanged by repetitive freeze-thawing, retains its normal pentameric arrangement, and is extremely resistant to proteolysis. Unless boiled, it does not disentangle into protomers in the presence of the sodium dodecyl sulphate, a strong anionic detergent. CRP is serum reliable, which significantly increases

its functionality as a clinical marker. Given these compelling findings, hypotheses about the physiological or pathophysiological effects of solubilized CRP subunits, so-called adapted CRP, or proteolytic cleavage broken pieces of CRP are highly improbable to be correct, and scientific proof for the presence of such moieties in vivo is unpersuasive (Tennent et al., 1995).

1.3. Functions of Human CRP

The significant evolutionary and phylogenetic preservation of the CRP molecule's presence and structure recommend that it is likely to perform a valuable role, and given its ligand binding selectivity and indirect impacts, this role might be connected to both innate protection against infectious disease and the appropriate safe handling and destruction of broken autologous cells and lipids. However, evaluating these hypotheses experimentally is incredibly difficult since, despite significant resemblance, CRP molecules in distinct species exhibit substantial differences in normal amount, acute phase protein behavior, fine ligand binding specificity, and indirect effects after ligand binding. Extrapolation from animals to humans is thus difficult, and supposedly preserved capabilities must be interoperable with these significant differences. Furthermore, effects of heterologous CRP in vivo, following management or transgenic countenance of human CRP in animals, are not unavoidably unpretentious effects of human CRP in humans (Baltz et al., 1982).

1.4. Synthesis of CRP

Hepatocytes generate the circulating CRP. Reports of extra-hepatic CRP synthesis by some other cell types have not always been reproducible, and while possibly relevant to prospective local effects of CRP, the participation to plasma concentrations may be negligible in comparison to that from the liver. Hepatic CRP synthesis is highly susceptible to pro-inflammatory cytokines such as interleukin (IL)-6, IL-1, and tumor necrosis factor so that almost any type of tissue injury, infection, or inflammatory processes, as well as most forms of adverse non-physiological'stress,' are linked to an increased propagated CRP value. CRP appears to be resolved from the plasma and

metabolised solely by hepatocytes, and the plasma half-life in humans of around 19h is the same for all individual irrespective of disease or percolating CRP concentration. The synthesized rate is thus the main indicator of plasma concentration (Vigushin et al., 1993).

It is extremely crucial for any viewpoint of the importance and functionality of CRP values to differentiate between modest increases in basic flow CRP values and massive growth in amplitude that take place very quickly following major stimuli, such as sepsis, acute trauma, or tissue necrosis, and which may persevere for months or years in people who have ongoing active inflammatory and tissue detrimental diseases, such as systemic infection and rheumatoid arthritis. Furthermore, because the CRP response is almost entirely nonspecific, it is neither feasible nor pharmacologically suitable to define CRP values in a participant in the absence of full clinical information on that person, including one with a history, medical examination, and the official results of all obtainable investigations (Pepys and Hirschfiel, 2003).

1.5. Molecular Imprinting Technology

Molecular imprinting is a method for generating synthetic recognition sites in polymeric matrices that varies from the template in terms of the size, shape, and spatial configuration of the functional groups. Molecular imprinting is a technique for creating custom binding sites that retain the shape, size, and functional groups of the template molecules. There are two main approaches to molecular imprinting, one based on removable covalent bonds and the other on non-covalent interactions between imprinted molecules (templates) and functional monomers. In covalent imprinting, the templates are typically covalently bound to relevant monomers such as 4-vinylphenylboronic acid and 4-vinylbenzylamine (Mosbach, 1994).

After polymerization, the covalent connection is severed, and the template is removed from the polymer. When MIPs rebind the guest molecule, the same covalent linkage is formed. Because of the greater continuity of covalent bonds, covalent imprinting procedures produce more homogeneous binding site diffusion. However, due to the necessity for rapidly reversible covalent interactions between templates and functional monomers to form equivalent rebinding linkages, covalent imprinting is recognised as a less flexible method. As a result, the number of covalent imprinting

templates is limited. Furthermore, because of the strong nature of covalent interconnection and the resulting slow binding and disassociation, as highlighted in the diagram below, reaching thermodynamic stabilization is exceptionally hard (Wulff, 1995).

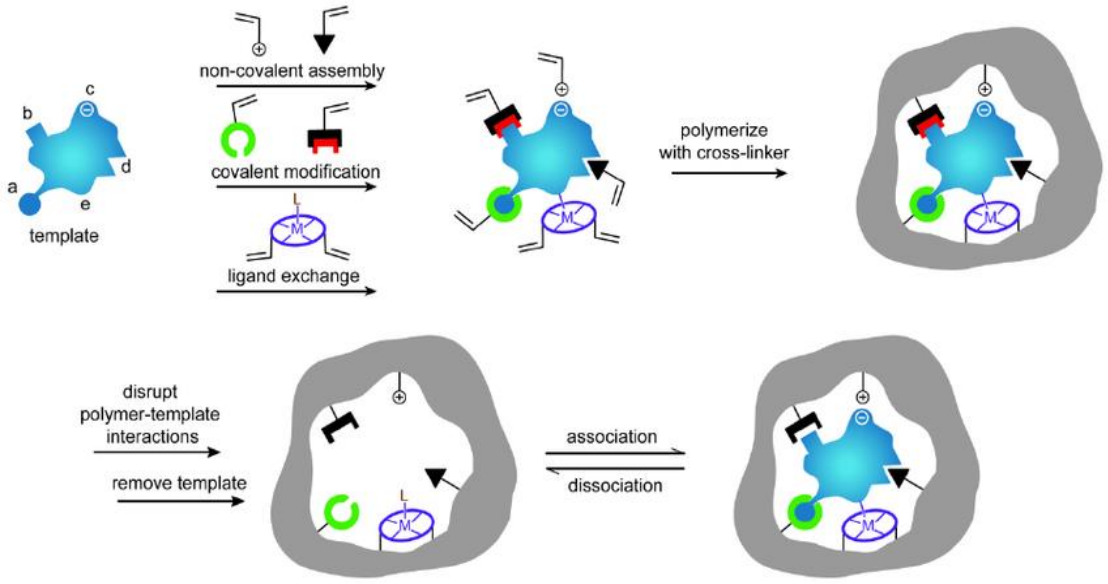

Figure 1.2. Schematic representation of the molecular imprinting process (Alexander C et al., 2006).

Non-covalent imprinting, on the other hand, has no such constraints. Template-monomer complexes are produced in a suitable solvent using various interactions such as hydrophobic interactions, ionic interactions, van der Waals forces, p-p interactions, and so on. Following polymerization and removal of the template, the functionalized polymeric matrix can rebind the target (template) by employing the same non-covalent interactions, greatly expanding the range of practical compounds that can be imprinted. Aside from the benefits mentioned above, another factor is the ease of operation, as only the mixing of templates and monomers in a particular solvent is considered necessary (Okutucu et al., 2009; Hasanah et al., 2021).

Currently, non-covalent imprinting has become MIT's most popular and common synthesis strategy. Surprisingly, after removing a covalently bonded template, non-covalent rebinding is also possible, which is referred to as a semi-covalent approach. This method provides an intermediate option in which the template is tightly bonded to a functional monomer, as in the covalent technique, but the template rebinding is based on

non-covalent interactions. It is distinguished by both high affinity covalent binding and mild non-covalent rebinding operational parameters, which will be mentioned in detail in the following sections. Although MIT enjoys substantial benefits and miscellaneous applications, it is also connected with many difficulties such as template outflow, inharmoniousness in aqueous media, low binding aptitude and slow mass transmission (Whitcombe et al., 1995; Chen et al., 2011).

This dissertation focuses on the current prominence of MIPs (including reagents and conventional reaction mechanisms), existing concerns, and several new appealing solutions to those challenges (including some significant advances in preparing well-designed MIPs, such as surface imprinting, semi-covalent imprinting, and dummy molecular imprinting), as well as illustrated applications of MIPs. Some novel MIP preparation techniques are also discussed, including controlled/living radical polymerization (CLRP), block copolymer self-assembly, ionic liquid as a solvent, and microwave-assisted heating. Finally, some attempts have been made to investigate MIT's potential development direction.

1.5.1. Main components of molecular imprinting

A Molecularly Imprinted Polymer is made up of the following components: a template, a functional monomer, a cross-linker, a solvent, and an initiator. Many factors influence the success of a Molecularly Imprinted Polymer, but the most important are the Molecularly Imprinted Polymer component and the interaction between template-monomers.

1.5.1.1. Template (target) molecule

According to one study, the physical properties and recognition of MIP are dependent on the successful interaction of template and monomer. During the pre-polymerization stage, this process occurs. The chosen functional monomer will interfere with the template, resulting in the formation of a stable template-monomer complex. As a result, functional monomers and templates must work in tandem. Based on the characteristics of the template-monomer interaction, MIP technology currently employs

different techniques (Mar and Wieczorek, 2019; Sánchez-González et al., 2019; Hasanah et al., 2021).

Furthermore, covalent, or non-covalent interactions between the template and functional monomer have established two different types of molecular imprinting strategies. These are the two techniques: The self-assembly method is the most utilized in the production of MIP. Non-covalent interaction forms template-monomer complexes in situ in this technique. Because of their ability to adapt, hydrogen bonds, electrostatic forces, and electrostatic interactions are the most used bonds in the manufacture of MIP. The advantages and disadvantages of MIP manufacturing technology based on covalent and non-covalent bonds are shown in the table below ((Hashim et al., 2014; Bakhtiar et al., 2019; Cuiet al., 2020).

Table 1.5.1. Comparison between Covalent and Non-Covalent Imprinting Techniques. Source: (Hasanah et al., 2021)

Imprinting Type	Covalent	Non-Covalent
Interaction	Reversible condensation reactions (ketal, acetal, esters, boronate, Schiff's bases)	Ionic interaction, hydrogen bonding, Van Der Waals forces
Advantage	More durable and rigid types of interactions The template-monomer complex is usually stable during the polymerization process Forming a polymer with a more homogeneous binding cavity	Flexible, fast, and straightforward binding interactions • Easy template molecule removal • Easy template-monomer complex preparation • Resulting in a MIP with high-affinity binding, greater affinity, and selectivity to the site
Disadvantage	- Strong covalent interactions result in slow binding and re-binding - Difficult to remove the template	Non-covalent interactions are sensitive to disruptions

The interaction of the template molecules and functional monomer, as well as the emergence of the polymerization mixture, can arise in one of three outcomes.

1. If the template is added at the exact time as the monomer, solvent, cross-linker, and initiator during the pre-polymerization step, the reaction medium will be very rich in functional monomers. Because of the cross-dominant linker's role, the polymerization

process will proceed quickly. A weak complicated forms between the template and the functional monomer, resulting in MIP with a low imprinting impact (Anfossi, et al., 2020).

2. If the template is added after the polymerization process has begun, a few minutes after the MIP- components have been added, the reaction medium will interconnect macro-monomers and a few monomers. Because of the nature of functional macro-monomers' versatility, they will freely re-arrange around the template to produce a MIP with a better imprinting effect.

3. If the template is added too late in the polymerization process, the reaction medium will be rich in preformed nanogel particles, which will additionally form a cross-linked macro-gel minutes after the optimum time of adding the template. The situation is made worse by the fact that the cross-linked nanogel particles are more restrictive than the functional macro-monomers. The resulting MIP is expected to have a reduced imprinting consequence (Hasanah et al., 2021).

1.5.1.2. Functional monomers

Functional monomers are one of the MIP elements whose characteristics will impact on the MIP's achievements. In molecular imprinting technology, functional monomers are critical for binding interactions. A MIP's binding site affinity will be influenced by the functional monomer. The functional monomers will interact with the template molecules during MIP pre-polymerization. MIP's success is dependent on the creation of a permanent template-monomer complex (Winingsih et al., 2022).

Furthermore, it is widely assumed that stronger interactions between the template and functional monomer will lead in a more sustainable template-monomer complex prior to polymerization, and thus a stronger imprinting efficiency of the resulting polymer. The monomers are arranged spatially around the template, and the location of the independent repeat units that interact with template molecules is fixed due to cross-linking. A polymer micro-porous matrix with micro-cavities with a three-dimensional structure supplementary to the template will be established as presented in the figure below (Zhong et al., 2018).

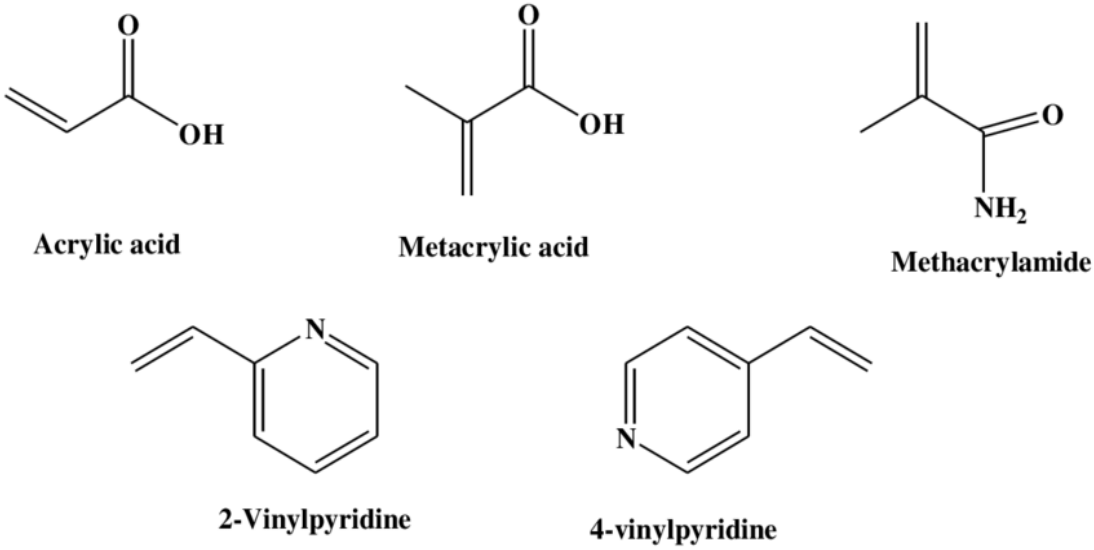

Figure 1.3. Structures of commercially available functional monomers used for imprinting optimization.

Notwithstanding, the lowest binding energy indicated the highest complex stability. When the imprinting ratio (template: monomer) was 1:5, the excess monomers increased their own correlation. In the meantime, time, the physical arrangement of the complex was unsteady due to the space hydrophobic interactions between the template and the functional monomer molecules. The wet laboratory experiment also revealed that the ratio (T: FM = 1:4) provided higher selectivity and adsorption capacity for template molecules toward analogous compounds. The most prevalent types of functional monomers are:I acidic compound such as methacrylic acid, (ii) alkaline compounds such as 4-vinyl pyridine, and (iii) pH neutral compounds such as styrene (Marć and Wieczorek, 2019).

1.5.1.3. Crosslinkers

As a MIP reagent, the cross-linker plays an important role in MIP formation. The cross-linker participates in the formation of the physical properties of polymers in MIP. The morphological features of the absorbent structure, three-dimensional frameworks, optimal stiffness, and the reliability of the MIP are the key characteristics of the polymer that are influenced by the existence of the cross-linker. The type and number of cross-

linkers used for polymerization are two crucial variables in the use of cross-linkers (Cui et al., 2020).

The greater the number of cross-linkers, the more reliable the porous material is. Zhao et al. (2020) investigated the effect of cross-linker concentration on MIP adsorption performance. Their findings demonstrated that the adsorption performance of a MIP increased with cross-linker concentration. After attaining optimum conditions, adding more cross-linker will not enhance adsorption performance; in fact, it will reduce adsorption performance. The most common cross-linking chemicals are trimethylolpropane trimethacrylate (TRIM), divinylbenzene (DVB), and ethylene glycol dimethacrylate (EGDMA) (Esfandyari-Manesh et al., 2013).

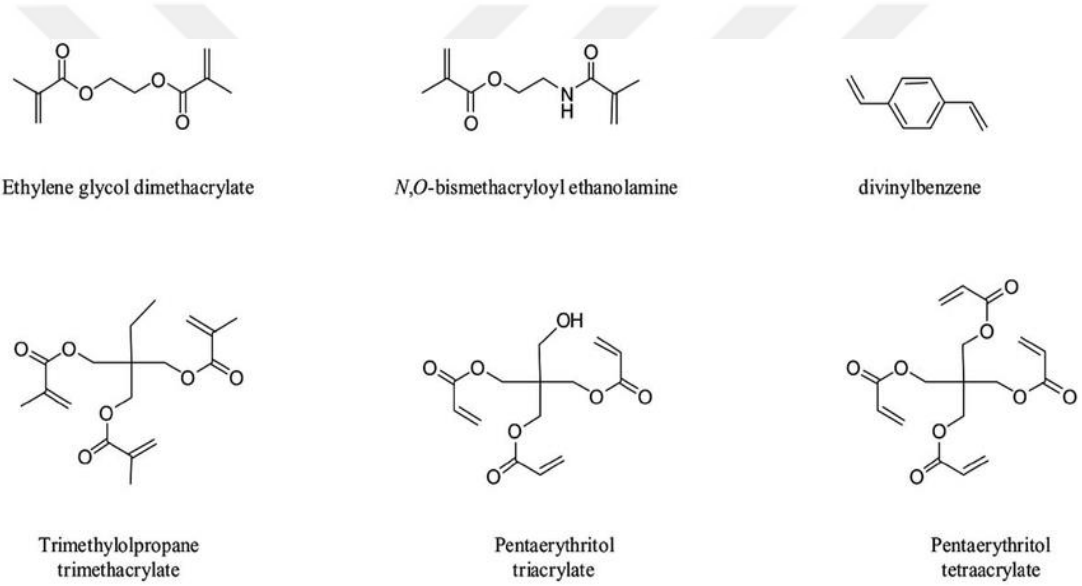

Figure 1.4. Common cross-linkers used in MIP preparation.

The presence of a cross-linker also influences MIP morphology, which influences MIP binding capacity. According to one study, lower cross-linker concentrations supply greater adsorption affinity. This phenomenon happens because the mean pore diameter declined as EGDMA increased, possibly resulting in greater sieving ability of these polymers, resulting in lower overall capacity. Several studies have been carried out to compare the cross-linkers commonly used in MIP. The use of TRIM and EGDMA in MIP with methacrylic acid (MAA) as the functional monomer and carbamazepine (CBZ) as the template has been evaluated by comparing (Holland et al., 2010; Rosengren et al., 2013).

The study found that MIP using TRIM as a cross-linker had higher binding capacity and more carbamazepine recognition sites than MAA-EGDMA, with MAA-TRIM binding capacity greater than 300 (around 300-500) micrograms CBZ and MAA-EGDMA binding capacity less than 300 micrograms CBZ, both measured at 180 minutes. Another study found that MIP with TRIM as a cross-linker has a higher binding capacity percentage of 45-50% than MIP with EGDMA as a cross-linker, which only has a binding capacity percentage of 40-45%. This may be influenced by the structure of TRIM and EGDMA. Three-branched chains in the TRIM molecule contain three vinyl groups, making TRIM more polymerization-friendly and causing in more rigid complementary recognition sites for the template than the EGDMA molecule, which only has two vinyl groups (Pengkamta et al., 2020).

1.5.1.4. Solvents

Solvents serve as a medium for reactions and have a major impact on template monomer interactions, which are critical elements to consider when creating a MIP. Solvents used in the production of MIP must interact with and dissolve all the ingredients, but they must not interfere excessively with the polymerization reaction process. solvents effected MIP adsorption selectivity using theophylline (THO) as a template and MAA as a functional monomer. When a high solubilization value is used in the synthesis of a MIP, the solvent protects the molecular interaction site while weakening the strong interaction between the monomer and template, resulting in a relatively poor molecular recognition ability of the MIP (Dong et al., 2007).

They tested three solvents, chloroform, tetrahydrofuran (THF), and dimethyl sulfoxide (DMSO), and discovered that DMSO had the highest affinity for THO and MAA but the lowest imprinting factor (IF), 1.0533, when compared to THF (IF = 1.1076) and chloroform (IF = 3.3197). The Imprinting Factor (IF) value represents the distribution ratio of a specific analyte on the imprinted polymer as well as under the same conditions as the non-imprinted polymer (NIP). An IF value greater than one indicates that the imprinting is good. MIP with chloroform as the solvent has the highest imprinting factor value because it interferes with the template-monomer interaction the least, resulting in the strongest hydrogen bonds between them (Dong et al., 2007).

MIP is typically synthesized in an organic solvent to enhance hydrogen bonding and electrostatic forces between the template and monomer. The polarity of the solvent has a significant impact on the template-monomer interactions. Less polar solvents promote the development of the template-monomer functional complex, whereas more polar solvents disrupt the interactions that form the template-monomer functional complex (Song et al., 2009).

1.5.1.5. Initiators

In hypothesis, any of the initiation techniques can be utilized to initiate free radical polymerizations in the existence of templates. However, there may be drivers for choosing one over the other arising from the system under consideration. When complication is driven by hydrogen bonds, lower polymerization temperatures are preferred, and photo-catalytically active initiators may be recommended because they can operate effectively at low temperatures (Cormack and Elorza, 2004).

As the radical source in free radical polymerization, a variety of initiators with various chemical properties may be utilized. In general, they are used at a lower level than the monomer, accounting for 1 mole of the total number of polymerisable double bonds. Depending on the chemical nature of the initiator, the rate and mode of biodegradation to radicals can be launched and controlled in a variety of ways, such as heat, light, and chemical/electrochemical means as illustrated in the figure below (Yan and Ho Row, 2006).

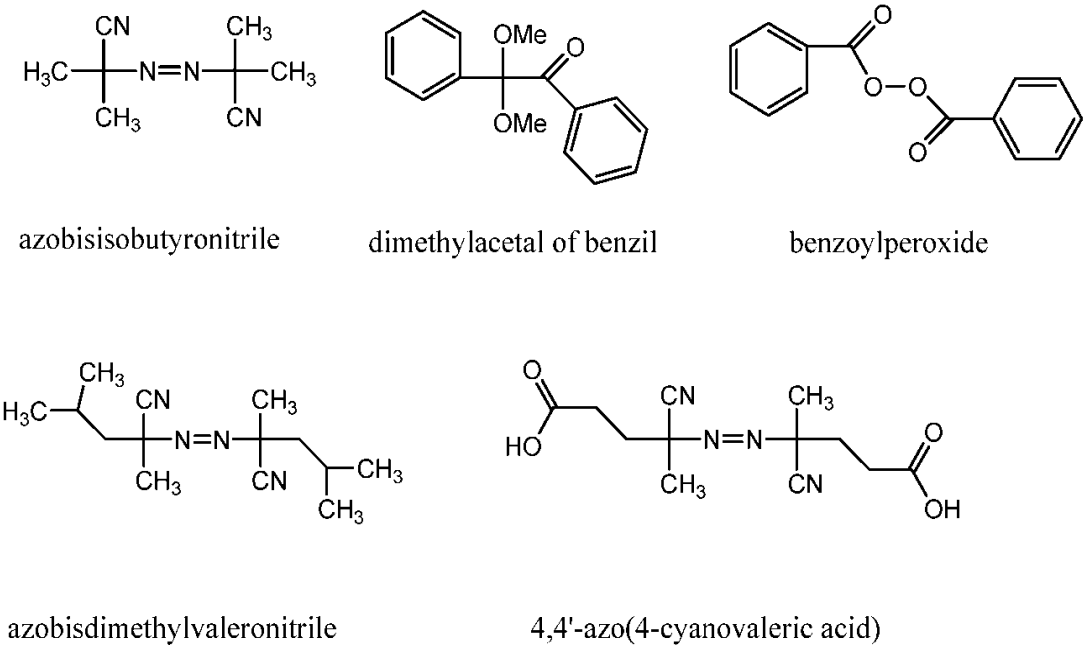

Figure 1.5. Chemical structure of common initiators (Yan and Ho Row, 2006).

As shown in the schematic above, oxygen gas retards free radical polymerizations; thus, to optimize monomer propagation rates and enable good batch-to-batch reproducibility of polymerizations, dissolved oxygen should be removed from monomer solutions immediately prior to proliferation. The expulsion of dissolved oxygen is as simple as ultra-sonication or sparging the monomer solution with an inert gas, such as nitrogen or argon (Yan and Ho Row, 2006).

1.5.2. Classification of methods MIPs

1.5.2.1. Covalent imprinting

The covalent imprinting framework involves the covalent alteration of the template, which is chemically bonded to the functional monomers in a controllable way. This is accompanied by the polymerisation step, during which the template remains covalently connected to the now polymeric monomer. Finally, the template is cleaved by a mild chemical reaction (such as hydrolysis or reduction), leaving the binding cavities behind. This method has several significant advantages, including the fact that the strong

interaction between the template and the functional monomer usually results in binding sites that are quite consistent (Wulff et al., 1982; Umpleby II et al., 2000).

However, both the separation of the chemically bound template and its successive rebinding are difficult because they constitute the disruption and re-establishment of covalent interactions, which slows the kinetic model of these processes significantly. This latter point must be considered, particularly in separation applications where the presence of fast rebinding kinetics is critical. Furthermore, prior derivatisation of the template is difficult using this method and is influenced by the chemical nature and accessible functional groups of the template (Ye and Mosbach, 2002; Zhu et al., 2010).

1.5.2.2. Non-covalent imprinting

The third method is known as non-covalent imprinting, which was pioneered by Mosbach and colleagues. It takes advantage of a variety of non-covalent bonds between the template and the monomers, including hydrogen, electrostatic, and hydrophobic interactions which including van der Waals forces. Because all of these interactions are weak, using an excess of monomers can result in more stable template-functional monomer complexes. This option is not without drawbacks, as it frequently results in a widespread distribution of non- homogenous binding sites (Mosbach et al., 1990; Umpleby II et al., 2000; Haupt, 2003).

Furthermore, the combination of this strategy and semi-covalent imprinting has lately been shown to improve the imprinting effect of poorly functionalized molecules. The prior chemical derivatisation of the template, however, persists a disadvantage of these combined approaches. Despite the disadvantages mentioned, the non-covalent imprinting approach is probably the most frequently used method for preparing MIPs due to its simplicity and faster template revocation and rebinding stages as presented in the table below (Alexander et al., 2006; Rosengren-Holmberg et al., 2009).

Table 1.5.2. Advantages and disadvantages of covalent and non-covalent imprinting (Komiyama et al., 2003)

İtem description	Covalent	Non-covalent
Synthesis of monomer template conjugate	Necessary	Unnecessary
Polymerization conditions	Rather free	Restricted
Removal of template after polymerization	Difficult	Easy
Guest-binding and guest-release	Slow	Fast
Structure of guest-binding site	Clearer	Less clear

Furthermore, the disintegrated target analyte interacts with the functional monomer implicated for characterizing the chemically active substituents of the target molecules during copolymerization via covalent, noncovalent, or covalently bonded interactions in the pre-polymerization mixture. As a result, molecular imprinting is divided into three types: covalent imprinting (pre-organized approach), non-covalent imprinting (self-assembly approach), and semicovalent imprinting, as shown in the figure below (Molinelli, 2004).

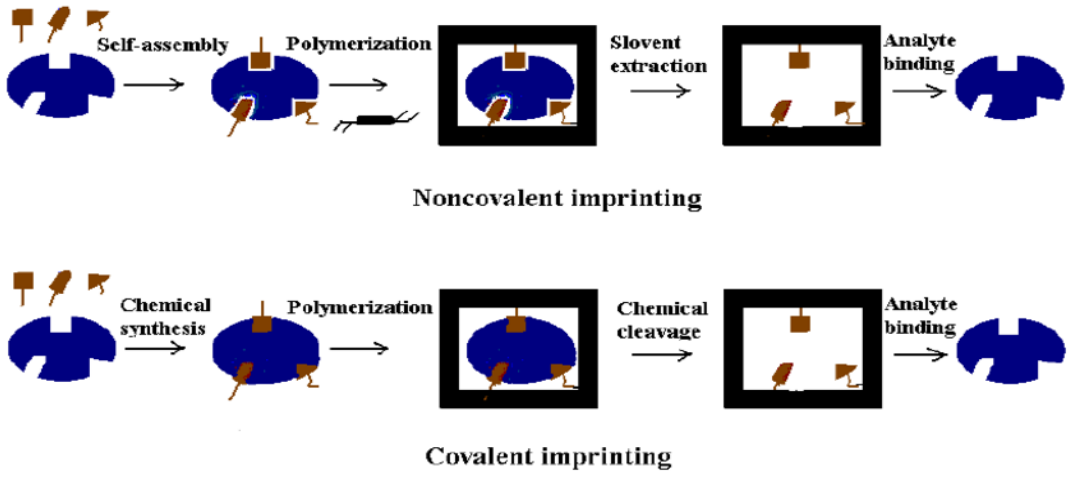

Figure 1.6. Principle of molecular imprinting (Molinelli, 2004).

1.5.2.3. Semi-covalent imprinting

In this approach, part of the monomer is also cleaved when the template is cleaved from the polymer (Figure 1.7). Sellergren and Andersson (1990) developed a variation of the previously described method in which the imprinting step is carried out by using polymerisation of the functional monomer bound to the template, while the rebinding process is carried out solely through non-covalent interactions. Hydrolysis removes the template, allowing the successive rebinding stage to take place via the formation of primarily hydrogen and electrostatic bonds (Mayes and Whitcombe, 2005). To overcome these issues, the template was cleaved by reducing the covalent bond with LiAlH4. For example, as opposed to a carboxylic group, a hydroxyl group was obtained using this methodology as highlighted in the following schematics (Byström et al., 1993; Whitcombe et al., 1995; Ikegami et al., 2004).

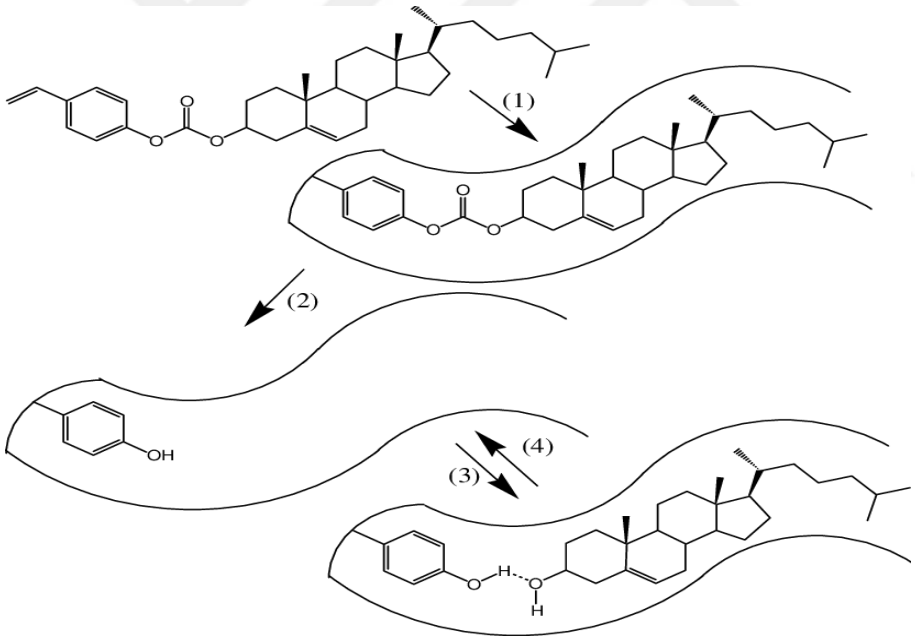

Figure 1.7. Semi-covalent molecular imprinting of cholesterol using the sacrificial spacer approach. Polymerization (1), cleavage and extraction (2), rebinding (association) (3), and dissociation (4) (Whitcombe et al., 1995).

1.5.3. Applications of imprinted Pplymers

1.5.3.1. Environmental monitoring

Concerns have been raised about the rising levels of pollutants in the ecosystem's water. Ecologically toxic ingredients that can be surveilled include dyes, contaminants, organic chlorine pesticide residues, mycotoxins, heavy metals, and antibiotics. These pollutants have the potential to harm public health, either explicitly or implicitly. Pollutants can pollute the considering the environmental mixtures: air, soil, atmosphere, sediment, flora and fauna. The pre-treatment sample's purpose is to remove matrix interference so that only the target analyte is procured. MIP is frequently used as a sorbent in pre-treatment samples with complex matrices because of its distinct characteristics in contrast to conventional adsorbent (Ndunda and Mizaikoff, 2016; Naseri et al., 2020).

MIP was utilized as a sorbent in the molecular imprinted solid-phase extraction (MI-SPE) pre-treatment approach, with the workable monomers methacrylic acid and tylosin serving as templates and was then analyzed using the LC-MS/MS method. As a result, MI-SPE demonstrated a high level of recognition of macrolides. At four contaminated concentration levels, the average percent recovering of macrolides was 62.6-100.9%, with intra-day and inter-day comparative standard deviation (S. D under 12.6%) (Song et al., 2018).

1.5.3.2. Food analysis

Environmental toxicants can enter the body through food or drinking water and have the potential to harm health. Pesticide and herbicide pollutants found in fruits, vegetables, and cereals, for example. Effective analytical methods and technologies are required to ensure food safety. Because MIP is a complex matrix sample, it can be used as a sorbent in food analysis. Dimethoate spiked in olive oil was tested using a core-shell magnetic-photonic dual responsive molecularly imprinted polymer (magnetic-photonic DR-MIP). Pre-concentration using a DR-MIP-based sorbent outperforms the MI-SPE method in terms of method and processing time. (Garcia et al., 2020).

1.5.3.3. Biomedical diagnostic

In the biomedical sector, MIP is identified as an artificial transcription factor with basic capabilities like natural receptors, one of which is the ability to recognize cells. MIP has several advantages over natural receptors, including higher affinity, better temperature predictability, faster preparedness, and lower costs. MIPs have specific recognition sites for target molecules such as antibodies and enzymes. Antibodies in the immune system recognize monoclonal antibodies with high specificity. MIP is frequently used as a substitute to antibodies in diagnostic procedures for diseases such as breast cancer, cardiac disease, and dengue fever. As a result, MIP functions as a biomarker because it can display specific features or measurable biologically produced differences in the body associated with specific illnesses or health conditions (Selvolini and Marrazza, 2017; Arshad et al., 2020).

1.5.3.4. Drug delivery systems (DDS)

DDS is a technique that delivers products and services to the desired location prior to drug discharge and absorption in to boost the drug's therapeutic properties and achieve the desired therapeutic effect. DDS must be able to control the amount and rate of drug release. As a DDS agent, MIP has several advantages, including a long shelf life, the ease of preparation, high chemical and physical consistency, and low cost. Suksuwan et al. (2015) used a covalent and physiological technique to deliver drug to cancer cells via an enantioselective receptor for (R)-thalidomide enantiomer designed in nanoparticles using methacrylic acid, a fluorescently active 2,6-bis (acrylamide) pyridine, and N,N-methylenebis-acrylamide. The results of his outcomes confirm that MIP nanoparticles, when joint with the right temperature at the target location, have the prospective to be operative drugs for attacking multidrug-resistant cells (Zaidi, 2020).

1.5.3.5. Molecularly imprinted polymers (MIPs) as biomimetic ligands

In the mid-1980s, researchers became interested in MIPs, also identified as plastic antibodies or tailor-made receptors, and these plastic antibodies are now used in a variety

of applications, such as bio-sensing. Before the artificial receptors are created, the operational monomers are formed from around template molecule using covalent, non-covalent, or semi-covalent interactions, as shown in the figure below. Polymerization then took place in a polymer matrix using the adequate cross-linker and initiator. Finally, the template molecule is extracted from the polymer matrix, resulting in the development of specific binding cavities that realize it predicated on its shape, size, and three-dimensional structure (Özgür et al., 2020).

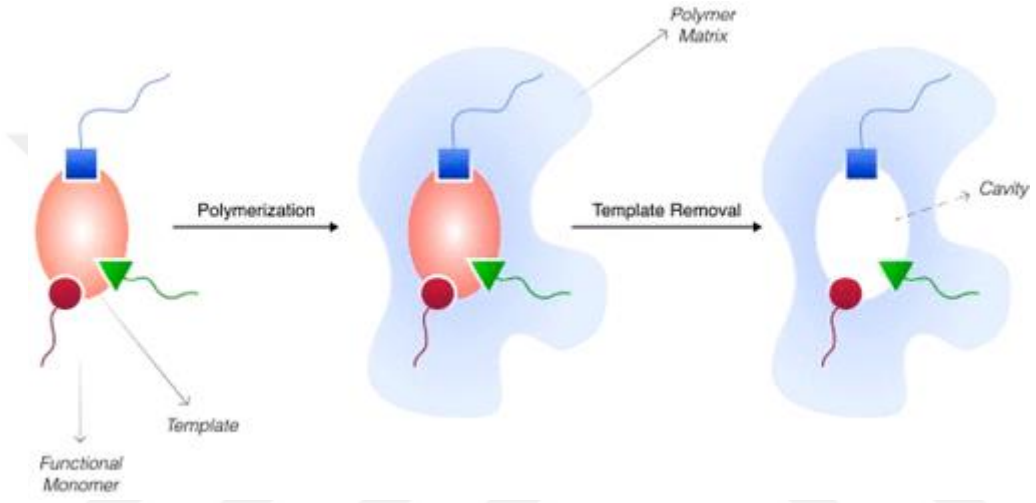

Figure 1.8. Schematic representation of MIPs. Source: (Topçu et al., 2022)

Although the functional monomer(s) and a template molecule are crucial when designing the specific binding cavities, monomer-monomer, monomer-template, or solvent-template communications can also influence the molecular and physical properties of the molecular recognition cavities. Numerical techniques, when contrasted with traditional thermodynamic models, provide much more detail about the pre-polymerization complex, and allow one to categorize polymer-ligand interconnections (Nicholls et al., 2011; Han et al., 2021).

1.5.4. Adsorption

Adsorption is the process by which a substance accumulates in higher concentrations on the surface of a molecular species. The gases hydrogen, nitrogen, and oxygen adsorb on activated charcoal. Meanwhile, we must distinguish between

adsorption and absorption. The two processes use entirely different mechanisms (Sheta, Elfeky and Boshra, 2020).

Two components are required for the adsorption process,

- Adsorbate: A substance that binds to the surface of another substance. For instance, H_2, N_2, and O_2 gases.
- Adsorbent: A substance's surface on which adsorbate adsorbs. For instance, charcoal, silica gel, and alumina.

1.5.5. Types of adsorptions

Based on interaction forces between adsorbate and adsorbent, adsorption is of two types.

1.5.5.1. Physical adsorption

This type of adsorption is also known as physisorption. Because the adsorbate and adsorbent have inadequate Van der Waals forces, this occurs. Van der Waals interactions are weak and far-reaching. These interactions can be evaluated as thermal motion by absorbing them as lattice vibrations. Physical adsorption enthalpy can be calculated by increasing the temperature of a sample with a known heat capacity. Enthalpy values are typically between 10 and 20 kJ/mol. Because this small enthalpy change is incomplete to break bonds, the molecule retains its distinctiveness even when physically adsorbed. Physical adsorption is most prevalent when the adsorbed material forms a multilayer structure because Van der Waals forces exist between the adsorbed molecules. Physical adsorption is a recurring event that occurs at low temperatures and rapidly. As a result, molecules that have been adsorbed by lessening the gas pressure or concentration can be conveniently expelled. Physical adsorption of gases involves forces such as condensation. Adsorption heat is immediately adjacent to condensed water heat for the same molecules. H_2 and N_2 gases, for instance, adsorb on coconut charcoal (Jones et al., 2013).

1.5.5.2. Chemical adsorption

Adsorption of this category is also known as chemical adsorption. It is caused by strong chemical pressures of the form of bonding between adsorbate and adsorbent. Consider iron nitride forming on the surface of an iron heated in N_2 gas at 623 K. Adsorption of a gas on a solid is an exothermic reaction that occurs spontaneously. Heat of adsorption is the amount of energy ejected when a unit mass of a gas is absorbed by the surface. In the case of chemisorption or chemical adsorption, particles confined to the surface keep a high standard by establishing a covalent bond and seek out centers with the highest coordination number with the adsorbed substance (Wester et al., 1994).

Aside from extraordinary cases in which chemical adsorption is expected to be exothermic, chemical adsorption enthalpy is much higher than physical adsorption enthalpy, with typical values ranging from 20 to 200 kJ/mol. During chemical adsorption, specific chemical bonds are formed in random areas of the surface. Adsorbed molecules do not typically occupy nearby regions, and adsorption is complete when the surface is completely covered. Physical adsorption weakens the bonds. Chemical adsorption can take place only in a single layer. Since the adsorbed molecules can connect, a second layer forms before the initial layer are finished (Kundu et al., 2014).

Comparison between physical and chemical adsorption

Physical adsorption characteristics:

1. Physical forces cause this type of adsorption.
2. Physisorption is an insignificant phenomenon.
3. This adsorption process is multi-layered.
4. Physical adsorption is non-specific and occurs throughout the adsorbent.
5. Surface area, temperature, pressure, and adsorbate nature all influence physisorption.
6. The activation energy is low (20 - 40 kg/mol).

Chemical adsorption characteristics:

1. This type of adsorption is caused by chemical forces.
2. It is a very powerful process.
3. Adsorption of this type is almost entirely a single-layered phenomenon.

4. Chemisorption is highly specific and occurs on the adsorbent at reaction centers.
5. Surface area, temperature, and adsorbate nature all influence chemisorption.
6. The activation energy is very high, ranging from 40 to 400 kJ/mol.

1.5.5.3. Displacement adsorption

It is caused by the electrical attraction of the adsorbed to the surface. In other words, it is concerned with the effects of the adsorbent's electrical attraction forces on the adsorbent. The electrical attraction between negatively charged adsorbate molecules and positively charged adsorbed ions diminishes diffusion impediments and thus intensifies adsorption efficiency. This class includes ion exchange. It is critical that the adsorbed and adsorbent surfaces, which have opposite electrical charges, attract each other in this case. As a result, ions with higher electrical charges and smaller diameters are better adsorbed. Even though adsorption is classified into three types, it is difficult to explain an adsorption process using a single type of adsorption. Overall, more than one category of adsorption is observed in an adsorption process. (Sarıkaya, 1997).

1.5.5.4. Ionic adsorption

Adsorption and successive exchange of ions between soil microparticles (clays, organic matter, sesquioxides, and amorphous minerals) are important processes. Soil colloids function a lot like a modern bank. They are the locations within the soil where ions of vital plant nutrients are held and designed to protect from leaching. Following that, nutrients can be "withdrawn" from colloidal "bank" sites and absorbed by plant roots. Through the addition of commercial fertilizers, lime, manures, and plant residues, these elements can be "deposited" or returned to the colloids. The charges on soil particles attract ions of negative charged (simple and complex) (Zhuang and Yu, 2002).

In temperate region soils, negative charges generally predominate on the soil particles (colloids), hence adsorbed cations are present in larger quantities than anions. Anion adsorption and transfer is comparatively more prevalent in more highly weathered soils (e.g., in the tropics), where 1:1 type clays and Fe/Al oxides are the most dominant type of colloids. The importance of ion exchange reactions such as cation exchange, anion

exchange, and base saturation Harry Stephen Thompson discovered the Ion Exchange phenomenon in England in 1850. Calcium sulfide was observed in the leachate after soil was leached (washed) with ammonium sulphate (Bizi and El Bachra, 2020).

The ammonium ion in the solution replaced calcium in the soil. $(NH_4)_2SO_4$ + Soil Ca = Soil $(NH_4)_2{}^+$ $CaSO_4$. Ion transfer takes place by which ions exchange between solids and liquids and/or between solid phases that are in close contact with each other. Ca^{2+}, Mg^{2+}, H^+, K^+, $NH_4{}^+$, and Na are the most common interchangeable cations. $SO_4{}^{2-}$, Cl^-, $PO_4{}^{-3}$, and $NO_3{}^-$ are the most common anions. The presence of remaining positive and negative charges on soil colloids causes ion exchange. The process of isomorphous replacements and ionization of hydrogen and hydroxide functional groups results in these residual charges. When soil solutions meet colloids, the negative charges attract positive charges and the positive charges attract negative-charged ions (Lin et al., 2017).

In addition, the ions attracted in this manner are reversible and have equivalent proportions. The exchange of cation is known as cation exchange, and the exchange of anion is known as anion exchange. Thomasway was the first to discover the cation exchange phenomenon (1850) Ion exchange is nature's second most essential reaction. The first is photosynthesis, which occurs in vegetation. Cation exchange capacity refers to the soil's ability to hold cation. C mol (P+)/kg is the unit. Anion exchange capacity is the ability to hold anion (AEC). C mol/kg is the unit of measurement (Doi et al., 2019).

1.5.6. Factors effecting adsorption

1.5.6.1. Effect of pH on adsorption

pH is the most significant factor that effects adsorption. The pH of the solution in which adsorption occurs influences the amount of adsorption for one or more reasons. Because hydrogen (H^+) and hydroxyl (OH^-) ions are strongly adsorbed, the pH of the solution influences the adsorption of other ions. Adsorption is affected by the ionization of an acidic or basic material, and pH effects adsorption as well, though it does not regulate the degree of ionization. The contact solution's pH is an important adsorption control variable. The adsorption capacity increases as the acidity of the contact solution increases. These variations can be explained by the competing between metal ions and

hydrogen ions, as well as the alteration of metal ion hydrolysis products with pH. Adsorption of different ions at different pH values is important only at specific pH values, whereas anionic ion adsorption occurs at low pH values and has nearly 100% ion removal efficiency. Adsorption of typical organic pollutants from water generally increases with decreasing pH (Cozmuta et al., 2012).

1.5.6.2. Effects of mixing speed

Mixing speed accelerates turbulence and reduces the penetration depth of the boundary layer around the adsorbent, resulting in greater liquid-phase mass transfer to eliminate dyes from the solution. An increment in flow rate is accompanied by a slight increase in the amount adsorbed.

1.5.6.3. Effects of temperature on adsorption

Temperature is an important factor in adsorption reactions. Adsorption decreases with increasing temperature, according to the adsorption theory, and molecules adsorbed earlier on a surface tend to disintegrate from the surface at higher temperatures. The amount of energy released when water vapor in the air is adsorbed onto the fiber surface is referred to as the heat of adsorption. Similarly, when moisture is desorbed from the fiber, the same amount of energy must be added. Even for a given fiber, the heat of adsorption is not constant, but rather changes depending on the environmental factors under which the adsorption or decomposition takes place. The micro-climatic relative humidity is the primary factor that effects heat of adsorption in most applications at extreme environmental pressures and temperatures, heat of adsorption can be treated as a function of humidity alone (Ghaddar and Jones, 2002).

Additionally, temperature is a critical factor in the adsorption process because it establishes the type of adsorption. Because the adsorption process is predominantly exothermic, the intensity of adsorption increases with annealing temperature. The changes in enthalpy in physical adsorption are known to be in the degree of condensation or crystallization reactions. As a result, small changes in temperature will not result in a significant change in the adsorption process. The total heat transmitted from solute

adsorption per unit weight is used to calculate the amount of heat alteration in the adsorption occasion. Adsorption heats in the gas phase are usually bigger than those produced during liquid phase adsorption (Canbazoğlu, 1996; Dilci, 2011).

1.5.6.4. Contact time

The contact time between both the adsorbent and the adsorbate is a critical factor in determining the extent of an adsorption mechanism. This is because it gives evidence on the adsorbate's sorption kinetics for a known initial dosage of the adsorbent (Singh et al., 2013).

1.5.6.5. Surface area

Adsorption is a surface phenomenon, and the intensity of adsorption is proportional to the specific surface area. The specific surface area is defined as the ratio of the area used for adsorption to the total surface area. The adsorbent should have a large surface area, pore volume, a specific pore distribution, and a particulate configuration. The adsorptive capacity of an adsorbent increases as its particle size decreases. The rate of adsorption varies with diameter, as the radius decreases, the amount adsorbed increases. Adsorption is affected by the adsorbent's surface area as well as its chemical structure and some of the procedures it has undergone. The adsorbing power of porous and granular surfaces is very high. For example, coal heated by passing water vapor over it under pressure is much more active than coal that has not undergone this treatment (Zeng et al., 2010).

1.5.6.6. Surface tension

Adsorption is related to surface reactions and the forces that accompany them (such as phase boundaries or surface boundaries). The effects of the previous mentioned forces can be lowered, and adsorption can be facilitated, to the significant degree that surface tension can be restricted. We expand and increase the surface by lowering surface tension. To reduce tension, the intermolecular bonds that form the liquid phase must be

broken, and bonds formed between these particles and the other phase. As a result, surface tension should beinvestigated to increase the surface area of a liquid (Weber Jr et al., 1991).

1.5.6.7. Effect of structural features

The chemical and physical characteristics of the adsorbents are the most important factors influencing the adsorption mechanism. Polar and nonpolar adsorbent materials are available. While electrical forces work in polar adsorbents, dispersion forces work in nonpolar adsorbents. The adsorbent's permeability and particle size are also significant considerations in the adsorption mechanism. Particulates in the adsorbent also have an impact on the adsorption process. Because contaminants alter the chemical and physical properties of the adsorbent, the quantity of adsorbed material varies. A side from the characteristics of the adsorbent materials, the electrical charges, polar characters, ion and molecular diameters of the adsorbed are significant factors in adsorption. Other important factors influencing adsorption efficiency include the features of the solvent in which the adsorbed substance is disintegrated and the solvent-adsorbed substance interrelations (Prakruthi et al., 2022).

1.5.7. Adsorption isoterms

The adsorption isotherm is the equilibrium relationship between the adsorbate in the liquid phase and the adsorbate on the adsorbent's surface at constant temperature. The following schematic illustrates the adsorption isotherms for nitrogen at 77 K up to the saturation pressure, P0, and the remaining fluids at 258 K for pressures up to 1 bar. The N_2 and SF_6 isotherms are clearly Type I, as shown by the inserts in this figure. For the three supercritical gases, the rate of take-up with pressure increases in proportion to the energy of the fluid-solid interactions. Because of its larger size and affinity for carbon, the rate of take-up of SF_6 is like that of N_2 despite the higher temperature (Biggs etal., 2006).

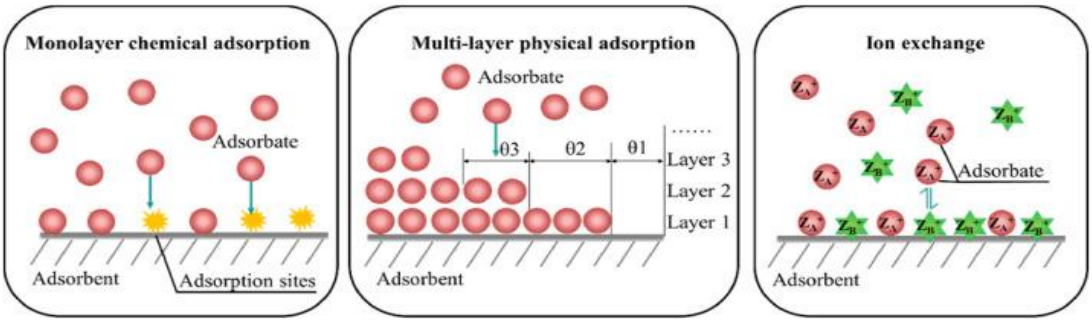

Figure 1.9. Adsorption isotherm models (Wang and Guo, 2020).

As can be observed from the above schematics, the adsorption isotherms for constituent materials are utilized to describe the adsorption of single components at a constant temperature in most cases, because thermodynamic characterization of the adsorbent surface is not feasible for functional targets. However, most adsorption isotherms will be linear only in narrow ranges; at low enough concentrations, the linear adsorption isotherm can be used. In explanatory chromatography, this linear relationship is frequently used. Several well-known equations, such as the BET equation, the Langmuir equation, and the Freundlich equation, have been expanded to describe the dynamic characteristics of adsorption equilibrium. These extensively used equations are restricted to model isotherms with a single curvature. Isotherms that displaying both curvatures cannot be described (Vallejos-Burgos et al., 2019).

The adsorption equilibrium can be expressed by relations known as the adsorption isotherm. Adsorption isotherms represent the relationship between the amount of chemical adsorbed per unit mass of the adsorbent and the solution concentration at equilibrium. In general, the relationship between the amount of substance adsorbed by the adsorbent at constant temperature and the equilibrium pressure or concentration is called the adsorption isotherm. Adsorption continues until an equilibrium is established between the concentration of the substance deposited on the adsorbent surface and the concentration of the substance remaining in the solution. After the adsorption equilibrium is established, there is no change in the adsorption amount and solution concentration.

Adsorption isotherms are functions that vary with the concentration of adsorbed substance. Equilibrium isotherms play a very important role in building models and designing adsorption systems. Isotherms in a certain condition fit a model, while in other conditions they do not. Therefore, there is no single model that is generally applicable.

New models can be developed by making some assumptions in the found models. Current studies are on changing the adsorbent or the adsorbed substance with the help of these models, generally using determined models (Slejko, 1985).

Many theoretical and experimental adsorption isotherm equations have been proposed and used by researchers to evaluate physical or chemical adsorption events. Langmuir, Freundlich Dubinin- Radushkevich (D-R) and Temkin are some of them (Sarıkaya, 1997).

1.5.7.1. Langmuir isotherm model

The Langmuir isotherm model is the easiest method and most commonly used in adsorption experiments after the lineal model based on a linear dependence between the adsorption rate and the number of free binding sites. Three principles underpin this isotherm: (a) Adsorption cannot proceed beyond monolayer coverage, (b) all surface binding locations are equivalent and can only facilitate one adsorbed template, and (c) a template's ability to bind at a given site is independent of the occupation of neighboring sites. The Langmuir theory makes the fundamental assumption that sorption occurs at specific homogeneous sites within the adsorbent. It is then assumed that once a template molecule has occupied a site, no further adsorption can occur there. In theory, a saturation value is approached beyond which no further sorption can occur (Baggiani et al., 2004; Cunliffe et al., 2005).

American physical chemist Irving Langmuir (1881-1957), who made important contributions to the field of biochemistry and colloid research examining thin molecular layers between solid and liquid surfaces and won the Nobel Prize in Chemistry in 1932 with these studies, developed a kinetic adsorption theory resulting from certain pressure and heat conditions. The underlying idea of this theory is the formation of a stable equilibrium state between a free gas and adsorbent. Said equilibrium is a situation where the number of molecules adsorbed on the solid surface in each time is equal to the number of molecules that leave the surface and pass into the gas phase. The adsorbed gas layer is a single molecule (Langmuir, 1918). The simplest model for monolayer adsorption is the Langmuir model (Mckay, 1996).

Langmuir isotherm accepted the following situations as true (Amık, 2014):

* The adsorbed substance is in the form of a monolayer molecule

*The adsorption equilibrium is a dynamic equilibrium, that is, the amount of material adsorbed in a time dt is equal to the amount of material separated from the solid surface.

*The rate of adsorption is proportional to the amount of substance and the uncovered surface of the solid, and the rate of desorption is also proportional to the surface previously covered by a monolayer molecule.

*Adsorbed molecules are not dissociated; the theory can be generalized in case of dissociation.

The mathematical equation for the curvilinear Langmuir isotherm is as follows:

$$q_e=\frac{bC_e}{1+bC_e} \quad (1.1)$$

The linear equation of can be expressed as follows:

$$\frac{C_e}{q_e}=\frac{1}{q_{max}\,b}+\frac{1}{q_{max}}C_e \quad (1.2)$$

b = Constant related to free energy or enthalpy of adsorption (L/mmol)

C_e = Amount of adsorbate remaining unadsorbed in solution at equilibrium (mM)

q_e =Amount of substance adsorbed per unit mass of adsorbent (μmol/g)

q_{max} =Maximum monolayer adsorption capacity (μmol/g)

A graph is drawn considering the Ce/qe values versus the Ce values. The slope and cut point of the obtained line gives the values of 1/qmax and 1/qmax.b. A low value of the Langmuir adsorption enthalpy constant (b) indicates that the adsorbent has a high affinity for the adsorbed substance. The maximum monolayer adsorption capacity (q_{max}) refers to the total number of binding sites on the adsorbent surface where adsorption can occur. The amount of adsorbed substance per unit mass of the adsorbent (q_e) gives the number of binding sites on the solid surface occupied by the adsorbed substance (Sarıkaya, 1997; Gürboğa, 2004).

An important parameter of the Langmuir isotherm model is the term 'R_L', which is a dimensionless constant and is called the separation factor or equilibrium parameter. R_L is expressed by the following equation:

$$R_L = \frac{1}{1+bC_0} \quad (1.3)$$

Where, C_0 is the initial concentration. b(L/mg) is the Langmuir constant. The R_L parameter gives important indications about the suitability of adsorption for the selected adsorbent-adsorbate pair (Sarıkaya, 1993).

There are four possible possibilities for the R_L value (Berkem and Baykut, 1980).

1. In the case of $0 < R_L < 1$, adsorption is appropriate.

2. In the case of $R_L > 1$, adsorption is not suitable.

3. The $R_L = 1$ condition indicates linearity of adsorption.

4. In the case of $R_L = 0$, the adsorption is irreversible.

1.5.7.2. Freundlich isotherm model

Several empirical models have been proposed to describe the continuous energy distribution for the sorption process observed using different solid surfaces. The Freundlich isotherm, presented in 1926 by Herbert Max Finley Freundlich as an empirical sorption isotherm for non-ideal sorption on heterogeneous surfaces as well as multilayer sorption, is the most common continuous distribution model. According to the equation, the isotherm was later theoretically derived assuming an exponentially decaying sorption site energy distribution (Umpleby et al., 2004): The mathematical expression of the Freundlich isotherm (Freundlich, 1906):

$$q_e = K_F C_e^{1/n} \quad (1.4)$$

C_e: Concentration of substance remaining in solution after adsorption (mg/L),

q_e: Amount of substance adsorbed on unit adsorbent (μmol/g),

K_F: It is a sure sign of adsorption. It shows the strength of the relationship between adsorbed and adsorbent [(μmol/g) (L/mmol)1/n]. High values of K_F indicate that the closeness of the adsorbent and the adsorbed material to each other is quite high.

n is an expression of the adsorption density. Generally, n values between 1 and 10 are an indication of good adsorption. The 1/n value is the heterogeneity factor and takes values in the range of 0–1. The more heterogeneous the surface, the closer to zero the 1/n value. The accuracy of this isotherm is better than the Langmuir isotherm in heterogeneous adsorption systems. If the Freundlich isotherm equation is made linear by taking the logarithm of both sides of the equation:

$$\ln q_e = \ln K_F + (1/n) \ln C_e \quad (1.5)$$

In addition, By plotting the variation of lnqe versus $\ln C_e$, the constants K_F and n are found (Chiou and Li, 2002). The y-axis of the line obtained from the graph gives the intersection point $\ln K_F$ and its slope gives 1/n. These values are also explanatory in terms of better understanding the nature of adsorption as Freundlich isotherm constants.

1.5.7.3. Temkin isotherm model

The Temkin isotherm model predicts that all molecules' adsorption heat decreases linearly with increasing adsorbent surface coverage, and that adsorption is categorized by an uniformly distributed of binding energies up to a maximum binding energy. The Temkin isotherm is used for systems where the decrease in sorption heat is linear instead of logarithmic (Ho et al., 2002).

Temkin adsorption isotherm is an adsorption isotherm that expresses the indirect effects of adsorbate-adsorbate interactions on adsorption. According to the Temkin isotherm, the heat of adsorption of all molecules in the layer decreases linearly. The following Equation can be used to describe the Temkin isotherm:

$$q_e = B.\ln (K_T.C_e) \quad (1.6)$$

The linearized form of the Temkin isotherm is also given in equation:

$$q_e = B.\ln(K_T) + B.\ln(C_e) \quad (1.7)$$

Where, B = RT/b, b: ($\ln C_e$ vs. q_e) is the Temkin constant of the adsorption temperature (J/mol); K_T is the Temkin isotherm constant (L/g), R is the gas constant (8.314 J/mol K), and T is the absolute temperature (K) (Piccin et al., 2011).

1.5.7.4. Dubinin-Radushkevich model

The D-R adsorption isotherms were derived by Dubinin-Radusckevich and coworkers based on the micropore volume-filling theory for adsorption from the gas phase. Pores with a pore diameter of less than 2 nm are called micropores, and pores with a diameter of 2–50 nm or sometimes 2–100 nm are called mesopores. Compared to adsorption in meso and macropores, the adsorption process is much stronger. The adsorbed molecules are more closely surrounded by the pore walls in the micropores.

Due to the force-distance characteristics of the adsorption forces [F(r) α 1/r3], the substance adsorbed in small pores interacts more with the pore walls. The microporous volume filling theory is related to the Eucken/Polanyi potential theory. In this theory, the characteristic adsorption potential curve is defined by a=f(A). Here, a adsorption is defined as the adsorption potential at

$$A=RT\ln(Ps/P) \quad (1.8)$$

A=0 is the saturation point. A defined for gases, similarly for solutions. A=RT is defined as ln(Cs/C).

The D-R isotherm describes the adsorption that takes place on an isodimensional and uniform porous structure. In this respect, D-R isotherms are like Langmuir adsorption isotherms. D-R isotherms are defined by the following equation (Singh and Pant, 2004).

$$\ln q_e = \ln q_m - \beta.\varepsilon^2 \quad (1.9)$$

Here; ε (polanyi potential) = [RT ln (1+(1/C_e)] (kJ/mol); q_e; Amount of CRP retained per unit weight (μmol/g); q_m: Adsorption capacity (μmol/g); C_e: Equilibrium

concentration of CRP (mM); β: Constant related to adsorption energy ($mol^2.kJ^{-2}$); R: Gas constant 8.314 x 10^{-3} kJ/ mol.K, T: Temperature (K). Langmuir and Freundlich isotherms do not give any information about the adsorption mechanism. Therefore, D-R isotherms are drawn to understand the type of adsorption. Using the k value calculated from the D-R isotherms, the mean energy (E) value of the adsorption can be calculated (Singh and Pant, 2004).

$$E= \frac{1}{\sqrt{2\beta}} \quad (1.10)$$

With the magnitude of these E values calculated with the formula, the effective reaction mechanism and the type of adsorption can be decided. If the E value is in the range of 8-16 kJ/mol, there is ion exchange. If E<8 kJ/mol, physical forces are effective in adsorption. If E>16 kJ/mol, the effective mechanism of adsorption is chemical sorption.

1.5.8. Adsorption kinetics

By understanding the kinetics of adsorption, the effective adsorbed substance-adsorbent contact time can be determined, and it can also be understood by which step of the adsorption the rate of the adsorption process is determined. Adsorption consists of four main steps (Do, 1998; Seader and Herley, 1998).

1. In the first stage, the adsorbed substance in the gas or liquid phase diffuses towards the boundary of a film layer covering the adsorbent. This step is called bulk fluid diffusion. Since the adsorption medium is generally mixed, this step is usually fast and is not rate-determining in adsorption. However, if the phase in which the adsorbent is located is immobile, this step may be the slowest and determining the rate of adsorption.

2. The substance to be adsorbed, reaching the film layer, passes through the stagnant part here and moves towards the pores of the adsorbent. This movement is called film mass transfer or boundary layer diffusion.

3. The adsorbed substance moves in the pore spaces of the adsorbent and moves towards the surface where adsorption will take place. This is called intraparticle diffusion

or pore diffusion. Boundary layer (film diffusion) and intraparticle diffusion stages generally effect the adsorption rate together.

4. Adsorption of the solute at an active site on the material surface (chemical reaction by ion exchange, complex formation and/or chelation). This is the fastest step of adsorption.

The last step is considered as the equilibrium reaction. The overall adsorption reaction rate is controlled by the slowest step. This step is film diffusion or pore diffusion. This mechanism is illustrated in Figure below.

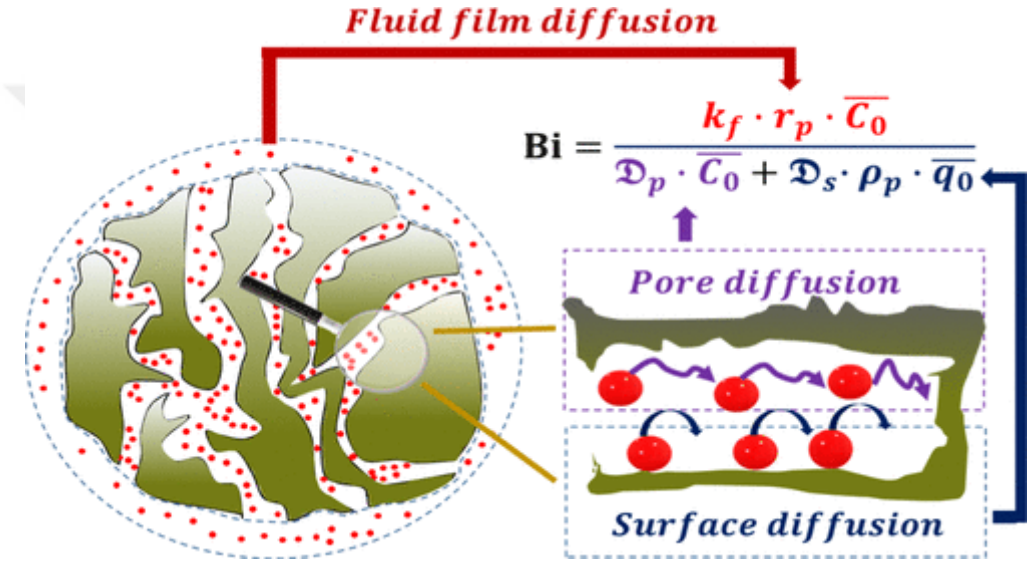

Figure 1.10. Illustration of diffusion steps of the adsorbate for liquid–solid adsorption.

External convection is the rate-limiting step in systems with weak mixing and dilute adsorbent concentration, small particle size adsorbent, and high affinity between adsorbent and adsorbent. On the contrary, in well-mixed systems, in the presence of adsorbent with large particle size, high adsorbed concentration, and low affinity between adsorbent and adsorbent, the intraparticle diffusion step limits the total transfer (Mogol, 2008).

Adsorption kinetics explains the reaction rate and the sorption process, which includes mass transfer, diffusion, and reaction on the adsorbent surface during adsorption. The adsorption process of adsorbates from aqueous solutions to the adsorbent consists of several phases, including external molecular diffusion over the boundary layer or diffusion film between the liquid phase as well as the adsorbent's external part; diffusion

that occurs within the adsorbent particles, allowing the adsorbate solution to enter the adsorbent pores; and the formation of physical or chemical bonds of the adsorbate at the active centers in the pores. The most common kinetic models used to monitor the kinetics of adsorption processes are Lagergren's pseudo-first-order model and Ho's pseudo-second-order model, while interfacial and particle diffusion models are most used to determine the mechanism of adsorption (Krstić, 2021).

1.5.8.1. Pseudo-first-order kinetic model

The Lagergren pseudo-first-order model assumes that the rate of change of solute uptake with time is directly proportional to the difference in saturation concentration and the quantity of solid uptake with time, which is widely appropriate over the early phase of an adsorption process. When adsorption occurs via diffusion through the interface, kinetics commonly follows the Lagergren pseudo-first-order rate equation. The linear form of the Lagergren pseudo-first-order model is as follows:

$$\ln(q_e - q_t) = \ln q_e - k_1.t \quad (1.11)$$

Here, qe and qt: amount of metal ion adsorbed at equilibrium and time t (min) k_1; first order adsorption rate constant (min^{-1}). The rate constant k_1 is calculated from the slope of the plot of ln (q_e-q_t) against t, and the theoretical qe value is calculated from the cut-off point of the graph (Sahoo and Prelot, 2020).

1.5.8.2. Pseudo-second-order kinetic model

The pseudo-second-order kinetic model predicts behavior over the entire range of adsorption by assuming that the rate-limiting process is chemical sorption or chemisorption. In this case, the adsorption rate is determined by adsorption capacity rather than adsorbate concentration. One significant advantage of this model over the Lagergren first order model is that the equilibrium adsorption capacity can be calculated from the model; thus, there is no need to evaluate adsorption equilibrium potential from experiment (Sahoo and Prelot, 2020).

The differential equation for the pseudo–second-order kinetics is given by:

$$\ln (q_e - q_t) = \ln q_e - k_1.t \quad (1.12)$$

Given by the relation. Here, q_e is the amount of substance adsorbed per gram of adsorbent at equilibrium (μmol/g), q_t is the amount of substance adsorbed per gram of adsorbent at any time (min), k_2 is the rate constant (g/mg.min). The initial adsorption rate is $h=k_2.qe_2$. The rate constant k_2 and theoretical qe values are calculated from the intercept and slope of the graph of t/qt against t, respectively.

1.5.8.3. Elovich kinetic model

The Elovich equation, first proposed in 1939, is satisfied in chemical adsorption processes and is appropriate for systems with non-homogenous adsorbing surfaces. The Elovich equation is extensively used in adsorption kinetics to characterize the framework of chemical adsorption (chemical reaction) in nature The Elovich equation is used to describe chemical adsorption kinetics. It is generally expressed as follows (Wu et al., 2009).

$$q_t = \frac{1}{\beta} \ln (\alpha\beta) + \frac{1}{\beta} \ln (t) \quad (1.13)$$

In this equation, α is the initial adsorption rate constant (μmol/g.min), β is the desorption constant (g/mg), and qt is the amount of substance adsorbed at time t (μmol/g). By plotting the qt values against the ln(t) values, the β constant from the slope and the α constant from the shear value are found.

1.5.8.4. Intraparticle diffusion model

The intra-particle diffusion model (IPD) introduced by Weber and Morris was used to analyze the kinetics of adsorption onto activated carbon fibers with phosphate groups in the expulsion of cadmium ions in aqueous environment. The intraparticle

diffusion adsorption kinetic model is one of the most widely used adsorption kinetic models. (Hu et al., 2019).

The intra-particle diffusion model can be written matematically as follows:

$$q_t = K_{id}. t^{1/2} + I \quad (1.14)$$

Here qt is the amount adsorbed per unit mass of the adsorbent at time t (min) and Kid is the intraparticle diffusion rate constant (μmol/g.min$^{-1/2}$). The value of I gives an idea of the thickness of the boundary layer, in other words, the greater the degree of intersection, the greater the boundary layer effect. In the intraparticle diffusion model, the rate step can be determined as one or a combination of more than one step. The first sharp segment observed in the $t^{1/2}$ versus q_t plot of intraparticle diffusion indicates the film diffusion segment. The second part is a further adsorption part, that is, the part where the intraparticle diffusion is the rate control degree. The third part is the final equilibrium part, and in this part, intraparticle diffusion begins to slow down due to the very little concentration of substance remaining in the solution (Chiu et al., 2004).

The linearity of the $t^{1/2}$ versus qt plot of intraparticle diffusion indicates the presence of intraparticle diffusion in adsorption. The fact that the line does not pass through the origin indicates that the rate limiting step is not only caused by intraparticle diffusion, but other kinetic models can also control the adsorption rate (Mezenner and Bensmaili, 2009; Şentürk and Büyükgüngör, 2013).

1.5.9. Adsorption thermodynamics

For the adsorption process, the enthalpy, entropy and free energy changes can be determined with the help of the equilibrium constant. These thermodynamic parameters are shown in the following equations (Nollet et al., 2003; Singh and Pant, 2003).

$$\Delta G° = - \ln Kd\ RT \quad (1.15)$$

$$\ln K_d = \frac{\Delta S^0}{R} - \frac{\Delta H^0}{RT} \quad (1.16)$$

Here, ΔG^o standard Gibbs free energy, ΔH^o standard enthalpy, ΔS^o standard entropy, R is the gas constant (8.3145 J/mol.K), and T is the temperature in Kelvin. Adsorption equilibrium is the constant:

$$K_d = \frac{C_A}{C_S} \quad (1.17)$$

K_d in the equation; is the thermodynamic distribution coefficient. C_A and C_S; adsorbed in equilibrium amount of CRP ions (mM) and remaining in solution in equilibrium adsorbed shows the amount of CRP ions (mM).

From the slope of the graph of lnKd vs. 1/T and the cutoff point, ΔG^o is the equation it is calculated from 1.14. The negative value of $\Delta H°$ indicates an exothermic behavior of adsorption and Negative values of $\Delta G°$ indicate that adsorption occurs spontaneously. The negative value of $\Delta S°$ is the solute-solution (i.e. adsorbent-liquid phase) interface. It shows a decrease in adsorbed concentration and on the solid phase indicates an increase in adsorbed concentration. If the positive value of $\Delta S°$ is solid-solution intermediate indicates that the randomness on the surface has increased (Goswami and Ghosh, 2005).

1.5.10. The aim of the study

The aim of this thesis is to detect CRP in human serum in a short time, with an easy and economical method, using molecular imprinting technique, which is a reliable technique for the preparation of affinity systems of C-Reactive Protein. For this purpose, molecular imprinted polymer (CRP-MIP) will be synthesized for selective adsorption of CRP.

After the characterization studies of the synthesized imprinted polymer, the re-bonding ability of the CRP-MIP with the batch polymerization process and the compatibility of the adsorption process with the kinetic and isothermal models and

thermodynamic expressions will be determined. Then the obtained data will be compared with the unprinted reference polymer (CRP-NIP).

2. LITERATURE REVIEW

The literature review for achieving the methods of this research has based on the previous collected works such as information about the Molecular imprinting and its components and applications in therapeutics and determinations of some medical parameters such as CRP. Moreover, as previously defined molecular imprinting is a technique used synthetic polymers for a specific target molecule. Molecularly imprinted polymers (MIPs) therefore have specific molecular recognition, one of the most important properties of biological antibodies. It can be used for applications where immunoassays, affinity separation, biosensors, and selective binding events such as directed synthesis and catalysis are important (Yıldırım, 2020).

MIP resin has better rebinding effectiveness for Thiamethoxam than MIP. Besides this, MIPs with particle sizes ranging from 53 to 75 m have the greatest efficiency of all imprinted polymers. Furthermore, provisional adsorption tests revealed that the MIP obtained achieved a maximum of equilibrium adsorption in roughly 30 minutes at pH 7.0, where the pesticides is in molecular form, favoring its retrieval. The results of the experiments revealed that MIP-GN/GCE not only had high sensitivity and retention properties for TMX, but it also had high reproducibility and renewability. Furthermore, the novel approach was successfully applied to the identification of TMX in brown rice samples (Xie et al., 2017; Silva et al., 2021).

Molecular recognition is critical in many biological systems. Molecular imprinting is among the most significant biological identification techniques, allowing host compounds to recognize and detect multiple molecules quickly, delicately, and discreetly. When contrasted with natural systems, molecular imprinting techniques have several advantages, including low cost, reliability, high recognition capacity, and long lifetime, allowing molecularly imprinted polymers to be utilized in a variety of biotechnological processes such as chromatography, therapeutic agents, nano-technology, and sensor technology (Silva et al., 2021).

Furthermore, sensors are essential tools due to their capacity to resolve a conceivably large number of practical situations in a variety of areas with numerous macromolecular objectives. Proteins, enzymes, nucleic acids, antibodies, viruses, and

cells are examples of macromolecules with numerous functions. Thus, macromolecule diagnosis has gained a lot of attention in terms of progress in most research findings. Because of their low cost, high precision, and consistency, macromolecule imprinted sensors will have a variety of uses (Saylan et al., 2017).

The created imprinted polymers exhibit high template specificity in both separate binding protocols and when constrained in competition with HSA. Intriguingly, we have shown that by modifying the template, the procedure can be employed to imprint HSA. Imprinted polymers derived from this protein had a much greater specificity for their native format than for CRP. They demonstrated that micro-contact imprinting is a feasible method for generating imprints of significantly larger proteins, which could be useful in the development of sensing element for the detection and quantifying of such species (Chou et al., 2005).

According to an additional research project, MIP-based analytical techniques can provide relatively simple examination and have been successfully applied to food volatile matter and off-odor analyzation with high specificity and intensity in recent times, with the expectation that this strategic approach will have broader application opportunities in the coming years. Almost every manufacturing will recommend the use of cutting-edge and bio-based materials produced by various polymerization approaches that facilitate restricted adsorption and desorption of target analytics and bioactive molecules. The future use of natural polymers and green heterogeneous catalysts is an important topic to think about when considering the future of MIP synthesizing (Cengiz et al., 2022).

According to numerous studies, the target species for molecular imprinting processes has augmented and include cells and micro-organisms. For instance, as a new category of nanosensors that empowers processing-free whole-cell bacterial diagnosis, the selective identification of pathogens (e.g., pathogenic bacterial strains) in living organisms using synthetic MIP bio-sensing formations has received considerable attention. Bacterial monitoring has historically relied on cultures and antimicrobial susceptibility testing tests, immunological tests, genotyping, and histopathological examination, all of which are time-consuming, costly, and labor-intensive procedures. Recent studies have shown that using MIPs can be a novel method for detecting pathogenic bacteria (Mustafa et al., 2022).

Molecular imprinting is a polymer matrix-based self-assembly technique that generates 3-D imprinting formations for a specific target molecule. MIPs have a number of cost advantages over other protein and nucleic acid-based sensing platforms. MIPs have a strong benefit in that they are highly specific for the template or target biomolecule. They are additionally more recalcitrant to higher temperatures and pressures as well as stronger, more physically rigorous, and undetectable to chemical reagents, bases, acids, and metal ions. MIPs are also economical to manufacture and have a lengthy shelf life when stored correctly at ambient temperature. Therefore, the electrode was modified to diagnose neonatal sepsis using MIPs equipped for CRP measurement (Balayan et al., 2022).

Molecular imprinting is a method that generates biorecognition sites in a polymeric material that are covalently and sterically supplementary to the predefined target molecules. Molecularly imprinted polymers (MIPs) have proved invaluable for the technique works best of smaller biological molecules to date. Nowadays, much emphasis is being placed on the molecular imprinting of bio-macro-molecules such as proteins and DNA. The imprinted polymers have outstanding chemical, structural, and surrounding temperature and are being used in place of costly biological antibodies for protein isolation, extraction, and identification. However, the major issues confronted in supramolecular imprinting are protein absorption in the polymer matrix, morphological versatility, dissolution rate, and completeness due to the number of organic compounds, and poor mass-transfer of the proteins (Kumar and Prasad, 2012).

Conventional protein molecularly imprinted polymers (MIPs) are applied to create biosensors for highly specific protein recognizing. These biosensors are based on the production of three-dimensional pores that are completely equivalent to the imprinted template molecules. Protein MIPs, as a modern trend of artificial recognition probes, can achieve recognition selectivity, but their diagnostic sensitivity and limit of detection (LOD) are not optimal (Cui et al., 2022).

C-reactive protein (CRP), an essential element of the immune system, is a diagnostic and therapeutic biomarker associated with cancer, cardiac disease, and neurological condition. As a result, the advancement of investigative techniques for accurate CRP analysis, including enzyme-linked immunosorbent experiment, quartz crystal microbalance, and spectroscopic immunoassay, is gaining traction for early

clinical diagnosis and therapeutic rehabilitation. These practices, however, are limited by time-consuming processing. For example, intricate operations, trivial pre-treatment steps, high cost, and reduced specificity. As a result, a strategy capable of determining CRP in a sensitive, selective, simple, accurate, versatile, low-cost, and rapid manner represents an encouraging trend (Cui et al., 2021).

Molecular recognition is essential in many living systems. The molecular imprinting technique (MIT) offers an appealing alternative for creating artificial molecular recognition probes. MIPs centered on MIT can be created through co-polymerization in the existence of functional monomers, template molecules, and other constituents such as cross-linking agents, initiators, and promoters. MIPs can produce many three-dimensional abscesses after the template molecules are retrieved. These three-dimensional cavities, which serve as highly particular recognition sites, are complementary in size, shape, and functionality to template molecules. As a result, MIPs can interfere with their biomolecules with pinpoint accuracy. Protein MIPs are a type of antibody imitate that has a high sensitivity and specificity for recognizing biological synapses (Chen et al., 2020).

Protein MIPs with three-dimensional polymer films equipped using template protein molecules and functional monomers can achieve extremely selective identification of target proteins premised on the three-dimensional cavities left in the polymers after removal of the template protein molecules as a younger generation of identifying microelectrodes. Protein MIPs, like MIPs, have three-dimensional cavities that are coherent to the template protein molecules regarding the functional group affiliation, size, and shape. As a result, interaction forces with rigorous selectivity happen disproportionately between the pores and target protein complexes. Protein MIPs have benefits over antibodies, like simple and inexpensive synthesizing, easy combined effect with actuators, long storage times, and consistency (Hu et al., 2021).

C-reactive protein (CRP) accumulation in serum is frequently used to determine the risk of heart attack, and it is linked to coronary heart disease, fibrosis and inflammatory processes, melanoma, and infectious diseases. Molecular imprinting, a low-cost advancement, can be employed for sensing and differentiating, among other things. Protein sensing and extraction from biological fluids are particularly interesting in the context of MIPs. Molecular imprinting of proteins traditionally uses the entire protein as

a template. Working with a delicate template like protein, on the other hand, necessitates extreme caution. Furthermore, protein molecules must be extracted from the MIP bulk before being recognized by this polymer. Epitope imprinting is an alternative molecular imprinting strategy that can generate protein-specific receptors (Lee et al., 2021; Bartold et al., 2022).

Due to the devoted architecture of the three-dimensional cavities engrained within the polymer, molecular imprinting of polymers is a procedure spearheaded more than 30 years ago that provides a different way to conventional bio - recognition techniques (e.g., the use of antibodies for the explication of immunosensors). As a result, molecularly imprinted polymers (MIPs), also known as "plastic antibodies," are competent of binding a specific analyte from a complex array with high specificity because they can act as receptor sites for target molecule recognizing. The basic reaction mechanism for MIP synthesis occurs in a complex mixture containing a based on the functional monomer, a cross-linker, an initiator, and the target molecule, all blended in an efficient leader liquid or mixtures of various solvents (Cieplak and Kutner, 2016).

To begin, a pre-polymerization compound is formed in which the template is confined to the monomer by various types of reactions, such as covalent, semi-covalent, non-covalent, or metal synchronised relationships. The energy required for removing the template varies depending on the kind of bonding, with covalent bonds requiring the most energy and non-covalent bonds requiring the least. As a result, non-covalent bond formation is more flexible, which makes it the preferred scheme for MIPs readiness. When the template molecule is excluded from the polymeric matrix, supplementary cavities with shape, framework and functional groups form which act as particular binding sites for the particles were originally taken (Abdel Ghani et al., 2016).

Polymer molecular imprinting MIPs have sparked interest in the scientific community due to their numerous advantages, including low costs, high stability and affinity for the target molecule, and ease of incorporation into standard fabrication methods. As a result, a wide range of MIP-based applications has been developed, including solid phase extraction, affinity separation, chemical sensors, immune-like assays, and controlled (targeted) drug delivery. Even though most MIP-related implementations are associated with attraction separation methods, the development of MIP-based sensors has been extensively researched. MIPs could be used to collect both

qualitative and quantitative data for analytes from a variety of classes, such as biomolecules (proteins, amino acids, and enzymes), drugs from pharmaceutical dosage forms or biological material (Uzuriaga-Sánchez et al., 2016).

Classical MIP manufacturing approaches (e.g., bulk synthesis) have some disadvantages, such as template discharges or inadequate expulsion, random selection of complex formation, slow mass flow, and non-periodic morphology. To address this challenge, various imprinting methodologies, such as in situ polymerization or core shell MIP synthesizing, were used. Since the appearance of drugs has become an inveterate pattern throughout most people's lives, their detection and evaluation has become critical. Analytical testing is a crucial key for exploring the involvement of unconnected or instrumental stimulants in the pharmaceutical companies, clinical pharmacology, forensics, or the surroundings, whether it is regarding medication management, doping, psychoactive substances, and quality assurance in the pharmaceutical sector, clinical pharmacognosy, forensics, or the climate (Niu et al., 2016).

MIPs have been investigated for many years in pharmaceutical analysis because they can remove only the preferred molecule. Selectivity could also be drastically enhanced by employing standard techniques as investigative techniques for MIPs-based sensors, with these techniques offering the exceptional possibility of disassembling the devices and acquiring hand-held or even point-of-care equipment (Florea et al., 2016).

3. MATERIALS AND METHODS

3.1. Materials

C-Reactive Protein (CRP), α1-Antitrypsin, α1-Acid glycoprotein, methacrylic acid (MAA), ethylene glycol dimethacrylate (EGDMA) 2,2′-azobis(2-methylpropionitrile) (AIBN), acetonitrile, acetic acid (CH_3COOH), methanol (MeOH) was obtained from Sigma-Aldrich (USA). All their agents used were of analytical grade.

- Multiple magnetic stirrer heaters (Wise Stir)
- Analytical Precision balance (Precisa)
- PH meter (620 Lab pH Meter)
- Oven (Core FN 400)
- UV spectrophotometer (Optizen POP)
- SEM (Scanning Electron Microscope) (Zeiss Evo 15 Model)
- FTIR Spectrophotometer (Bio-Rad-Win-IR spectrophotometer)
- TGA/DSC (Setaram Labsys Evo Gravimetric Analyzer 1600, France)
- Distilled water device (Thermo Scientific)
- Filter paper, (Whatman No.41)
- Micropipette and drip tip
- 200 mesh sieves
- Desiccator
- Glass materials, in the experiments, flasks, beakers, measuring tapes of various sizes, balloons used with jugs, pipettes and tubes.

3.2. Synthesis of CRP-MIP

The bulk polymerization method was used to prepare the MIP for C-reactive protein. For the synthesis, 20 mL of acetonitrile solution (CH_3CN) was mixed with 675 μL of methacrylic acid ($C_4H_6O_2$), which is soluble in warm water and miscible with most organic solvents. Next, 10 μL of C-reactive protein (CRP) was heated and after half an

hour, nitrogen gas was opened for 15 minutes and 0.05 g of AIBN (2,2'-azobis-isobutyro-nitrile) and 6.04 mL of ethylene glycol dimethacrylate (EGDMA) were added. Then it was polymerized in an oil bath at 70°C for 24 hours. After 24 hours, the solution was washed with water and methanol and placed in an oven at a temperature of 60°C for 24 hours, after which the solution was ground (Jain et al., 2020).

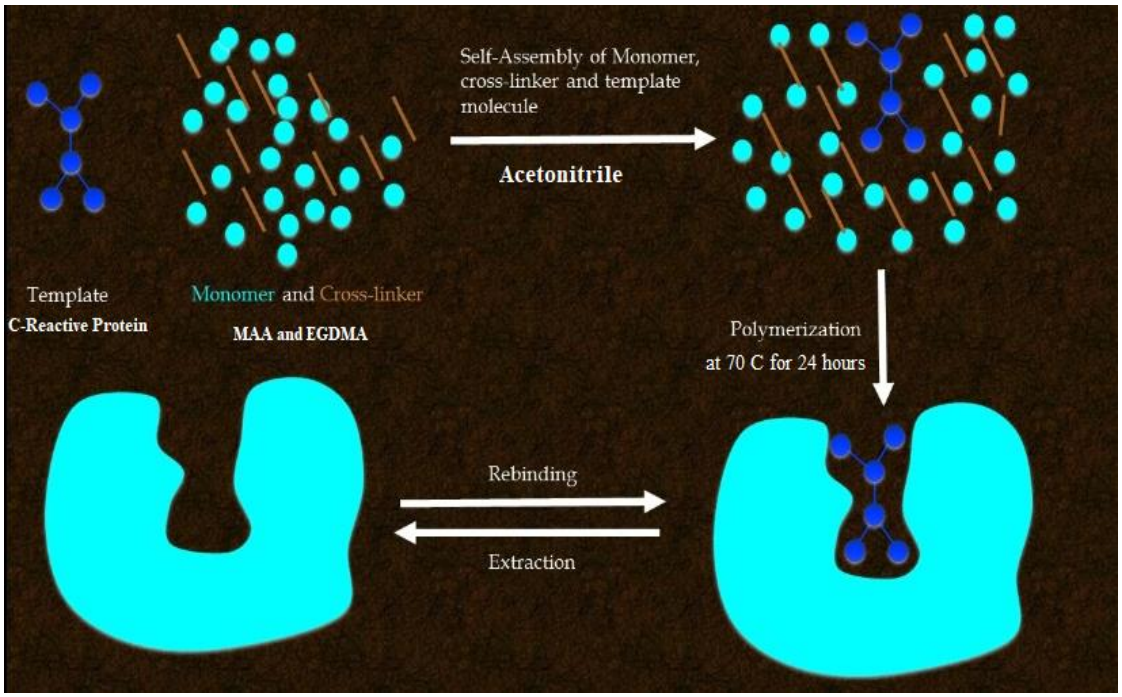

Figure 3.1. Schematic illustration for the synthesis of a molecularly imprinted polymer.

3.3. Synthesis of NIP

The NIP for C-reactive protein was created using the bulk polymerization procedure. 20 mL of acetonitrile solution (CH_3CN) was mixed with 675 μL of methacrylic acid ($C_4H_6O_2$), which is soluble in warm water and miscible with most organic solvents. Then they were heated for 30 minutes in acetonitrile solution methacrylic acid. After that, the mixture was exposed to nitrogen gas for an extended period (15 min.). To further protect the solution for polymerization the initiator 0.05 g Azobis isobutyro nitrile (AIBN), an organic compound was added to the solution with 6.04 mL cross-linker (EGDMA). Then it was polymerized in an oil bath at 70°C for 24

hours. After 24 hours, the solution was washed with water and methanol, and the solution was placed in an oven at a temperature of 60°C for 24 hours,

3.4. Removal of the Template CRP from CRP-MIP

The synthesized CRP imprinted polymer (MIP) was packed in cellulose cartridges, placed in the soxhlet chamber, and extracted in a methanol-acetic acid (4:1) mixture for 48 hours. Then the MIP was washed several times with methanol and distilled water and dried in an oven at 60°C for 24 hours. The dried polymer was brought as a fine powder and kept in a desiccator.

3.5. Characterization of Polymers

3.5.1. SEM (scanning electron microscope) analysis

SEM is one of the most important test instruments for in situ analysis of micro areas. It has the advantages of high resolution, great depth of field, high magnification, and strong stereoscopic vision. Photographs taken with SEM have higher magnification and clearer definitions than those of optical microscopy.

The surface morphology of the polymer particles (MIP and NIP) was investigated using scanning electron microscopy (SEM) (Figure 3.2). The images of MIP and NIP are similar in size and surface morphology, but MIP has gaps, possibly due to the structure of the target molecule (C-reactive protein). Figure 3.2 (a and b) also shows that the imprinted polymers have irregular particles and heterogeneous structures. The ordered nature of the non-embossed polymer is since no specific binding sites for the analyte were created.

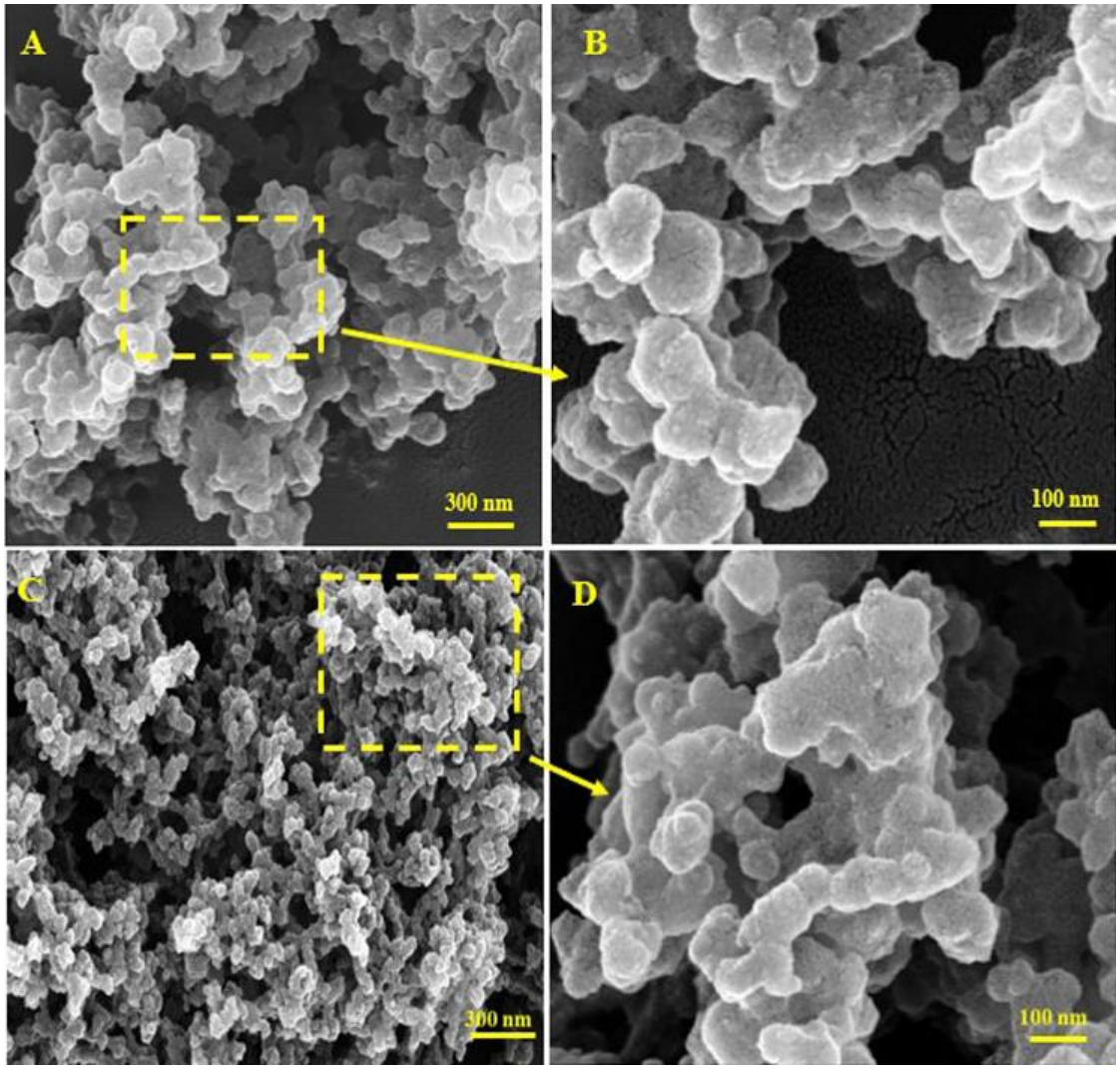

Figure 3.2. SEM of polymers; (a, b) MIP and (c, d) NIP.

3.5.2. FT-IR (fourier transform-infrared) spectrum analysis

Infrared spectroscopy is a method based on the measurement of the absorption of energy by molecules between the visible region and the microwave region. This energy region, which has a frequency between 3.8×10^{14} and 3.0×10^{11} Hz (wavelength 700-100000 nm), is defined as the general infrared region and is divided into subgroups as near, mid, and far infrared regions. Structural characterization of polymers of the synthesized adsorbent to be used in the study was made using Bio-Rad-Win-IR model FT-IR spectrophotometer. Spectra were obtained by scanning in the range of 4000-400 cm^{-1}.

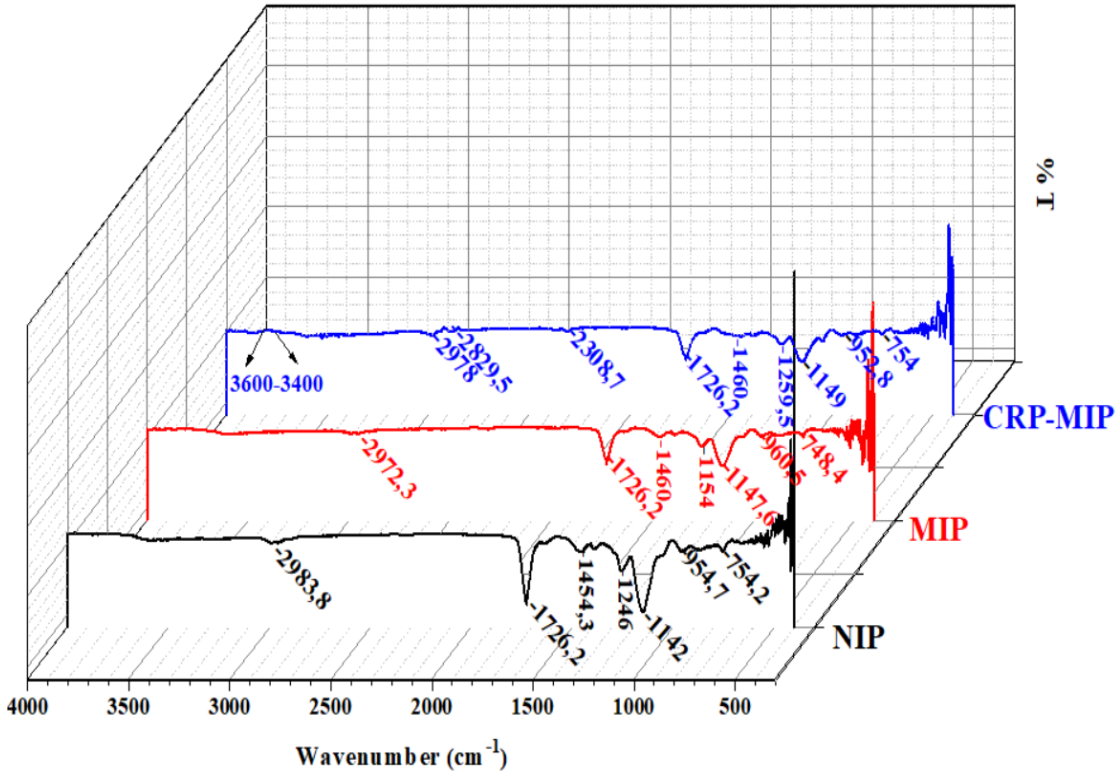

Figure 3.3. FTIR spectra of (a) uneluted CRP-MIP (b) eluted MIP and (c) NIP.

Figure 3.3 shows the infrared spectra of unresolved MIP (CRP-MIP), eluted MIP, and NIP. The peaks from 3600 cm^{-1} to 3400 cm^{-1} are the stretching vibrations of O-H and N-H, respectively. 2978 cm^{-1} and 2829 cm^{-1} are the stretching vibrations of =C-H and C-H, respectively. 1726 cm^{-1} and 1640 cm-1 were the stretching vibrations of C=O and C=C, respectively. The peaks at 1295 cm^{-1} and 1149 cm^{-1} were the stretching vibrations of C-O in carboxyl and ester, respectively, indicating the presence of MAA and EGDMA (Mei, et al., 2016). After washing, the spectrum of the MIP (Figure 3.3.b) is like the spectrum of the unprinted polymer (Figure 3.3c). This shows that the template molecule has been removed from the polymer. Therefore, it provides an advantage when studying the binding behavior.

3.5.3. Thermogravimetric analysis (TGA)

Thermal stability, glass transition temperature and melting temperature values of CRP-MIP and CRP-NIP, TGA analyzes were determined using Setaram Labsys Evo Gravimetric Analyzer 1600 model device. Approximately 10 mg of sample was placed in

a ceramic crucible and analyzed at a heating rate of 10°C/min with a flow of 100 mL/min under Argon atmosphere in the range of 25-550°C. TGA thermo-grams of CRP-MIP and CRP-NIP are given in Figure 3.4.

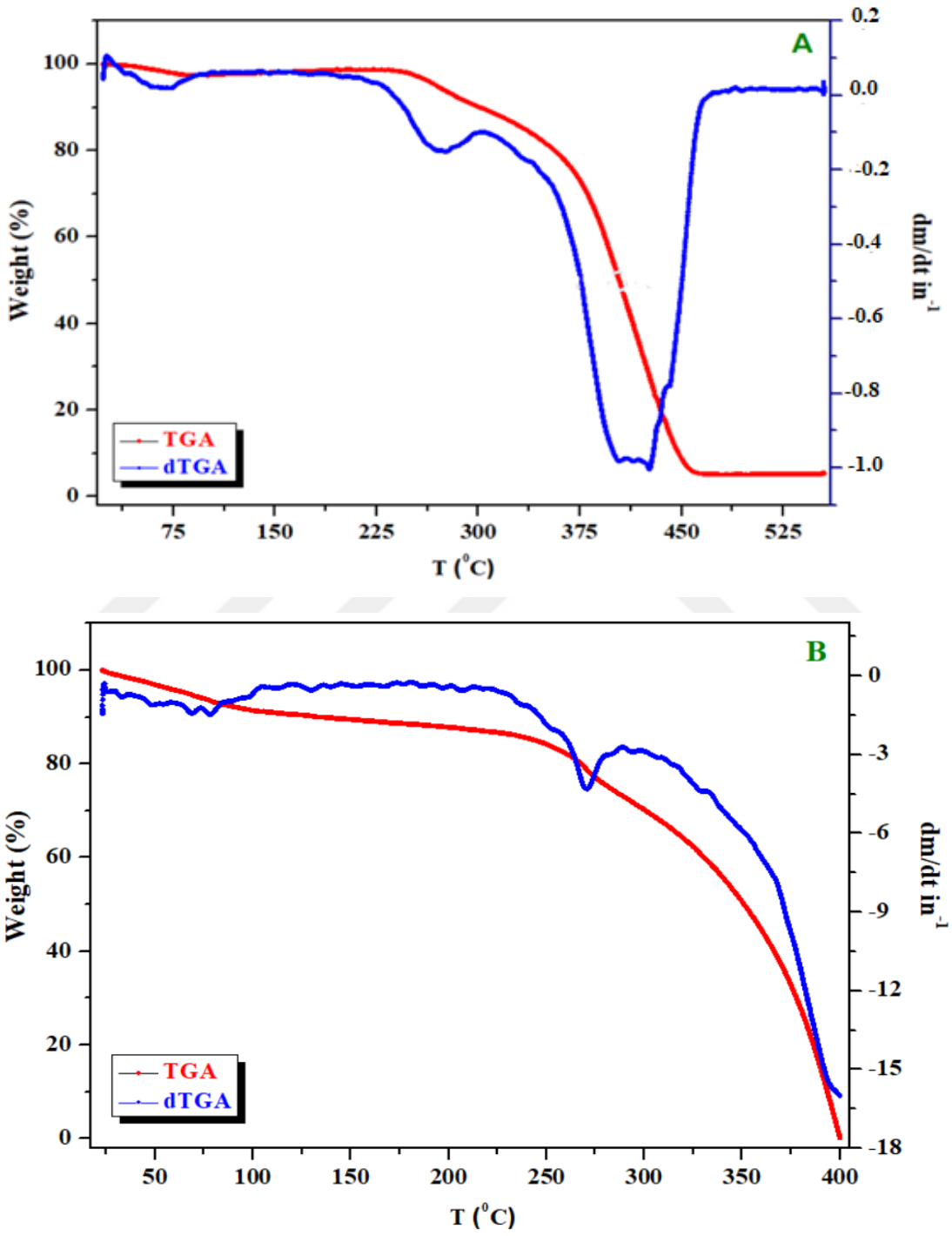

Figure 3.4. TG and dTG curves (a) CRP-MIP (b) CRP-NIP.

The TGA thermogram from CRP-MIP (Fig. 3.4a) shows three-digit decomposition. These decompositions start at 68ºC, 273ºC, and 413ºC, as shown in the derived diagram. In the first decomposition step, about 3% of the substance consisting of low molecular weight components such as absorbed water, solvent and monomer are removed from the polymer. In the 2nd and 3rd decomposition steps, the polymer chain structure is degraded. 50% substance loss occurred at 403ºC (Th). When heated to 550ºC, 95% of the polymer decomposed and the remaining 5% remained intact.

From the TGA thermogram plot of CRP-NIP (Figure 3.4b), there is a two-stage decay. These decays start at 74 ºC and 271 ºC, as can be seen from the derivative plot. In the first decomposition step, about 6% of the matter is removed. In the second decomposition step, the polymer chain structure is degraded. 50% of the material loss occurred at 350ºC (Th). CRP-NIP Polymer was completely degraded at 400ºC. Looking at the graphs of CRP-MIP and CRP-NIP TGA, CRP-MIP has higher thermal stability. This stability also leads to a slowing down of the degradation.

4. RESULTS

4.1. Adsorption Studies

Adsorption of CRP on CRP-MIP and NIP from aqueous solutions was performed in a batch procedure. CRP solutions with different concentrations and pH values were contacted with the polymers at different temperatures for different times. To adjust the pH, 1 M NaOH and 1 M HNO_3 solutions were used in the studies. When adsorption is complete, the polymers are removed from the solution by filtration with filter paper. The amount of CRP remaining in the solution medium was measured using a UV spectrophotometer at 300 nm.

The amounts of CRP adsorbed were calculated from the difference among the initial and equilibrium concentrations. qe (μmol/g), the amount of CRP adsorbed per adsorbent, the percentage of removal (%) were determined as follows.

$$q_e = \frac{(C_i - C_e).V}{m} \quad (4.1)$$

$$\% \text{ Removal degree} = \frac{C_i - C_e}{C_i} \times 100 \quad (4.2)$$

Where, C_i and C_e are the initial and equilibrium CRP concentration (mM); Solution volume is V (mL) and the quantity of adsorbent is m (mg). Stock CRP solutions were prepared at 5 mM concentration. Used the concentrations of the solutions were calculated according to the formula $M_1.V_1 = M_2.V_2$ and diluted from the stock solution.

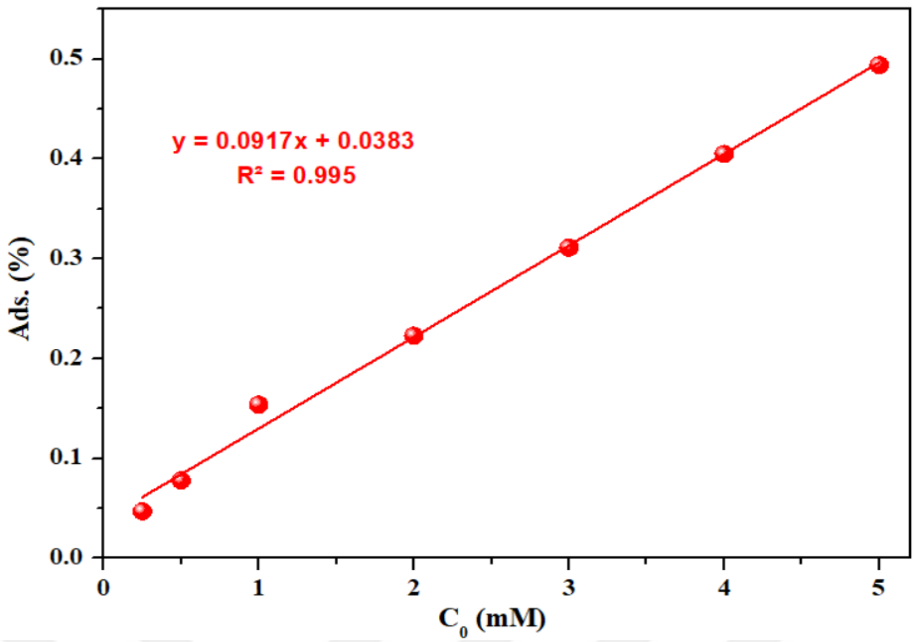

Figure 4.1. Calibration plot for CRP determination.

In the preparation of the calibration curve, the calibration curve prepared from different solutions of the CRP was used to determine the CRP concentrations before and after adsorption in the study. While the calibration curve was being drawn, the solutions prepared at 5, 4, 3, 2, 1, 0.5, and 0.25 mM concentrations were read against distilled water at 300 nm, and the resulting values were plotted against the concentration.

Calculations were made using the formula y=ax+b (R=0.9950) obtained from the regression analysis of the calibration curve.

4.2. Adsorption of C-Reactive Protein by CRP-MIP

4.2.1. Contact time effect and kinetic studies

Contact time is an important parameter that effects adsorption. The diagram of the removal efficiency (%) and q_e (μmol/g) as a function of time for adsorption of CRP solutions with a concentration of 1 mM is shown in Figure 4.2.

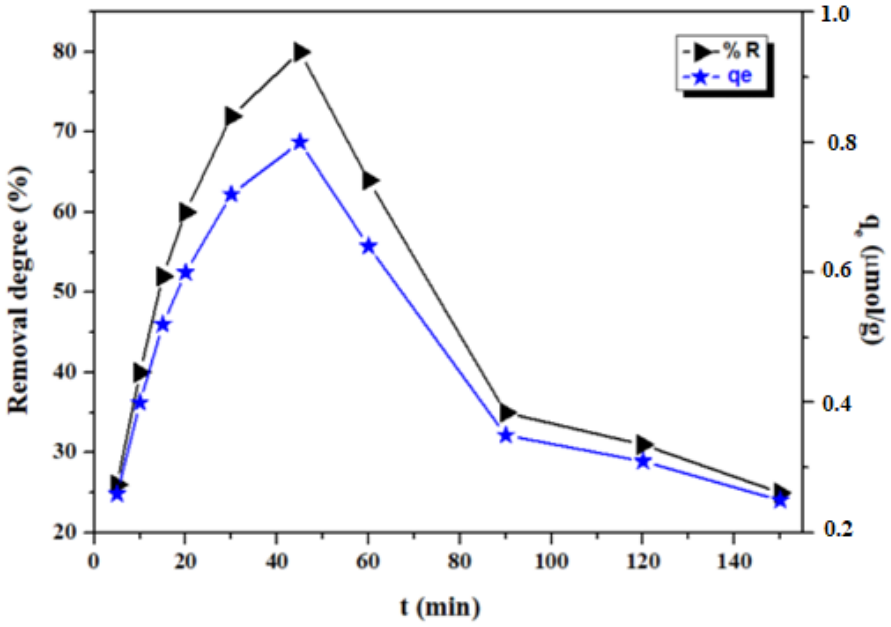

Figure 4.2. Effects of contact time on CRP adsorption (pH: 5, CRP cons.: 1 mM, adsorbent 10 mg, T: 25°C, V:10 mL, 500 rpm).

Figure 4.2 shows that adsorption efficiency in the CRP adsorption studies at CRP-MIP increases with time, peaking at the 45th minute. At this optimal time, the adsorption efficiency was 80% and the q_e value was determined to be 0.8 μmol/g. It was observed that the adsorption efficiency and q_e value decreased with longer adsorption studies.

For the kinetic evaluations of the adsorption of CRP on CRP-MIP, the diagram (Figure 4.2) was used for the effect of contact time on adsorption. The fit of CRP adsorption to the first-order kinetic pseudo model, second-order kinetic pseudo model, intraparticle diffusion model, and Elovich's kinetic model, whose mathematical equations are given in Section 1.10, was examined. The plots of the kinetic models drawn with the data obtained from the equations are shown in Figure 4.3. The kinetic parameters are given in Table 4.1.

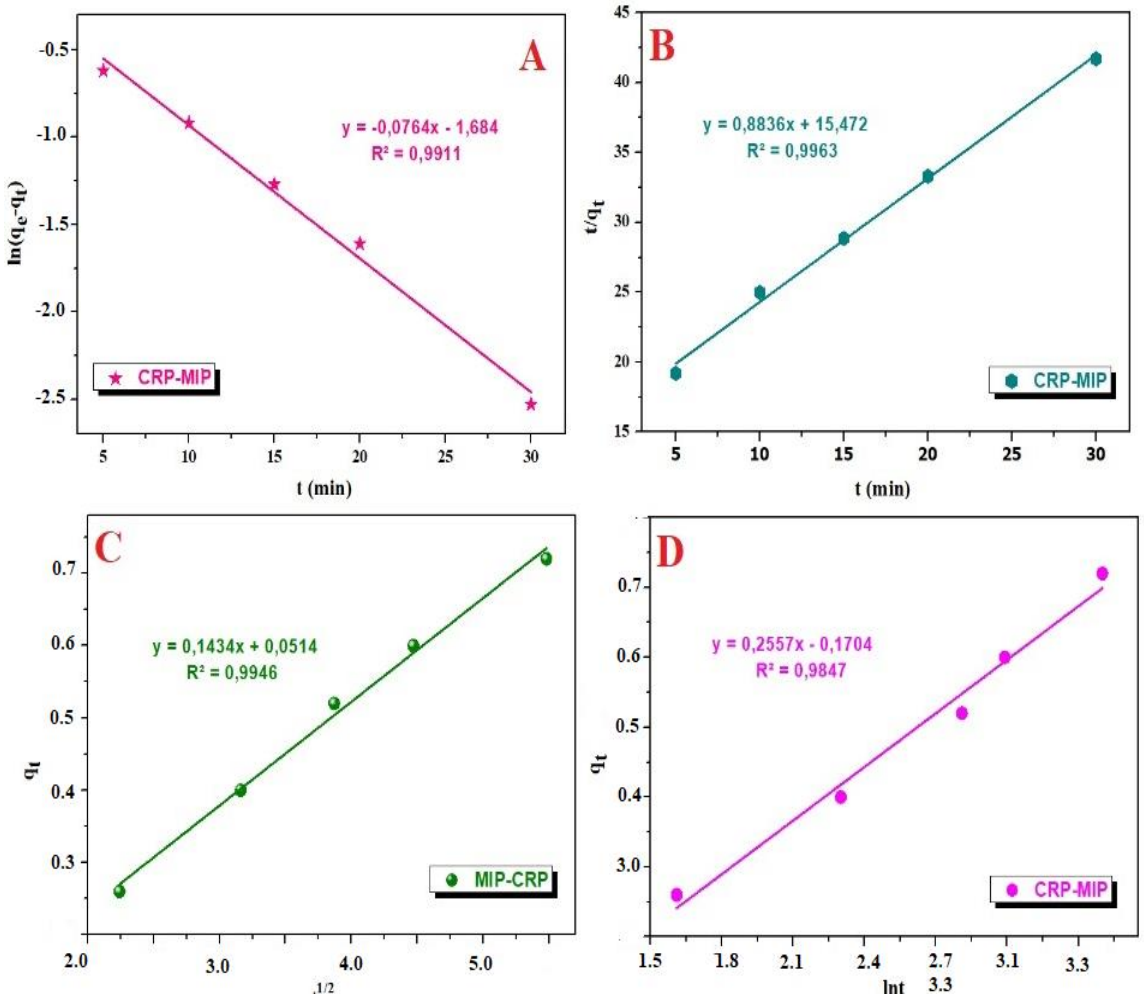

Figure 4.3. Kinetic studies for CRP adsorption on CRP-MIP; (a) pseudo-first order, (b) pseudo-second order, (c) Intraparticle-diffusion, (d) Elovich kinetic models.

Table 3.1.1. Kinetic parameters of CRP adsorption onto CRP-MIP

Models	Parameters	CRP-MIP
Pseudo-first order	q_e (μmol/g)	0.19
	k_1 (1/min)	0.08
	R^2	0.9911
	q_{exp} (μmol/g)	0.8
Pseudo-second order	q_e (μmol/g)	1.1
	k_2 (g/μmol.min)	0.05
	R^2	0.9963
	q_{exp} (μmol/g)	0.8
Elovich	α (μmol/g.min)	0.13
	β (g/μmol)	3.91
	R^2	0.9847
Weber-Morris intra-particle diffusion	k (μmol/g.$min^{1/2}$)	0.14
	I (μmol/g)	0.05
	R^2	0.9946

Examination of Table 4.1 shows that the most appropriate adsorption kinetic model for CRP is the second-order pseudo-rate equation. This equation is used to explain the adsorption behavior at low concentrations. From the table, the correlation coefficient R^2 of the second-order rate equation is very close to 1 (0.9963) and the qe value calculated from the equation (1.1) gives a result closer to the experimental q_e (0.8).

The pseudo-first-order kinetic model, Elovich kinetics, and intraparticle diffusion model showed lower agreement with the CRP adsorption mechanism, as they had lower correlation values. The Elovich kinetic model, on the other hand, unlike the first and second order pseudorate equations, cannot predict any mechanism present in the system. Adsorption kinetics is usually controlled by several mechanisms.

Hai et al. (2020) conducted a study on the fullerene functionalized magnetic molecularly imprinted polymer and obtained the results of the rate constants of reaction kinetic models. They used two kinetic models included Pseudo first order kinetic equation and Pseudo second order kinetic equation and their values of R^2 were 94.3% and 98.6 %

respectively. The results of the current study is slightly hugher than these results so, our results can be verified and reliable for further analysis of the research. Although, the values of qe were 23.3 μmol/g and 34.6 μmol/g respectively obtained by the Pseudo first order kinetic equation and Pseudo second order kinetic equation as compared to the current results which was much smaller 0.19 μmol/g and 1.1 μmol/g.

4.2.2. pH effect

The effect of pH on adsorption was determined by working in 1 mM CRP solution between pH 4-10. Figure 4.4 shows the values for the effectiveness of pH on adsorption.

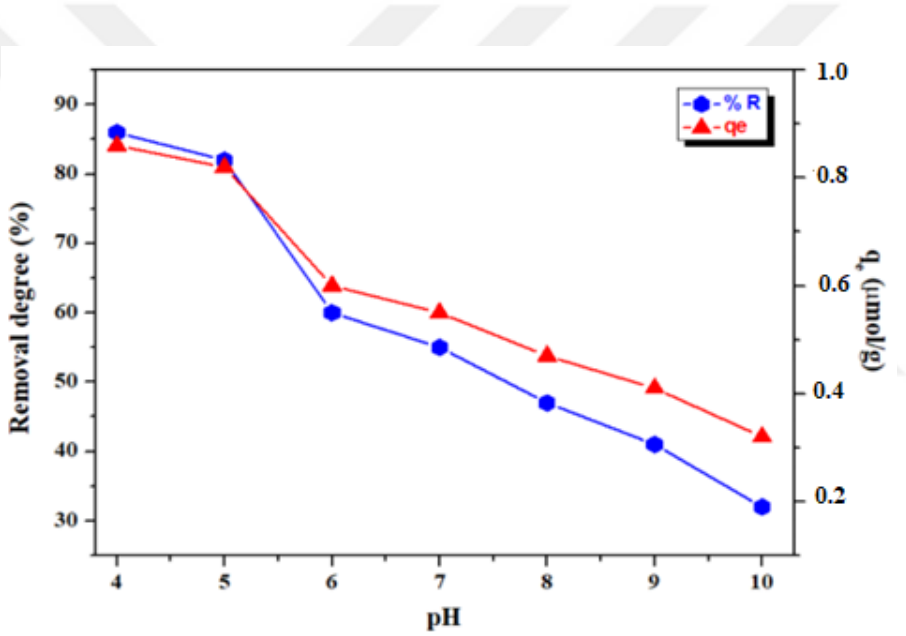

Figure 4.4. Effects of pH on CRP adsorption (t: 45 min, adsorbent 10 mg, CRP conc.: 1 mM, T: 25°C, V: 10 mL, 500 rpm).

The figure 4.4 has presented that both the amount of removal degree (%) and qe (μmol/g) are proportional with the pH values over the entire observations. While the adsorption capacity of CRP was high at pH 4, no decrease was observed in the adsorption capacity between pH 5 and 10. In other words, as the pH values increase, lower efficiency of the adsorption rate and smaller qe value are obtained.

Asiabi et al. (2016) confirmed that manufactured molecular imprinted polymers accumulate the target analyte at neutral pH, but this occurrence is entirely contingent on

the presence of analyte acidic or basic organic compounds and the nature of organic functional effectively available inside the cavities of MIPs. The pH of the medium influences the adsorption of Congo red dye MIP. This is due to the chemical evolution by natural selection of the binding sites of cavities present within the MIP as well as the active functional groups of dye obtainable for bonding. These findings are consistent with the findings of this study.

4.2.3. Initial concentration effect and isotherm studies

Different concentrations of CRP solutions (0.25-5 mM) were used to determine the effect of the initial concentration. To determine the amount of CRP adsorbed by CRP-MIP at these concentrations, the change graph of removal degree (%) and q_e (µmol/g) versus varying initial concentration is given in Figure 4.5.

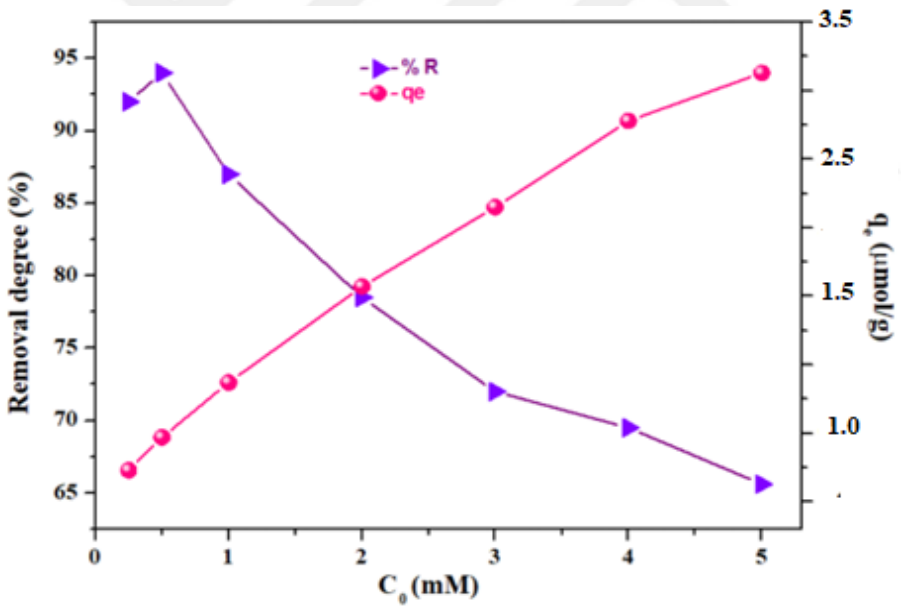

Figure 4.5. Effects of initial concentration on CRP adsorption (t: 45 min, adsorbent 10 mg, pH:4, T: 25°C, V: 10 mL, 500 rpm).

When Figure 4.5 is examined, it is seen that the highest removal degree was obtained at 0.5 mM concentration. At higher concentration values, as shown in the figure, it is seen that the removal degree decreased and q_e increased. When higher concentration values are increased, the adsorption efficiency decreases, whereas the qe value increases

against the fixed amount of adsorbent due to the increase in the ion concentration in the solution medium. One of the most important features that emerged in this experiment is that both the degree of removal and q_e intersect when the initial concentration value is 2 mM. Mathematically, the intersection point is referred to as the chemical break point analysis or equilibrium state (Figure 4.5).

The graph of change of initial concentration versus removal degree (%) at constant temperature for the adsorption of CRP on CRP-MIP is shown in Figure 4.5. The isotherm graphs drawn using this graph and using the mathematical equations expressed for adsorption isotherms in Section 1.9 are given in Figure 4.6 and adsorption isotherm parameters are given in Table 4.2.

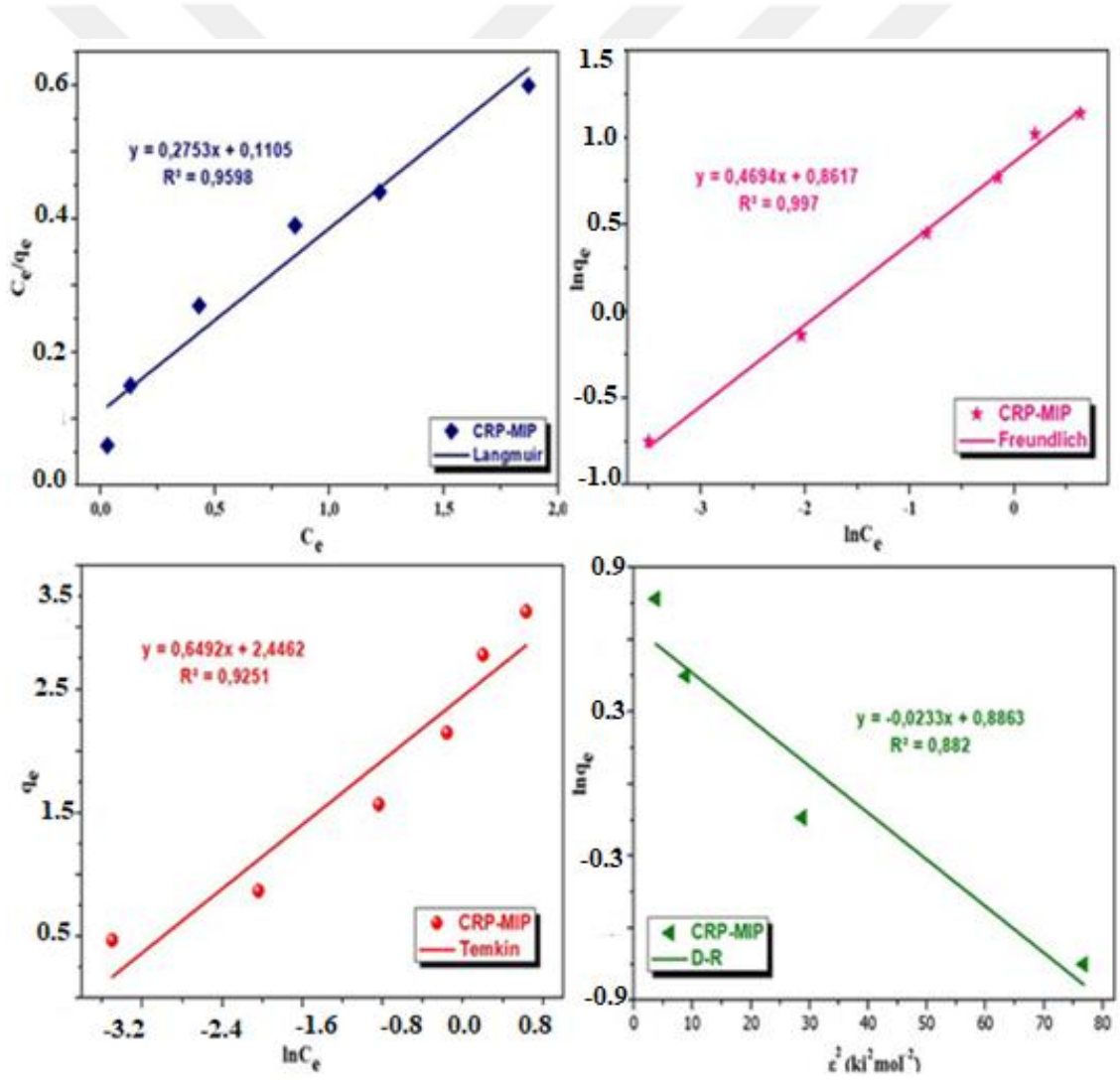

Figure 4.6. Isotherm plots for CRP adsorption on CRP-MIP.

Table 3.1.2. Isotherm parameters of CRP adsorption onto CRP-MIP

Models	Parameters	CRP-MIP
Langmuir	q_{max} (μmol/g)	3.63
	b (L/mmol)	2.5
	R_L	0.44
	R^2	0.9598
Freundlich	K_f [(μmol/g)(L/mmol)$^{1/n}$)]	2.37
	N	2.13
	R^2	0.9970
Temkin	b_T	0.65
	KT (L/mol)	43.09
	R^2	0.9251
Dubinin-Radushkevich	q_{max} (μmol/g)	2.43
	β (1/mol^2.J^2)	0.023
	E (J/mol)	4.66
	R^2	0.8820

It was determined that CRP adsorption applied to Freundlich, Langmuir, Temkin and Dubinin-Radushkevich (D-R) isotherm models is more compatible with Freundlich isotherm than these four isotherm models. Freundlich model for adsorption on heterogeneous surfaces is implemented. The correlation coefficient calculated from the drawn Freundlich isotherm was found to be R^2=0.997. One parameter that determines the adsorption process is the favorite, i.e. the n-value, which results from Freundlich's isotherm equation. The n value calculated as 2.13 for CRP is in the range of 1<n<10.

According to the Langmuir equilibrium isotherm, the maximum adsorption coefficient (qmax) of the monolayer was determined to be 3.63 μmol/g. The average E value of adsorption energy calculated from the Dubinin-Radushkevich adsorption isotherm gives an indication of the reaction mechanism operative in adsorption. If E<8 kJ/mol, physical forces are at work in adsorption. Since the calculated E values for CRP are 4.66 kJ/mol, the adsorption of CRP can be defined as physical adsorption.

4.2.4. Temperature effect and thermodynamic studies

Temperature has an important effect on adsorption, depending on the motion of the particles and whether the adsorption mechanism is endothermic or exothermic. When adsorption is exothermic, adsorption capacity increases as ambient temperature decreases. On the other hand, if the adsorption is endothermic, the adsorption capacity increases with increasing temperature.

The change graph of removal degree (%) and qe (μmol/g) of CRP adsorption from solution onto CRP-MIP at varying temperatures (20-50°C) is given in Figure 4.7.

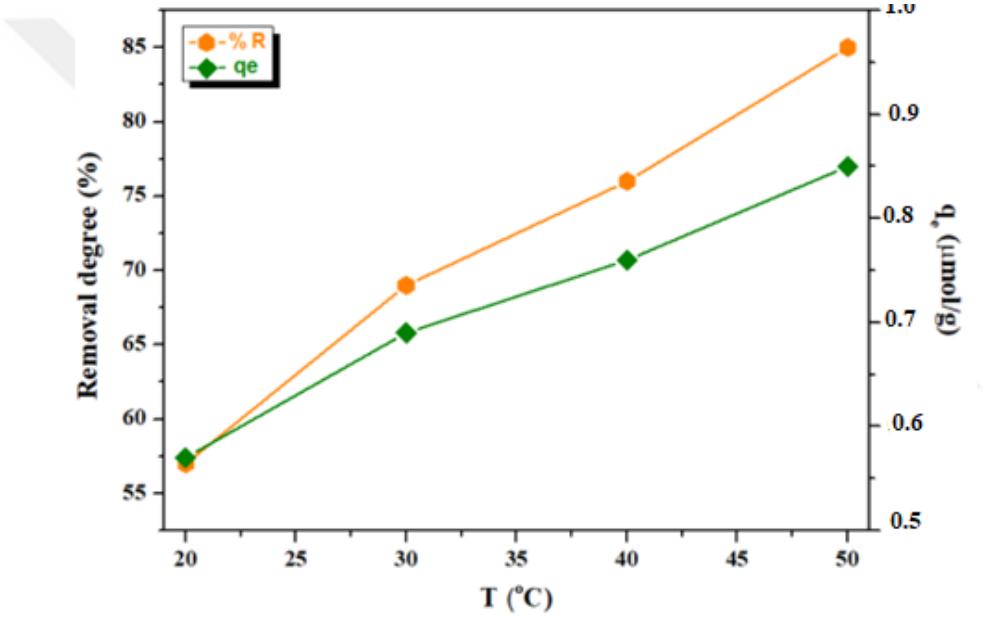

Figure 4.7. Effects of temperature on CRP adsorption (t: 45 min, pH: 4, adsorbent 10 mg, V: 10 mL, CRP conc.: 0.5 mM, 500 rpm).

The impacts of temperature on CRP adsorption is correlational effect with both the parameters shown in the Figure 4.7 since as the percentage of removal degree and qe are increasing continuously with raising temperature over the entire observations of the temperature which is ranging from 20°C to 50°C, as can be seen from the illustrations when the initial temperature is set on 20°C, the value of qe and removal degree is minimum and their figures are increasing with the increased temperature. The optimum values are obtained when the temperature is 50°C. The maximum percentage of removal degree is reached to around 85% when the temperature is 50°C.

The graph of change of $\ln K_d$ against (1/T), drawn with the help of Figure 4.7 and using the mathematical equations for the thermodynamic expressions given in Section 1.11, is given in Figure 4.8. Adsorption enthalpy (ΔH^o) is calculated from the slope of this graph and adsorption entropy (ΔS^o) values are calculated from its shift. Adsorption free energy (ΔG^o) value is calculated with the help of adsorption enthalpy (ΔH^o) and adsorption entropy (ΔS^o) values. These calculated parameters of adsorption thermodynamics are shown in Table 4.3.

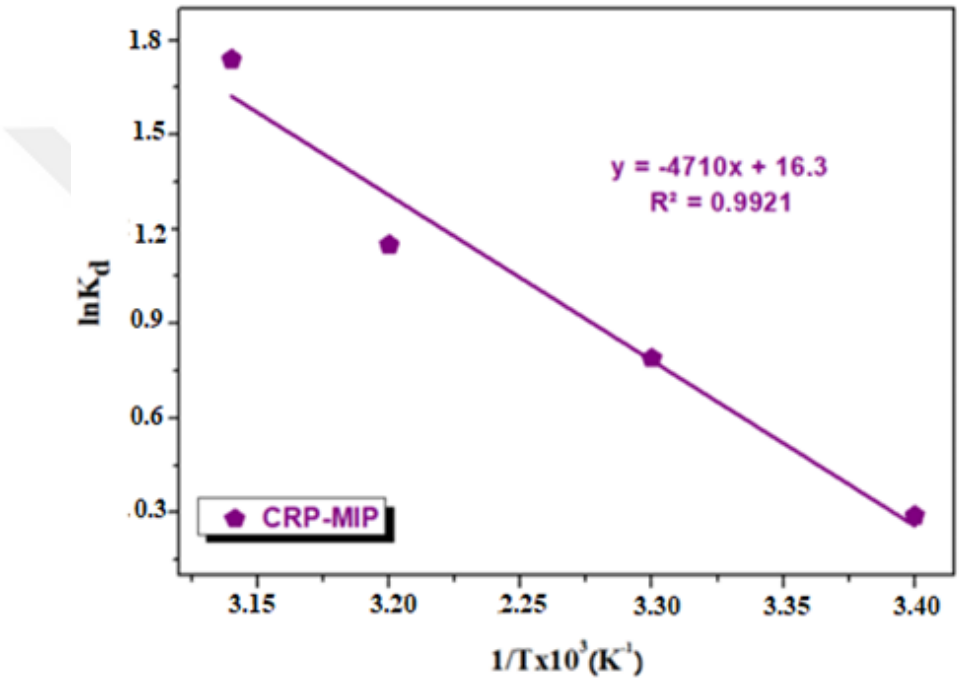

Figure 4.8. The Van't Hoff plots for the CRP adsorption on CRP-MIP.

Table 3.1.3. Thermodynamics parameters of CRP adsorption on CRP-MIP

	Temperature (K)	ΔH° (kJ/mol)	ΔS° (J/mol K)	TΔS° (kJ/mol)	ΔG° (kJ/mol)
CRP-MIP	293	39.16	135.5	39.7	-0.71
	303			41.06	-1.99
	313			42.41	-2.99
	323			43.77	-4.67

Looking at the value of adsorption enthalpy given in Table 4.3, the positive value of ΔH° for CRP adsorption shows that the adsorption processes are endothermic. A ΔH°

value less than 40 kJ/mol indicates that adsorption is a physical process. Since the values of adsorption enthalpy in this study were calculated to be less than 40 kJ/mol, it can be said that the adsorption is a physical adsorption, and this result is consistent with the result of isothermal models.

The values of Gibbs free energy of adsorption were calculated as -2.59 kJ/mol. The fact that the ΔG° values reach more negative values with increasing temperature implies that the tendency of adsorption processes to run spontaneously increases at high temperatures In spontaneous events, entropy (ΔS°) increases with increasing disorder.

4.3. Adsorption of C-Reactive Protein by CRP-NIP

Adsorption studies were performed to remove CRP from aqueous solutions by using CRP-NIP as adsorbent. Optimal conditions were determined by examining the effects of contact time, pH, temperature, and initial concentration that effect adsorption in studies conducted by the batch method.

4.3.1. Contact time effect and kinetic studies

Contact time, one of the parameters effecting adsorption, was studied for CRP by using CRP-NIP adsorbent. The graphs of a removal degree (%) and qe (μmol/g) versus varying time of studies performed at 25ºC and pH 5.0 at different contact times for 1 mM CRP solutions are given in Figure 4.9.

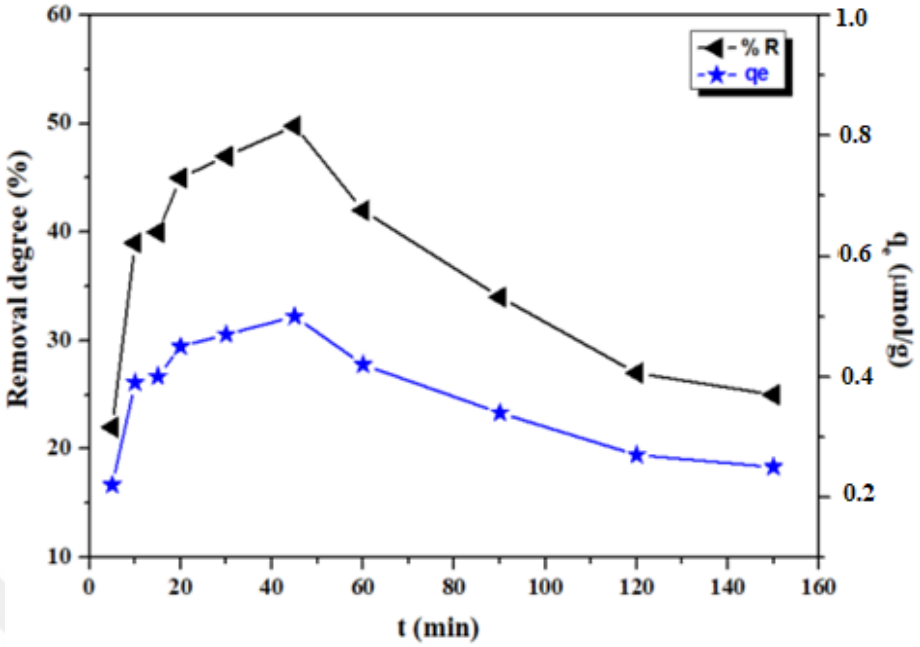

Figure 4.9. Effects of contact time on CRP adsorption (CRP conc.: 1 mM, T: 25°C, V: 10 mL, pH: 5, adsorbent 10 mg, 500 rpm).

According to Figure 4.9, in adsorption studies using CRP-NIP adsorbent, the adsorption efficiency that increased over time reached its maximum value at the 45th minute. The adsorption efficiency at this optimum time was determined as 49.8%, qe 0.5 μmol/g. As the time continues, the adsorption efficiency decreases. For this reason, the optimum contact time was determined as 45 minutes and was also used in other parameter studies.

For the kinetic evaluations of CRP adsorption on CRP-NIP, the first-order kinetic pseudo-model, second-order kinetic pseudo-model, intraparticle diffusion model, and Elovich kinetic model whose mathematical equations are given in Section 1.10, are shown in Figure 4.9 for the effect of contact time on adsorption. The suitability was tested. The graphs of the kinetic models drawn with the data obtained from the equations are shown in Figure 4.10, and the parameter values of the kinetic models are listed in Table 4.4.

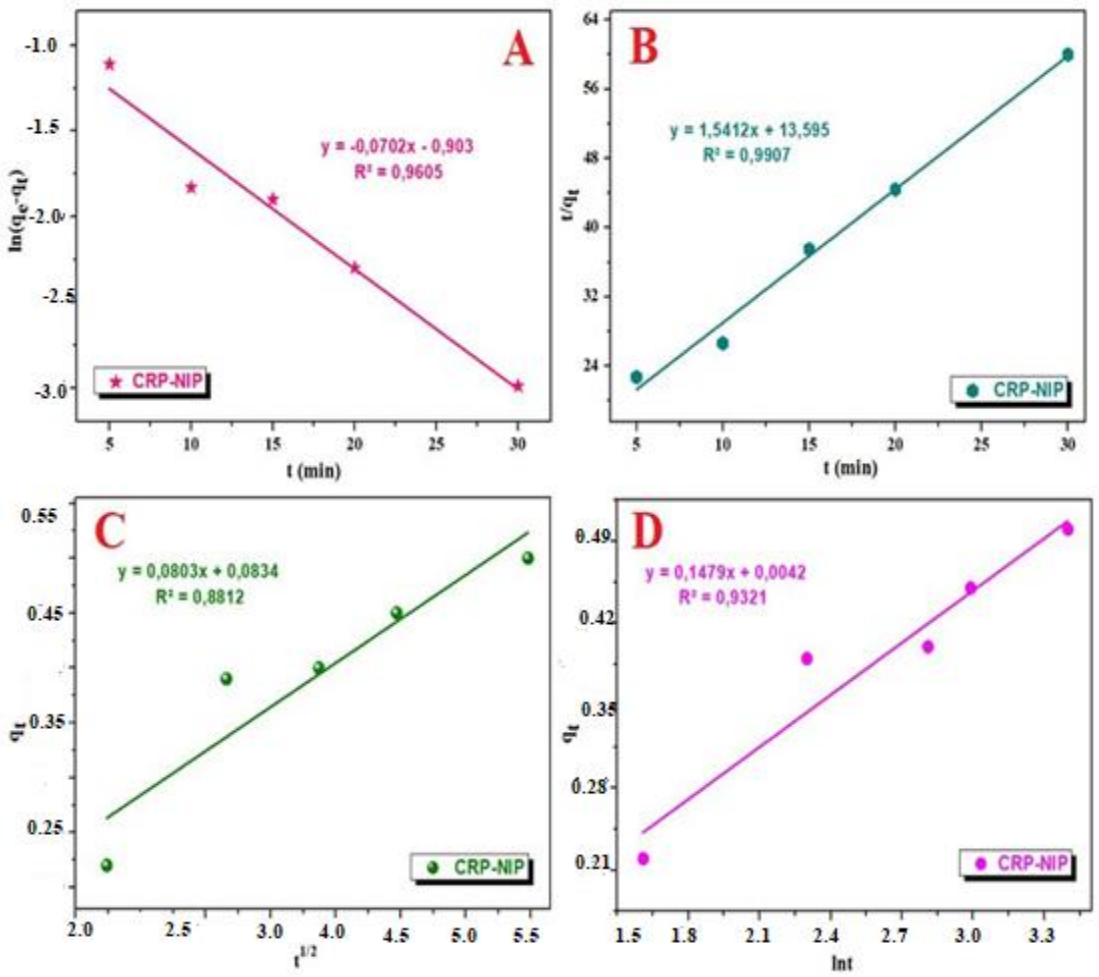

Figure 4.10. Kinetic studies for CRP adsorption on CRP-NIP; (a) pseudo-first order, (b) pseudo-second order, (c) Intraparticle-diffusion, (d) Elovich kinetic models.

Table 4.3.1. Kinetic parameters of CRP adsorption on CRP-NIP

Models	Parameters	CRP-NIP
Pseudo-first order	q_e (μmol/g)	0.4
	k_1 (1/min)	0.07
	R^2	0.9605
	q_{exp} (μmol/g)	0.55
Pseudo-second order	q_e (μmol/g)	0.65
	k_2 (g/μmol.min)	0.17
	R^2	0.9907
	q_{exp} (μmol/g)	0.55
Elovich	α (μmol/g.min)	0.15
	β (g/μmol)	6.76
	R^2	0.9321
Weber-Morris intra-particle diffusion	k (μmol/g.$min^{1/2}$)	0.08
	I (μmol/g)	0.083
	R^2	0.8812

After analyzing Table 4.4, it is found that the most appropriate adsorption kinetic model for CRP adsorption on CRP-NIP is the second-order pseudo-rate equation. From the table, the correlation coefficient R^2 of the second-order rate equation is very close to 1 (0.9907) and the q_e value calculated from the equation (0.65) shows a result near to the experimental q_e (0.55).

Although the pseudo-first-order rate equation has a correlation coefficient closer to 1 for CRP than the Elovich kinetic and intraparticle diffusion model, it is less compatible with adsorption mechanisms since the q_e value is farther from the q_{exp} value. The overall adsorption reaction rate is controlled by the slowest step.

In the intraparticle diffusion graphs given in Figure 4.10c, the adsorption rates of CRP ions are controlled not only by intraparticle diffusion but also by boundary layer (film) diffusion, due to the graph line that does not pass through the origin.

According to López et al. (2020), the results of $q_{e,exp}$ and $q_{e,cal}$ differ significantly in the first-order model, but are nearly identical in the second-order case. Furthermore, the R^2 values show a much better fit with the second order model. As a result, the pseudo-second-

order mechanism was prominent; however, chemisorption may be the rate-limiting step in controlling binding. The pseudo-second order model assumes that chemisorption is the ratelimiting step. When the outcomes of the diffusion model and the chemical model are compared, it is clear that the chemical model is particularly fit to the data of their complicated system. Despite the fact that R^2 is high in both cases, the pseudo-second order model produces better results in the kinetic analysis. The results of the current work compatible with the results obtained by (López et al., 2020).

4.3.2. pH effect

To define the effect of initial pH onto CRP adsorption on NIP; CRP solutions at a concentration of 1 mM at 25ºC were shaken in the pH range of 4-10. The graph of (removal degree (%) and qe (µmol/g) for the adsorbed CRP amounts is given in Figure 4.11.

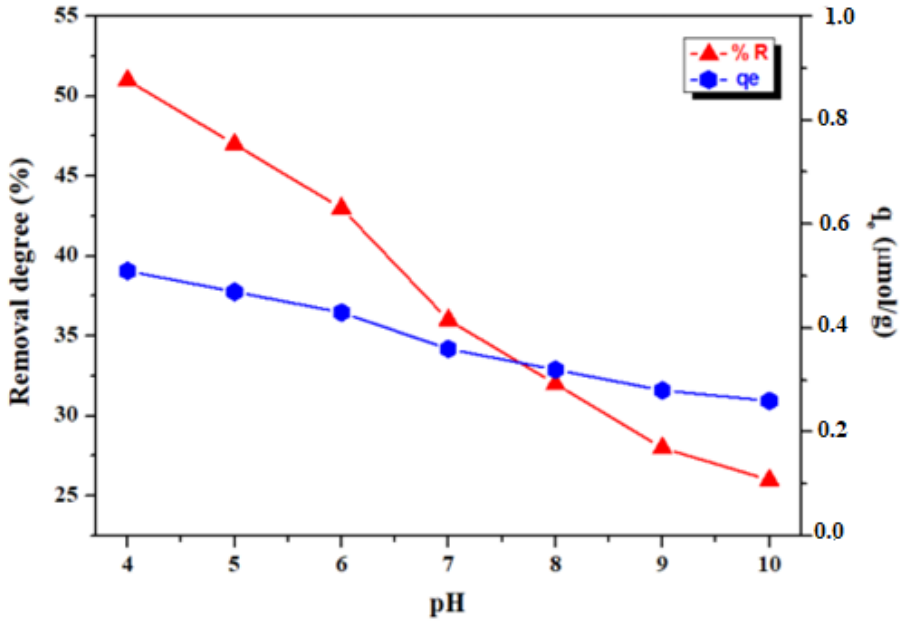

Figure 4.11. Effects of pH on CRP adsorption (t: 45 min, adsorbent 10 mg, T: 25°C, CRP cons.: 1 mM, V: 10 mL, 500 rpm).

Examining Figure 4.11, it was found that the maximum removal efficiency of 51% was achieved at pH 4. Moreover, the optimum amount of qe (0.51 µmol/g) was obtained

in acidic medium. As the pH of the medium increases, the value for the degree of removal (%) decreases. In general, more CRP was adsorbed at lower pH of the adsorption solution

4.3.3. Initial concentration effect and isotherm studies

To determine the effect of initial concentration on CRP adsorption on NIP; CRP solutions of different concentrations (range 0.25-5 mM) were shaken for 45 minutes. The graph of (%) removal degree and qe (μmol/g) values against varying concentrations for adsorbed CRP amounts is shown in Figure 4.12.

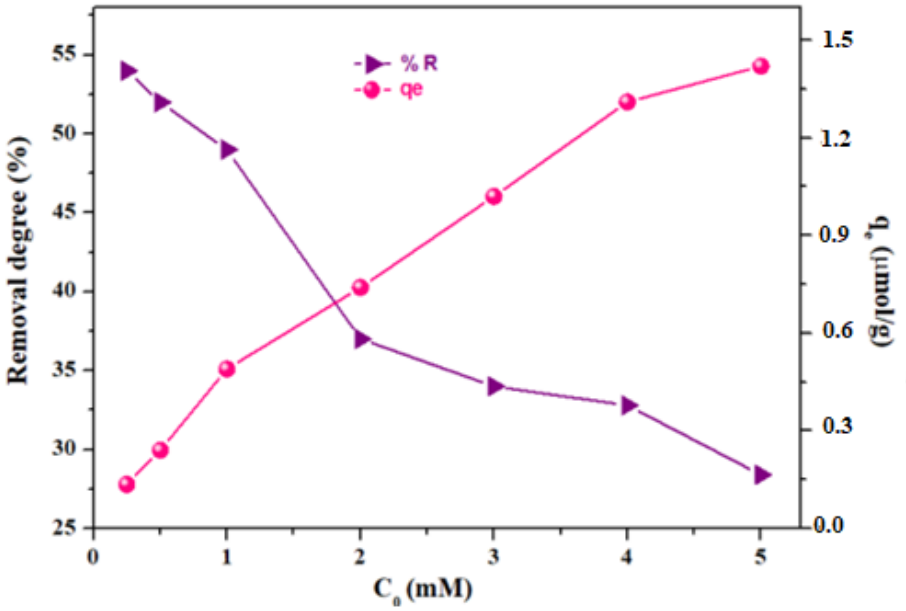

Figure 4.12. Effects of initial concentration on CRP adsorption (t: 45 min, V: 10 mL, pH:4, adsorbent 10 mg, 500 rpm, T: 25°C).

As Figure 4.12 shows, there is a disproportionate relationship between the degree of adsorption and the initial concentration since the degree of removal is high when the concentration is low. In general, the maximum degree of removal (54.6%) occurs when the initial concentration is 0.25 mM, which drops dramatically to 28% at the high concentration of 5 mM. Also, the crossover occurs when the initial concentration is 1.5 mM, where the removal degree value is about 40%, indicating that the adsorption is less efficient at low initial concentrations than at higher removal degrees.

The graphs of four different models used by CRP-NIP to determine the conformity of CRP adsorption to isotherm models are shown in Figure 4.13. The isotherm parameters obtained from the graphics are given in Table 4.5.

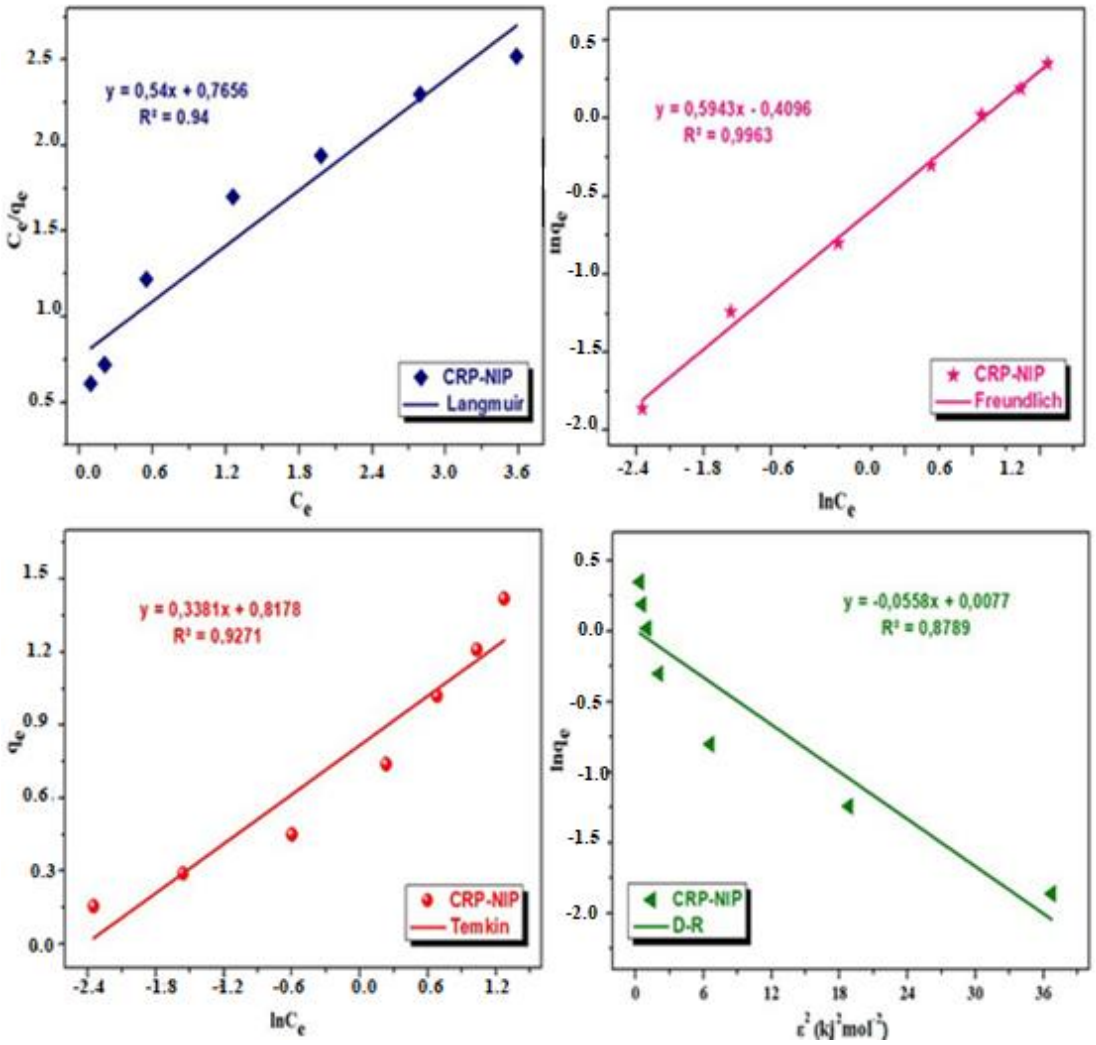

Figure 4.13. Isotherm plots for CRP adsorption on CRP-NIP.

Table 4.3.2. Isotherm parameters of CRP adsorption onto CRP-NIP

Models	Parameters	CRP-NIP
Langmuir	q_{max} (μmol/g)	1.85
	b (L/mmol)	0.71
	R_L	0.85
	R^2	0.94
Freundlich	K_f [(μmol/g)(L/mmol)$^{1/n}$)]	0.66
	n	1.68
	R^2	0.9963
Temkin	b_T	0.34
	K_T (L/mol)	11.08
	R^2	0.9271
Dubinin-Radushkevich	q_{max} (μmol/g)	1.01
	β (1/mol^2.J^2)	0.06
	E (J/mol)	2.89
	R^2	0.8789

Evaluation of the correlation coefficients calculated in Table 4.5 shows that CRP adsorption on CRP-NIP can be explained by Freundlich's isothermal model, whose correlation coefficient is closer to 1 (R^2=0.9963) and is more consistent with this model.

The value for q_{max} determined with the Langmuir model was 1.85 μmol/g for CRP-NIP. The RL values were also calculated to be 0.85, and since these values were within a range of $0<R_L<1$, CRP-NIP adsorption with the adsorbent can be realized and are suitable adsorptions.

Since the E value is calculated from the Dubinin-Radushkevich adsorption isotherm equation for the adsorption of CRP (2.89) E<8 kJ/mol, it was concluded that the adsorption of CRP on NIP is physical adsorption. Additionally, the Temkin model on the other hand can be concluded as another compatible method to apply for the CRP adsorption on NIP as it has a high percentage of R^2 as compared to the Dubinin-Radushkevich model. In contrast to the Freundlich, Langmuir, and Temkin models the

Dubinin-Radushkevich approach has a negative slope on the regression lines in which the value of lnq_e is continuously declining.

According to a study performed on isotherm parameters and conducted by (Lin, et al., 2020), it was calculated the parameters of Langmuir and Frendlich for PR-Cell-NIP and they determined the qe value as 53.48 μmol/g. As compared to our results obtained in this research the results of (Lin et al., 2020) on PR-Cell-NIP obtained by Langmuir was much higher than our results and the variatio of the results was very high because our results were 1.85 μmol/g. On the other hand, the obtained value of b-parameter in (L/mg) was 0.0047 which was much smaller than the results of this study in wich the b-value was 0.71 L/mg. Moreover, the R^2-value obtained by Languir isotherm models was 99% as compared to the obtained figure of this study (R^2=94%). In contrast to the Languir isotherm models, the results obtained by the Frenduich isotherm model was very steady as it had a very high (R^2=99.86%) which resembles the findings of the current study (R^2=99.63%) and support the suitability of the model is very reliable to the experimental research conducted on CRP-NIP. Overall, despite of having small variations in the obtained results of the whole parameters by both the Langmuir and Frenduich models, ther are also more similarities existent in particular the R^2-value by Frenduich model was very high and it was also close to the results obtained by (Lin et al., 2020). Consequently, the high R^2 values evidenced that the PR-Cell-NIP adsorption data followed both the Langmuir and Freundlich models. The Freundlich model, on the other hand, better describes the adsorption of PR-Cell-NIP than the Langmuir model.

4.3.4. Temperature effect and thermodynamic studies

To determine the effects of temperature on CRP adsorption, it was studied in a water bath in a multi-stirrer heater at temperatures ranging from 20-50ºC. The change graph of removal degree (%) and qe (μmol/g) against the changing temperature because of the adsorption processes is given in Figure 4.14.

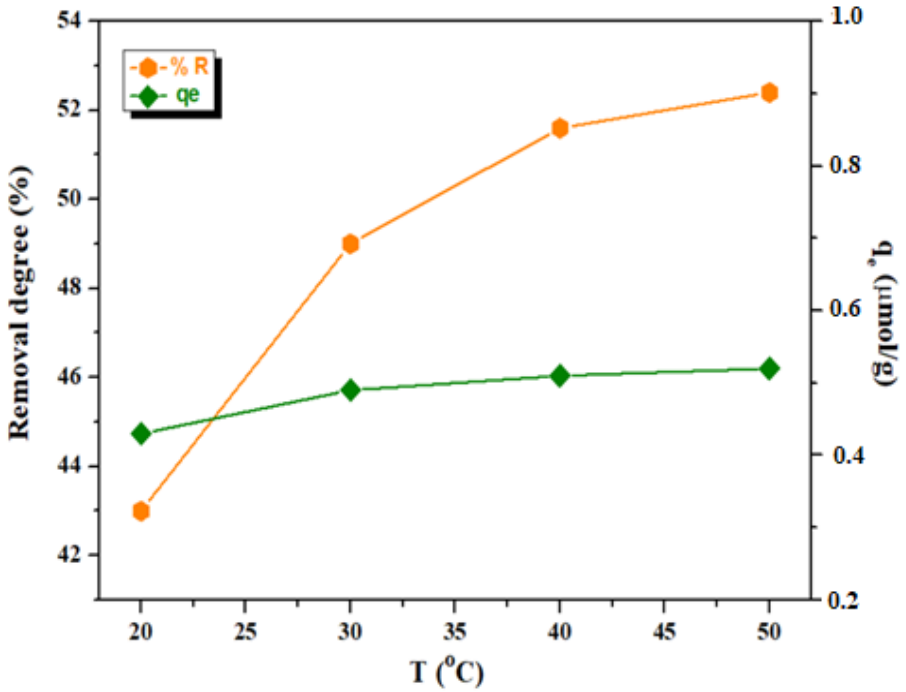

Figure 4.14. Effects of temperature on CRP adsorption (t: 45 min, pH:4, adsorbent 10 mg, V: 10 mL, CRP conc.: 0.25 mM, 500 rpm).

The percent removal degree and q_e shown in Figure 4.14 increase continuously with increasing temperature throughout all temperature observations ranging from 20°C to 50°C. As can be seen from the figures, when the initial temperature is set to 20°C, the qe value and the degree of removal are minimum, and their values increase with increasing temperature. Optimum values are obtained when the temperature is 50°C. The maximum removal degree percentage reaches 52.3% when the temperature is 50°C.

The effect of temperature on the adsorption of CRP on CRP-NIP was studied and the results were reported (Figure 4.14). With these results, the graph of change of $\ln K_d$ against (1/T) drawn using the equations regarding thermodynamic expressions in Section 1.11 is given in Figure 4.15, and the parameters of adsorption thermodynamics are shownn in Table 4.6.

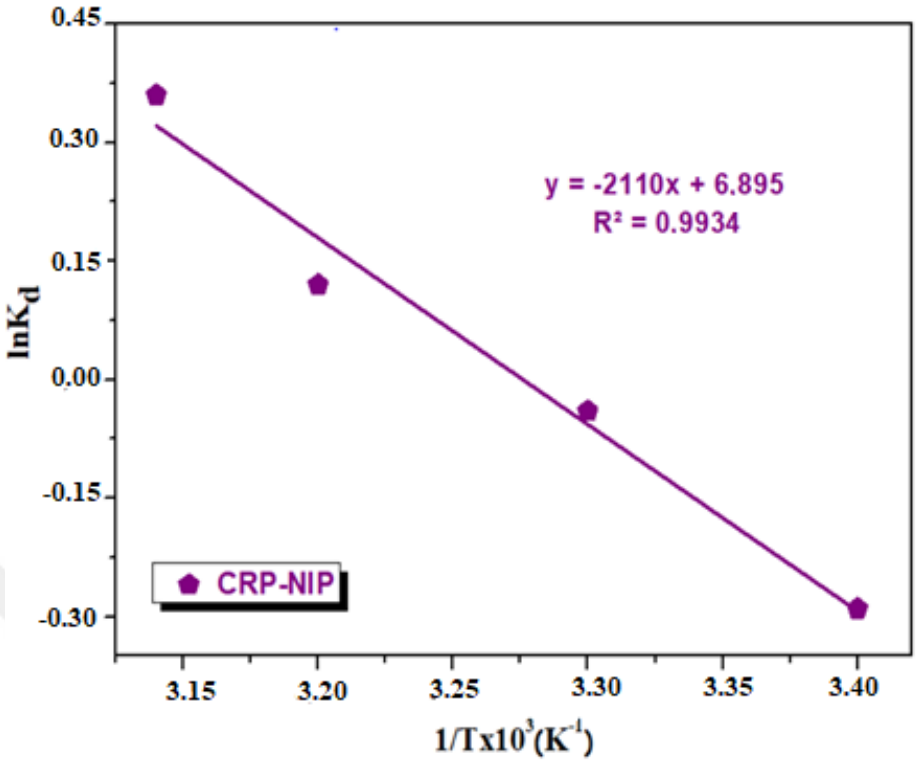

Figure 4.15. The Van't Hoff plots for the CRP adsorption on CRP-MIP.

Table 4.3.3. Thermodynamics parameters of CRP adsorption on CRP-MIP

	Temperature(K)	ΔH° (kJ/mol)	ΔS° (J/mol K)	TΔS° (kJ/mol)	ΔG° (kJ/mol)
CRP-NIP	293	17.54	57.33	16.8	0.71
	303			17.37	0.1
	313			17.94	-0.31
	323			18.52	-0.97

According to the data obtained from Table 4.6, the fact that the adsorption enthalpies (ΔH°) for CRP-NIP have positive values indicates that the adsorption mechanisms are endothermic, and the adsorption increases with increasing temperature. Adsorption enthalpy values less than 40 kJ/mol (17.54) show that adsorption events can be explained by physical adsorption. The physical adsorption phenomenon determined in equilibrium adsorption isotherms agrees with the result obtained from the adsorption enthalpy values.

Negative values of Gibbs free energy (ΔG°) indicate that CRP-NIP adsorption occurs freely. The fact that ΔG° values reach more negative values with increasing temperature means that the tendency of adsorption processes to run themselves increases at high temperatures. Adsorption entropy (ΔS°), another measure of self-adsorption, was found to be positive for CRP-NIP adsorption, confirming that the adsorptions occur voluntarily. The fact that the adsorption entropy has a positive value indicates that the randomness occurring at the interface increases and the affinity of CRP-NIP to adsorbents increases.

4.4. Selectivity Studies

To determine the selectivity of the adsorbent CRP-MIP toward the CRP molecule, 1-antitrypsin and 1-acid glycoprotein molecules (Figure 4.16), which are positive acute-phase reactants like CRP and are present in plasma, were selected as competing compounds. The solutions of CRP, α1-antitrypsin and α1-acid glycoprotein were treated at an initial concentration of 1 mM with the adsorbents CRP-MIP and CRP-NIP under previously determined optimal conditions (45 min, pH: 4.0, 25C and 500 rpm). The amount of α1-antitrypsin and α1-acid glycoprotein remaining in the solution due to the adsorption process was investigated by measuring with a UV spectrophotometer at 230 and 250 nm, respectively. The results obtained are shown in Figure 4.16. As a result of this study, it was found that CRP-MIP is highly selective compared to competing compounds.

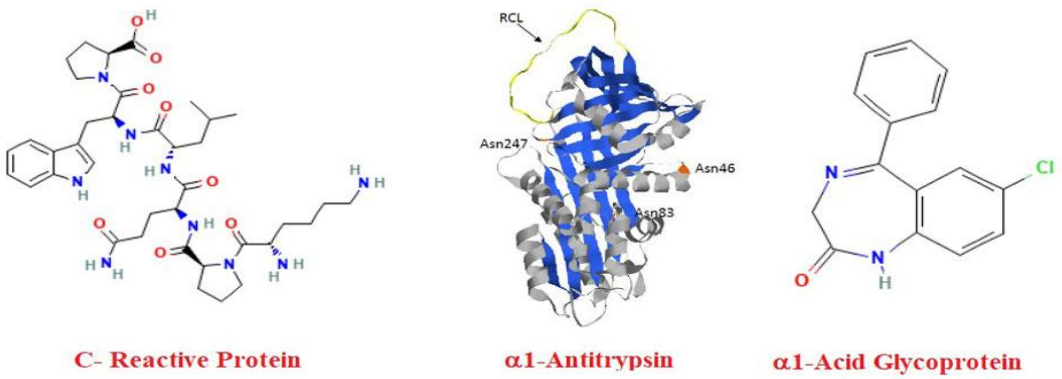

Figure 4.16. Formula structures of the compounds used.

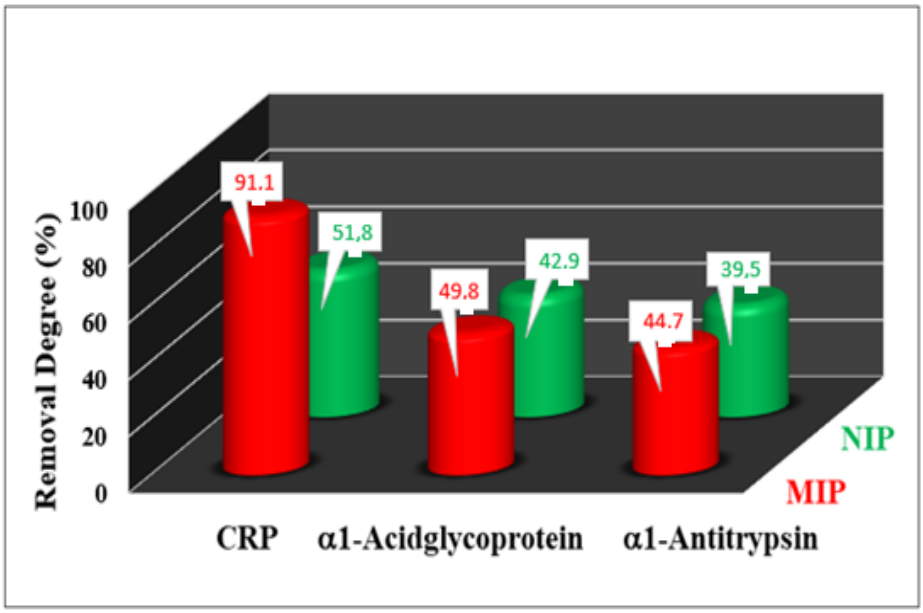

Figure 4.17. Adsorption yield of MIP and NIP for CRP, α1-asiglikoprotein and α1-antitripsin compounds (contact time: 45 min, adsorbent: 10 mg, temperature: 25 °C, C_0=1 mM, pH; 4.0).

4.5. Rebinding of CRP to Imprinted Polymer in Human Serum

The study on selective reabsorption of CRP from human serum was performed with 1:10; 1:20 diluted human serum with concentrations of 0.5 mM and 0.25 mM CRP, respectively. As a result of the adsorption process, 0.74 μmol/g and 0.22 μmol/g CRP were rebound to CRP-MIP using the UV spectrophotometer, corresponding to 37% and 91% recoveries, respectively. The successful rebinding of CRP to CRP-MIP from crude human serum with a high recovery rate of 91% demonstrated the highly selective properties of the synthesized imprinted molecule for CRP.

5. DISCUSSION AND CONCLUSION

C-reactive protein has both proinflammatory and anti-inflammatory effects. It is not only a marker of inflammation or infection, but also has a diversity of biological functions and properties. CRP is often used clinically to detect disease and monitor response to treatment. Therefore, it is important to measure CRP levels easily, sensitively, and reliably.

Molecularly imprinted polymers are next-generation smart materials with selective recognition sites for the desired molecule or ion in a three-dimensional crosslinked polymer structure. These materials are made by polymerizing functional and crosslinking monomers around the desired template molecule. In this work, a molecularly imprinted polymer (CRP-MIP) was synthesized for the selective adsorption of C-reactive protein, an important biomarker, from human serum. SEM for the characterization studies of the polymer structure with CRP recognition sites, FT-IR and TGA/DSC analyzes were performed.

The rebinding capacity of CRP to the imprinted polymer (CRP-MIP) synthesized from aqueous solutions was calculated to be 3.63 mg per dry gram of CRP-MIP polymer. In addition, the selectivity of the imprinted polymer was studied in the presence of competing substances with similar molecular structure (1-antitrypsin and 1acid glycoprotein). In the study, it was found that the selectivity of the imprinted polymer in the recognition of CRP was higher than that of the competing substances. Moreover, the successful re-binding of CRP from diluted human serum to CRP-MIP at a high rate of 91% showed that the synthesized imprinted polymer was highly selective for CRP.

Adsorption of CRP from solutions to imprinted polymers (CRP-MIP) was also investigated by a batch polymerization process. Application of the adsorption process to isothermal and kinetic models and determination of thermodynamic expressions were performed, and the results were compared with the unimprinted reference polymer (CRP-NIP).

By applying the adsorption data obtained with different contact times to the adsorption kinetics, the suitability of the first-order pseudo-kinetic equation, the second-order pseudo-kinetic equation, the intraparticle diffusion model, and Elovich's kinetic

model for CRP adsorption was investigated. In adsorption studies using both CRP-MIP and CRP-NIP, the adsorption mechanism was determined to be consistent with the pseudo-second-order kinetic equation, as it has a higher correlation coefficient and the examined q_e value gives results closer to the experimental q_{exp} value. The fact that the kinetics is second order proves that the step that determines the rate is realized by a chemical process such as complexation or ion exchange and that adsorption depends on concentration.

The suitability of adsorption data obtained with different CRP concentrations at constant temperature for Langmuir, Temkin, Dubinin-Radushkevich and Freundlich isotherms was investigated. Examining the isotherm graphs and isotherm parameters of adsorption of CRP on the adsorbents CRP-MIP and CRP-NIP, it was found that the adsorption process was more consistent with the Freundlich isotherm due to its high correlation coefficient. The fact that the RL distribution constant value calculated to determine the adsorption feasibility is in the range of $0<RL<1$ in both adsorbents proves the availability. In addition, since the mean adsorption energy (E) values determined from the Dubinin-Radushkevich isotherm were found to be $E<8$ kJ/mol for the two adsorbent materials used, it was determined that the CRP adsorption type was physical adsorption. By investigating the adsorption thermodynamics because of the adsorption of CRP on CRP-MIP and CRP-NIP at varying temperatures; Standard adsorption entropy change ($\Delta S°$), enthalpy ($\Delta H°$), and free energy change ($\Delta G°$) values were determined with the help of the data obtained from the (1/T) versus $\ln K_d$ graph. In studies with these two adsorbents, the increase in the adsorption percentage as the temperature rises and the positive $\Delta H°$ value ($\Delta H°>0$) indicates that the adsorption mechanisms are endothermic. Moreover, the fact that $\Delta G°$ reaches larger negative values with increasing temperature for each adsorbent used indicates that the adsorption processes occur spontaneously, i.e., voluntarily, at high temperatures. In such events that occur spontaneously, the entropy increases with increasing disorder.

In view of all these studies, it seems that the synthesized adsorbent CRP-MIP can be used as an alternative method for the diagnosis of CRP from blood and has the potential to be used commercially due to its selectivity.

REFERENCES

Abdel Ghani, N.T., Mohamed El Nashar, R., Abdel-Haleem, F.M. and Madbouly, A., 2016. Computational design, synthesis, and application of a new selective molecularly imprinted polymer for electrochemical detection. ***Electroanalysis*, 28** (7): 1530-1538.

Alexander, C., Andersson, H.S., Andersson, L.I., Ansell, R.J., Kirsch, N., Nicholls, I.A., O'Mahony, J. and Whitcombe, M.J., 2006. Molecular imprinting science and technology: a survey of the literature for the years up to and including 2003. ***Journal of Molecular Recognition: An Interdisciplinary Journal*, 19** (2): 106-180.

Amık, O., 2014. *AC/PAN Kompozit Adsorban Kullanılarak Uranyum Adsorpsiyonunun İncelenmesi.* (yüksek lisans tezi, basılmamış). EÜ, Fen Bilimleri Enstitüsü, Bornova, İzmir.

Anfossi, L., Cavalera, S., Di Nardo, F., Spano, G., Giovannoli, C. and Baggiani, C., 2020. Delayed Addition of Template Molecules Enhances the Binding Properties of Diclofenac-Imprinted Polymers. ***Polymers*, 12** (5): 1178.

Arshad, R., Rhouati, A., Hayat, A., Nawaz, M.H., Yameen, M.A., Mujahid, A. and Latif, U., 2020. MIP-based impedimetric sensor for detecting dengue fever biomarker. ***Applied Biochemistry and Biotechnology*, 191** (4): 1384-1394.

Asiabi H, Yamini Y, Seidi S, Ghahramanifard F., 2016. Preparation and evaluation of a novel molecularly imprinted polymer coating for selective extraction of indomethacin from biological samples by electrochemically controlled in-tube solid phase microextraction. ***Anal Chim Acta*, 913**: 76–85.

Baggiani, C., Giraudi, G., Giovannoli, C., Tozzi, C. and Anfossi, L., 2004. Adsorption isotherms of a molecular imprinted polymer prepared in the presence of a polymerisable template: Indirect evidence of the formation of template clusters in the binding site. ***Analytica Chimica Acta*, 504** (1): 43-52.

Bakhtiar, S., Bhawani, S.A. and Shafqat, S.R., 2019. Synthesis and characterization of molecular imprinting polymer for the removal of 2-phenylphenol from spiked blood serum and river water. ***Chemical and Biological Technologies in Agriculture*, 6** (1): 1-10.

Baltz, M.L., De Beer, F.C., Feinstein, A., Munn, E.A., Milstein, C.P., Fletcher, T.C., March, J.F., Taylor, J., Bruton, C., Clamp, J.R. and Davies, A.J.S., 1982. Phylogenetic aspects of C-reactive protein and related proteins. ***Annals of the New York Academy of Sciences*, 389** (1): 49-75.

Baraliakos, X., Szumski, A., Koenig, A.S. and Jones, H., 2019, June. The role of C-reactive protein as a predictor of treatment response in patients with ankylosing spondylitis. ***In Seminars in arthritis and rheumatism*, 48** (6): 997-1004.

Bartold, K., Iskierko, Z., Borowicz, P., Noworyta, K., Lin, C.Y., Kalecki, J., Sharma, P.S., Lin, H.Y. and Kutner, W., 2022. Molecularly imprinted polymer-based extended-gate field-effect transistor (EG-FET) chemosensor for selective determination of matrix metalloproteinase-1 (MMP-1) protein. ***Biosensors and Bioelectronics*, 208:** 114203.

Biggs, M.J., Buts, A., Cai, Q. and Seaton, N.A., 2006. Absolute assessment of adsorption-based microporous solid characterisation methods. ***Studies in Surface Science and Catalysis*,** 79-86.

Bizi, M. and El Bachra, F.E., 2020. Evaluation of the ciprofloxacin adsorption capacity of common industrial minerals and application to tap water treatment. ***Powder Technology,* 362,** 323-333.

Braun, J., Brandt, J., Listing, J., Zink, A., Alten, R., Golder, W., Gromnica-Lhle, E., Kellner, H., Krause, A., Schneider, M. and Sörensen, H., 2002. Treatment of active ankylosing spondylitis with infliximab: a randomised controlled multicentre trial. ***The Lancet,* 359** (9313): 1187-1193.

Canbazoğlu, M., 1996. Dünyada Altın ve Gümüş Madenciliğinde Kullanılan Sıvı Atık Arıtma Teknikleri, Türkiye'de Altın Madenciliği. ***Yurt Madenciliği Geliştirme Vakfı***, Ankara. 75-108.

Cengiz, N., Guclu, G., Kelebek, H., Capanoglu, E. and Selli, S., 2022. Application of Molecularly Imprinted Polymers for the Detection of Volatile and Off-Odor ***Compounds in Food Matrices***. ACS omega.

Chen, F., Mao, M., Wang, J., Liu, J. and Li, F., 2020. A dual-step immobilization/imprinting approach to prepare magnetic molecular imprinted polymers for selective removal of human serum albumin. ***Talanta,* 209**: 120509.

Chen, L., Xu, S. and Li, J., 2011. Recent advances in molecular imprinting technology: current status, challenges and highlighted applications. ***Chemical Society Reviews,* 40** (5): 2922-2942.

Chen, Y., Zhu, Y., Wang, Z., Li, Y., Wang, L., Ding, L., Gao, X., Ma, Y. and Guo, Y., 2011. Application studies of activated carbon derived from rice husks produced by chemical-thermal process-A review. ***Advances in Colloid and Interface Science,* 163** (1): 39-52.

Chiu, H.C., Hsiue, T. and Chen, W.Y., 2004. FTIR-ATR measurements of the ionization extent of acrylic acid within copolymerized methacrylated dextran/acrylic acid networks and its relation with pH/salt concentration-induced equilibrium swelling***. Polymer,* 45** (5): 1627-1636.

Chou, P.C., Rick, J. and Chou, T.C., 2005. C-reactive protein thin-film molecularly imprinted polymers formed using a micro-contact approach. ***Analytica Chimica Acta***, **542** (1): 20-25.

Cieplak, M. and Kutner, W., 2016. Artificial biosensors: How can molecular imprinting mimic biorecognition? ***Trends in Biotechnology,* 34** (11): 922-941.

Cormack, P.A. and Elorza, A.Z., 2004. Molecularly imprinted polymers: synthesis and characterisation. ***Journal of Chromatography B,* 804** (1): 173-182.

Costa Lopes, A.S., Carualho, S.M.L., Brasil, D.S.B., Mendes, R.A., Lima, M.O., 2015.

Cozmuta, L.M., Cozmuta, A.M., Peter, A., Nicula, C., Nsimba, E.B. and Tutu, H., 2012. The influence of pH on the adsorption of lead by Na-clinoptilolite: Kinetic and equilibrium studies. ***Water Sa,* 38** (2): 269-278.

Cui, F., Zhou, Z. and Zhou, H.S., 2020. Molecularly imprinted polymers and surface imprinted polymers based electrochemical biosensor for infectious diseases. ***Sensors,* 20** (4): 996.

Cui, M., Che, Z., Gong, Y., Li, T., Hu, W. and Wang, S., 2022. A graphdiyne-based protein molecularly imprinted biosensor for highly sensitive human C-reactive protein detection in human serum. ***Chemical Engineering Journal,* 431**: 133455.

Cui, M., Gong, Y., Du, M., Wang, K., Li, T., Zhu, X., Wang, S. and Luo, X., 2021. An antifouling electrochemical biosensor based on a protein imprinted hydrogel for human immunoglobulin G recognition in complex biological media***. Sensors and Actuators B: Chemical,* 337**: 129820.

Cunliffe, D., Kirby, A. and Alexander, C., 2005. Molecularly imprinted drug delivery systems. ***Advanced drug Delivery Reviews,*** **57** (12): 1836-1853.

Dilci, Y., 2011. ***Amidoksim Destekli Poliester Liflere Metal Adsorpsiyonu*** (yüksek lisans tezi, basılmamış). BÜ, Fen Bilimleri Enstitüsü, Yozgat.

Do, D.D., 1998. ***Adsorption Analysis****:* Equilibrium and Kinetics, Series on Chemistry Engineering. Imperial College Press, Singapore. 145.

Doi, A., Ejtemaei, M. and Nguyen, A.V., 2019. Effects of ion specificity on the surface electrical properties of kaolinite and montmorillonite. ***Minerals Engineering,*** **143:** 105929.

Dong, W., Yan, M., Liu, Z., Wu, G. and Li, Y., 2007. Effects of solvents on the adsorption selectivity of molecularly imprinted polymers: Molecular simulation and experimental validation. ***Separation and purification technology,*** **53** (2): 183-188.

Esfandyari-Manesh, M., Javanbakht, M., Shahmoradi, E., Dinarvand, R. and Atyabi, F., 2013. The control of morphological and size properties of carbamazepine-imprinted microspheres and nanospheres under different synthesis conditions. ***Journal of Materials Research,*** **28** (19): 2677-2686.

Florea, A., Hosu, O., Ciui, B. and Cristea, C., 2016. ***Molecularly imprinted polymer-based sensors for biomedical and environmental applications***. Scrievener Publishing, NJ, USA. 283-325.

Garcia, R., Carreiro, E.P., Lima, J.C., Gomes da Silva, M., Costa Freitas, A.M. and Cabrita, M.J., 2020. Assessment of dimethoate in olive oil samples using a dual responsive molecularly imprinting-based approach. ***Foods,*** **9 (**5): 618.

Ghali, K., Ghaddar, N. and Jones, B., 2002. Empirical evaluation of convective heat and moisture transport coefficients in porous cotton medium. ***Journal of Heat Transfer,*** **124** (3): 530-537.

Goswami, S. and Ghosh, U.C., 2005. Studies on adsorption behaviour of Cr (VI) onto synthetic hydrous stannic oxide. ***Water SA,*** **31**(4): 597-602.

Gürboğa, G., 2004. ***Sezyum ve Stronsiyum Adsorpsiyonu İçin TiO2-SiO2 Jel Küreciklerinin Hazırlanması ve Adsorpsiyon Koşullarının İncelenmesi*** (doktora tezi, basılmamış). EÜ, Nükleer Bilimler Enstitüsü, İzmir.

Hai, J.H. Lee, C., Kapila Y.L., Chaffee, B.W., Armitage, G.C., 2020. Antibiotic prescribing practices in periodontal surgeries with and without bone grafting. ***Journal of Periodontology,*** **91** (4): 508-515.

Han, F., Zhou, D.B., Song, W., Hu, Y.Y., Lv, Y.N., Ding, L., Zheng, P., Jia, X.Y., Zhang, L. and Deng, X.J., 2021. Computational design and synthesis of molecular imprinted polymers for selective solid phase extraction of sulfonylurea herbicides. ***Journal of Chromatography A,*** **1651:** 462321.

Hanauer, S.B. and Sandborn, W., 2001. Management of Crohn's disease in adults. *The* ***American journal of gastroenterology,*** **96** (3): 635.

Hasanah, A.N., Safitri, N., Zulfa, A., Neli, N. and Rahayu, D., 2021. Factors Affecting Preparation of Molecularly Imprinted Polymer and Methods on Finding Template-Monomer Interaction as the Key of Selective Properties of the Materials. ***Molecules,*** **26 (**18): 5612.

Hashim, S.N., Boysen, R.I., Schwarz, L.J., Danylec, B. and Hearn, M.T., 2014. A comparison of covalent and non-covalent imprinting strategies for the synthesis of stigmasterol imprinted polymers. ***Journal of Chromatography A,*** **1359**: 35-43.

Haupt, K., 2003. Peer reviewed: molecularly imprinted polymers: the next generation. ***Analytical Chemistry,*** **75** (17): 376-A.

Holland, N., Frisby, J., Owens, E., Hughes, H., Duggan, P. and McLoughlin, P., 2010. The influence of polymer morphology on the performance of molecularly imprinted polymers. ***Polymer,*** **51** (7): 1578-1584.

Hu, Y., Guo, X., Chen, C. and Wang, J., 2019. Algal sorbent derived from Sargassum horneri for adsorption of cesium and strontium ions: equilibrium, kinetics, and mass transfer. ***Applied microbiology and biotechnology,*** **103** (6): 2833-2843.

Hu, Z., Zhou, X., Duan, J., Wu, X., Wu, J., Zhang, P., Liang, W., Guo, J., Cai, H., Sun, P. and Zhou, H., 2021. Aptamer-based novel Ag-coated magnetic recognition and SERS nanotags with interior nanogap biosensor for ultrasensitive detection of protein biomarker. ***Sensors and Actuators B: Chemical*****, 334:** 129640.

Jain, U., Soni, S., Balhara, Y.P.S., Khanuja, M., Chauhan, N., 2020. Dual-Layered Nanomaterial-Based Molecular Pattering on Polymer Surface Biomimetic Impedimetric Sensing of a Bliss Molecule, Anandamide Neurotransmitter. ***ACS Omega,*** **5:** 10750-10758.

Jones, A.C., O'Callahan, B.T., Yang, H.U. and Raschke, M.B., 2013. The thermal near-field: Coherence, spectroscopy, heat-transfer, and optical forces. ***Progress in Surface Science,*** **88** (4): 349-392.

Krstić, V., 2021. Role of zeolite adsorbent in water treatment. In Handbook of Nanomaterials for ***Wastewater Treatment,*** 417-481.

Kumar, D. and Prasad, B.B., 2012. Multiwalled carbon nanotubes embedded molecularly imprinted polymer-modified screen-printed carbon electrode for the quantitative analysis of C-reactive protein. ***Sensors and Actuators B: Chemical*****, 171**: 1141-1150.

Kundu, T., Mitra, S., Patra, P., Goswami, A., Díaz Díaz, D. and Banerjee, R., 2014. Mechanical downsizing of a gadolinium (III)-based metal–organic framework for anticancer drug delivery. ***Chemistry–a European journal,*** **20** (33): 10514-10518.

Lee, M.H., Thomas, J.L., Su, Z.L., Yeh, W.K., Monzel, A.S., Bolognin, S., Schwamborn, J.C., Yang, C.H. and Lin, H.Y., 2021. Epitope imprinting of alpha-synuclein for sensing in Parkinson's brain organoid culture medium**. *Biosensors and Bioelectronics*****, 175**: 112852.

Lin, Y.C., Wang, H.P., Gohar, F., Ullah, M.H., Zhang, X., Xie, D.F., Fang, H., Huang, J. and Yang, J.X., 2017. Preparation and copper ions adsorption properties of thiosemicarbazide chitosan from squid pens. ***International Journal of Biological Macromolecules,*** **95:** 476-483.

Lopez-Moreno, M., Lopez, M.T.I., Miguel, M., Garces-Rimon, M., 2020.Physical and Psychological effect related to food habits and lifestyle changes derived from Covid-19 home confinementin the Spanish population. ***Nutrients,*** **12** (11): 34-45.

Marć, M. and Wieczorek, P.P., 2019. Introduction to MIP synthesis, characteristics and analytical application. ***In Comprehensive Analytical Chemistry***, **86**: 1-15.

Mckay, G., 1996. ***Use of Adsorbents For The Removal of Pollutions From Wastewater***. CRC Press, New York. 186.

Mei, X.Q., He, X.P., Wang, J.T., 2016. Molecularly imprinted polymer as efficient sorbent of solid-phase extraction for determination of gonyautoxin 1,4 in seawater followed by high-performance liquid chromatography-fluorescence detection, ***Analytical Bioanalytical Chemistry,*** **408:** 5737-5743.

Mezenner, N.Y. and Bensmaili, A., 2009. Kinetics and thermodynamic study of phosphate adsorption on iron hydroxide-eggshell waste. ***Chemical Engineering Journal,*** **147** (2-3): 87-96.

Mogol, B.A., 2008. ***Adsorban Reçineler Kullanılarak Şeker Şurubu ve Elma Suyu Renginin İyileştirilmesi*** (yüksek lisans tezi, basılmamış). HÜ, Fen Bilimleri Enstitüsü, Ankara.

Mosbach, K. and Ramström, O., 1996. The emerging technique of molecular imprinting and its future impact on biotechnology**.** ***Bio/technology,*** **14** (2): 163-170.

Mosbach, K., 1994. Molecular imprinting. ***Trends in biochemical sciences,*** **19** (1): 9-14.

Mustafa, Y.L., Keirouz, A. and Leese, H.S., 2022. Molecularly imprinted polymers in diagnostics: accessing analytes in biofluids. ***Journal of Materials Chemistry B.***

Naseri, M., Mohammadniaei, M., Sun, Y. and Ashley, J., 2020. The use of aptamers and molecularly imprinted polymers in biosensors for environmental monitoring: A tale of two receptors. ***Chemosensors,*** **8** (2): 32.

Ndunda, E.N. and Mizaikoff, B., 2016. Molecularly imprinted polymers for the analysis and removal of polychlorinated aromatic compounds in the environment: a review**.** ***Analyst,*** **141** (11): 3141-3156.

Nicholls, I.A., Andersson, H.S., Golker, K., Henschel, H., Karlsson, B.C., Olsson, G.D., Rosengren, A.M., Shoravi, S., Suriyanarayanan, S., Wiklander, J.G. and Wikman, S., 2011. Rational design of biomimetic molecularly imprinted materials: theoretical and computational strategies for guiding nanoscale structured polymer development. ***Analytical and Bioanalytical Chemistry,*** **400** (6): 1771-1786.

Niu, M., Pham-Huy, C. and He, H., 2016. Core-shell nanoparticles coated with molecularly imprinted polymers: a review. ***Microchimica Acta,*** **183** (10): 2677-2695.

Nollet, H., Roels, M., Lutgen, P., Van der Meeren, P. and Verstraete, W., 2003. Removal of PCBs from wastewater using fly ash. ***Chemosphere, 53*** (6): 655-665.

of Benzene and Toluene. ***American Journal of Analytical Chemistry,*** **6:** *528-538.*

Okutucu, B., Önal, S. and Telefoncu, A., 2009. Noncovalently galactose imprinted polymer for the recognition of different saccharides. ***Talanta,*** **78** (3): 1190-1193.

Özgür, E., Topçu, A.A., Yılmaz, E. and Denizli, A., 2020. Surface plasmon resonance based biomimetic sensor for urinary tract infections. ***Talanta,*** **212**:120778.

Pang, M., Liu, B., Kano, N. and Imaizumi, H., 2015. Adsorption of chromium (VI) onto activated carbon modified with $KMnO_4$. ***Journal of Chemistry and Chemical Engineering,*** **9***:* 280-287.

Pengkamta, T., Mala, M., Klakasikit, C., Kanawuttikorn, P., Boonkorn, P., Chuaejedton, A. and Karuehanon, W., 2020. Synthesis and Evaluation of Molecularly Imprinted Polymer as a Selective Material for Vanillin. ***Suan Sunandha Science Technology Journal 7***:1-6.

Pepys, M.B. and Hirschfield, G.M., 2003. C-reactive protein: a critical update. ***The Journal of Clinical Investigation,*** **111** (12): 1805-1812.

Piccin, J.S., Dotto, G.L. and Pinto, L.A.A., 2011. Adsorption isotherms and thermochemical data of FD&C Red n 40 binding by chitosan. ***Brazilian Journal of Chemical Engineering,*** **28**: 295-304.

Prakruthi, K., Ujwal, M.P., Yashas, S.R., Mahesh, B., Kumara Swamy, N. and Shivaraju, H.P., 2022. Recent advances in photocatalytic remediation of emerging organic pollutants using semiconducting metal oxides: an overview. ***Environmental Science and Pollution Research,*** **29** (4): 4930-4957.

Rahman, I.A., Saad, B., Shaidan, S. and Rizal, E.S., 2005. Adsorption characteristics of malachite green on activated carbon derived from rice husks produced by chemical–thermal process. ***Bioresource Technology,*** **96** (14): 1578-1583.

Rosengren, A.M., Karlsson, B.C. and Nicholls, I.A., 2013. Consequences of morphology on molecularly imprinted polymer-ligand recognition. ***International Journal of Molecular Sciences,*** **14** (1): 1207-1217.

Rosengren-Holmberg, J.P., Karlsson, J.G., Svenson, J., Andersson, H.S. and Nicholls, I.A., 2009. Synthesis and ligand recognition of paracetamol selective polymers: semi-covalent versus non-covalent molecular imprinting. ***Organic & Biomolecular Chemistry,*** **7** (15): 3148-3155.

Rushton, G.T., Karns, C.L. and Shimizu, K.D., 2005. A critical examination of the use of the Freundlich isotherm in characterizing molecularly imprinted polymers (MIPs). ***Analytica chimica acta,*** **528** (1): pp.107-113.

Sahoo, T.R. and Prelot, B., 2020. Adsorption processes for the removal of contaminants from wastewater: the perspective role of nanomaterials and nanotechnology**.** ***In Nanomaterials for the Detection and Removal of Wastewater Pollutants***, 161-222.

Sánchez-González, J., Peña-Gallego, Á., Sanmartín, J., Bermejo, A.M., Bermejo-Barrera, P. and Moreda-Piñeiro, A., 2019. NMR spectroscopy for assessing cocaine-functional monomer interactions when preparing molecularly imprinted polymers**.** ***Microchemical Journal,*** **147**: 813-817.

Saylan, Y., Yilmaz, F., Özgür, E., Derazshamshir, A., Yavuz, H. and Denizli, A., 2017. Molecular imprinting of macromolecules for sensor applications. ***Sensors,*** **17** (4): 898.

Seader, J.D., Herley, E.J., 1998. ***Separation Process Principles***. John Wiley and Sons, New York, ABD.

Selvolini, G. and Marrazza, G., 2017. MIP-based sensors: promising new tools for cancer biomarker determination**.** ***Sensors,*** **17** (4): 718.

Senturk, I. and Buyukgungor, H., 2013. Equilibrium and Kinetic Studies on the Biosorption of 2-chlorophenol and 4-chlorophenol by Live Aspergillus niger. ***Ekoloji,*** **22** (88): 1-12.

Sheta, N.M., Elfeky, Y.A. and Boshra, S.A., 2020. Cardioprotective efficacy of silymarin liquisolid in isoproterenol prompted myocardial infarction in rats. ***Aaps Pharmscitech,*** **21** (3): 1-16.

Silva, C.F., Menezes, L.F., Pereira, A.C. and Nascimento Jr, C.S., 2021. Molecularly Imprinted Polymer (MIP) for thiamethoxam: A theoretical and experimental study. ***Journal of Molecular Structure,*** **1231:** 129980.

Singh, T.S. and Pant, K.K., 2004. Equilibrium, kinetics and thermodynamic studies for adsorption of As (III) on activated alumina**.** ***Separation and Purification Technology,*** **36** (2):139-147.

Sohrabi, H., kholafazad Kordasht, H., Pashazadeh-Panahi, P., Nezhad-Mokhtari, P., Hashemzaei, M., Majidi, M.R., Mosafer, J., Oroojalian, F., Mokhtarzadeh, A. and de la Guardia, M., 2020. Recent advances of electrochemical and optical biosensors for detection of C-reactive protein as a major inflammatory biomarker. ***Microchemical Journal,*** **158**: 105287.

Solem, C.A., Loftus Jr, E.V., Tremaine, W.J., Harmsen, W.S., Zinsmeister, A.R. and Sandborn, W.J., 2005. Correlation of C-reactive protein with clinical, endoscopic, histologic, and radiographic activity in inflammatory bowel disease. ***Inflammatory Bowel Diseases,*** **11** (8): 707-712.

Song, X., Wang, J. and Zhu, J., 2009. Effect of porogenic solvent on selective performance of molecularly imprinted polymer for quercetin. ***Materials Research,*** **12**: 299-304.

Song, X., Zhou, T., Li, J., Zhang, M., Xie, J. and He, L., 2018. Determination of ten macrolide drugs in environmental water using molecularly imprinted solid-phase extraction coupled with liquid chromatography-tandem mass spectrometry. ***Molecules,*** **23** (5):1172.

Srinivasan, N., Rufino, S.D., Pepys, M.B., Wood, S.P. and Blundell, T.L., 1996. A superfamily of proteins with the lectin fold. ***Chemtracts Biochemistry and Molecular Biology,*** **6:** 49-164.

Suksuwan, A., Lomlim, L., Rungrotmongkol, T., Nakpheng, T., Dickert, F.L. and Suedee, R., 2015. The composite nanomaterials containing (R)-thalidomide-molecularly imprinted polymers as a recognition system for enantioselective-controlled release and targeted drug delivery. ***Journal of Applied Polymer Science,*** **132** (18).

Surface Modification of Commercial Activated Carbon (CAG) for the Adsorption

Tennent, G.A., Lovat, L.B. and Pepys, M., 1995. Serum amyloid P component prevents proteolysis of the amyloid fibrils of Alzheimer disease and systemic amyloidosis. ***Proceedings of the National Academy of Sciences,*** **92** (10): 4299-4303.

Thompson, D., Pepys, M.B. and Wood, S.P., 1999. The physiological structure of human C-reactive protein and its complex with phosphocholine. ***Structure, 7*** (2): 169-177.

Topçu, A.A., Kılıç, S., Özgür, E., Türkmen, D. and Denizli, A., 2022. Inspirations of Biomimetic Affinity Ligands: A Review. ***ACS omega.*** 14-19.

Umpleby II, R.J., Baxter, S.C., Bode, M., Berch Jr, J.K., Shah, R.N. and Shimizu, K.D., 2001. Application of the Freundlich adsorption isotherm in the characterization of molecularly imprinted polymers. ***Analytica Chimica Acta,*** **435** (1): 35-42.

Umpleby II, R.J., Baxter, S.C., Rampey, A.M., Rushton, G.T., Chen, Y. and Shimizu, K.D., 2004. Characterization of the heterogeneous binding site affinity distributions in molecularly imprinted polymers**.** ***Journal of Chromatography B,*** **804**(1): 141-149.

Umpleby II, R.J., Bode, M. and Shimizu, K.D., 2000. Measurement of the continuous distribution of binding sites in molecularly imprinted polymers. ***Analyst,*** **125** (7): 1261-1265.

Uzuriaga-Sánchez, R.J., Khan, S., Wong, A., Picasso, G., Pividori, M.I. and Sotomayor, M.D.P.T., 2016. Magnetically separable polymer (Mag-MIP) for selective analysis of biotin in food samples**.** ***Food chemistry,*** **190**: 460-467.

Vallejos-Burgos, F., Ohba, T. and Kaneko, K., 2019. ***Fundamental aspects of supercritical gas adsorption.*** In Nanoporous Materials for Gas Storage. Springer, Singapore. 13-40.

Vigushin, D.M., Pepys, M.B. and Hawkins, P.N., 1993. Metabolic and scintigraphic studies of radioiodinated human C-reactive protein in health and disease**.** ***The Journal of Clinical Investigation,*** **91** (4): 1351-1357.

Wang, J. and Guo, X., 2020. Adsorption isotherm models: Classification, physical meaning, application and solving method. ***Chemosphere,*** **258**:127279.

Weber Jr, W.J., McGinley, P.M. and Katz, L.E., 1991. Sorption phenomena in subsurface systems: concepts, models and effects on contaminant fate and transport. ***Water Research,*** **25** (5): 499-528.

Wester, R.C., Bucks, D.A.W. and Maibach, H.I., 1994. Human in vivo percutaneous absorption of pyrethrin and piperonyl butoxide. ***Food and Chemical Toxicology,* 32** (1): 51-53.

Whitcombe, M.J., Rodriguez, M.E., Villar, P. and Vulfson, E.N., 1995. A new method for the introduction of recognition site functionality into polymers prepared by molecular imprinting: synthesis and characterization of polymeric receptors for cholesterol. ***Journal of the American Chemical Society,* 117** (27): 7105-7111.

Winingsih, W., Ibrahim, S. and Damayanti, S., 2022. Purification of Andrographolide Methanolic Extract Using Molecularly Imprinted Polymer Prepared by Precipitation Polymerization. ***Scientia Pharmaceutica,* 90** (2): 27.

Wu, F.C., Tseng, R.L. and Juang, R.S., 2009. Characteristics of Elovich equation used for the analysis of adsorption kinetics in dye-chitosan systems. ***Chemical Engineering Journal,* 150** (3): 366-373.

Wulff, G., 1982. Selective binding to polymers via covalent bonds. The construction of chiral cavities as specific receptor sites. ***Pure and Applied Chemistry,* 54** (11): 2093-2102.

Wulff, G., 1995. Molecular imprinting in cross-linked materials with the aid of molecular templates a way towards artificial antibodies. ***Angewandte Chemie International Edition in English***, **34** (17): 1812-1832.

Xie, T., Zhang, M., Chen, P., Zhao, H., Yang, X., Yao, L., Zhang, H., Dong, A., Wang, J. and Wang, Z., 2017. A facile molecularly imprinted electrochemical sensor based on graphene: application to the selective determination of thiamethoxam in grain. ***RSC Advances,* 7** (62): 38884-38894.

Yan H. and Ho Row K., 2006, Characteristic and Synthetic Approach of Molecularly Imprinted Polymer. ***International Journal of Molecular Sciences,* 7**: 155-178.

Ye, L. and Mosbach, K., 2002, Molecularly imprinted materials: towards the next generation, ***Mater. Res. Soc. Symp. Proc.,* 723*:*** 51-59.

Yıldırım, M., 2020. ***Recognition of angiotensin II via molecularly imprinted polymers*** (yüksek lisans tezi, basılmamış). ATÜ, Fen Bilimleri Enstitüsü, Adana.

Zaidi, S.A., 2020. Molecular imprinting: A useful approach for drug delivery. ***Materials Science for Energy Technologies***, **3**: 72-77.

Zeng, X., Yu, T., Wang, P., Yuan, R., Wen, Q., Fan, Y., Wang, C. and Shi, R., 2010. Preparation and characterization of polar polymeric adsorbents with high surface area for the removal of phenol from water. ***Journal of Hazardous Materials,* 177** (3): 773-780.

Zhong, M., Wang, Y.H., Wang, L., Long, R.Q. and Chen, C.L., 2018. Preparation and application of magnetic molecularly imprinted polymers for the isolation of chelerythrine from Macleaya cordata. ***Journal of Separation Science,* 41** (16): 3318-3327.

Zhu, R., Zhao, W., Zhai, M., Wei, F., Cai, Z., Sheng, N. and Hu, Q., 2010. Molecularly imprinted layer-coated silica nanoparticles for selective solid-phase extraction of bisphenol A from chemical cleansing and cosmetics samples. ***Analytica Chimica Acta,* 658** (2): 209-216.

Zhuang, J. and Yu, G.R., 2002. Effects of surface coatings on electrochemical properties and contaminant sorption of clay minerals***. Chemosphere,* 49** (6): 619-628.

GENİŞLETİLMİŞ TÜRKÇE ÖZET
(EXTENDED TURKISH SUMMARY)

MOLEKÜLER BASKILI POLİMERLER İLE C-REAKTİF PROTEİNİN BELİRLENMESİ

TAWFEEQ, Abdulqader Taher
Yüksek Lisans Tezi, Kimya Anabilim Dalı
Supervisor: Dr. Öğr. Üyesi Çiğdem ÖTER
Şubat 2023, 101 sayfa

C-Reaktif protein (CRP), pentraksin protein grubunun bir üyesidir. CRP, karaciğer tarafından patojenik enfeksiyonla sınırlı çeşitli tıbbi durumlarda iltihaplanma sırasında üretilen bir akut faz proteini olarak kabul edilir. CRP klinik olarak genellikle hastalığın prognozunu belirlemek ve tedaviye yanıtı izlemek için kullanılır. Serum CRP konsantrasyonunun hızlı, güvenilir ve kolay bir şekilde ölçülebilmesi çok önemlidir. Bu nedenle, CRP için seçici tanıma bölgelerine sahip üç boyutlu çapraz bağlı moleküler baskılı polimer sentezlendi ve karakterizasyon analizleri (SEM, FT-IR ve TGA) yapıldı. Sentezlenen polimerlerin CRP'nin sulu çözeltide adsorpsiyonu yoluyla bağlanma yetenekleri detaylı olarak değerlendirildi ve referans olarak kullanılan baskısız bir polimerin (CRP-NIP) yetenekleri ile karşılaştırıldı. Baskı etkisi ile hazırlanan MIP'nin şablon molekül CRP'yi seçici olarak adsorbe ettiği gözlendi. Bu etki, α1-antitripsin ve α1-asit glikoprotein gibi farklı pozitif akut faz reaktanlarına karşı adsorpsiyon yetenekleri test edilerek değerlendirildi.

CRP'nin sulu çözeltilerden polimer adsorbanlar üzerine adsorpsiyon işlemi; denge, kinetik ve termodinamik koşullar açısından değerlendirilmiş ve bu koşullar altında süreci açıklamak için gerekli parametreler hesaplanmıştır. Adsorpsiyon verileri: Langmuir, Freundlich, Dubinin-Radushkevich ve Temkin izoterm modelleri, Pseudo birinci dereceden kinetik model, Pseudo ikinci dereceden kinetik model, Elovich kinetik modeli ve partikül içi difüzyon modeli incelenmiş ve termodinamik parametreler ΔG°, ΔH° ve ΔS° hesaplanmıştır. .

Anahtar kelimeler: MIP, C-Reaktif Protein, Adsorpsiyon kinetiği, İzoterm ve termodinamik.

1. GİRİŞ

1.1. C-reaktif proteinin (CRP) Klinik Kullanımı

CRP, inflamatuar, patojenik, koroner kalp hastalığı, romatoid artrit ve çok çeşitli diğer metabolik hastalıklarda artan akut faz inflamatuar bir proteindir. Aslında, CRP sadece enflamatuar hastalığın ana belirteci değil, aynı zamanda enflamatuar süreçlerin önemli bir düzenleyicisi olarak kabul edilebilir. Birçok araştırmacı, CRP'nin vasküler doku biyolojisindeki rolünü inceledi ve bu aracı maddenin periferik dokulardaki spesifik rolünü tanımak için daha fazla araştırmaya ihtiyaç olduğunu fark etti. Son yıllarda CRP tespiti için biyo-algılama düzenlemesinde birçok strateji uygulanmıştır; buna rağmen iyon konsantrasyonu ve sıcaklık gibi bazı kısıtlamalar bu biyosensörlerin performansını etkiler. Sonuç olarak, yerinde teşhis için uygun ve kullanımı kolay CRP biyosensörlerini oluşturmak için daha fazla çaba gerekmektedir. Bunun yanı sıra, CRP biyobelirteçlerinin diğer protein belirteçleri ile etkileşimi, aşılması gereken önemli zorluklar sunar (Sohrabi ve ark., 2020).

1.2. CRP'nin Yapısı

C-reaktif protein, farklı fakat yakından ilişkili protein, serum amiloid P bileşeni (SAP) ile birlikte, lektin kat süper ailesine ait olan pentraksin protein ailesini içeren, glikosile edilmemiş dolaşımdaki bir plazma proteinidir. Her bir pentraksin, disk benzeri bir konfigürasyonda siklik pentamerik simetri ile düzenlenmiş beş özdeş kovalent olmayan ilişkili alt birimden oluşur ve spesifik ligandlara karakteristik kalsiyuma bağlı bağlanmaya sahiptir (Şekil 1). Her bir CRP protomeri düzleştirilmiş β-jellyroll lektin kıvrımına sahiptir ve bir yüzünde, B yüzünde veya bağlayıcı yüzünde protein karboksilat ve amid yan zincirleri ile koordineli olarak birbirinden sadece 4. Å bağlanmış iki kalsiyum iyonu içeren bir cep taşır.

1.3. İnsan CRP'sinin İşlevleri

CRP molekülünün hem varlığının hem de yapısının kayda değer evrimsel ve filogenetik korunması, yararlı bir role sahip olabileceğini ve ligand bağlama özgüllüğü ve ikincil etkileri göz önüne alındığında, bu rolün hem enfeksiyona karşı doğuştan gelen bağışıklıkla ilişkili olabileceğini düşündürmektedir. Bununla birlikte, bu olasılıkları deneysel olarak test etmek son derece zordur çünkü önemli yapısal benzerliğe rağmen, farklı türlerdeki CRP molekülleri normal konsantrasyonda, akut faz proteinleri olarak davranışta, ince ligand bağlanma özgüllüğünde ve ligand bağlanmasından sonraki ikincil etkilerde büyük farklılıklar gösterir. Bu nedenle, hayvanlardan insanlara ekstrapolasyon yapmak zordur ve varsayılan olarak korunan işlevlerin bu büyük farklılıklarla uyumlu olmasını gerektirir. Ayrıca, hayvanlarda insan CRP'sinin uygulanmasını veya transgenik ekspresyonunu takiben in vivo heterolog CRP'nin etkileri, insan CRP'sinin insanlarda gerçek etkileri olmak zorunda değildir (Baltz ve ark., 1982).

1.4. CRP Sentezi

Dolaşımdaki CRP, hepatositler tarafından üretilir. Diğer bazı hücre tipleri tarafından ekstrahepatik CRP sentezi raporları her zaman tekrarlanabilir olmamıştır ve muhtemelen CRP'nin potansiyel lokal etkileri ile ilgili olmasına rağmen, plazma konsantrasyonlarına katkısı karaciğerden gelenlere göre çok az olabilir. Hepatik CRP sentezi, interlökin (IL)-6, IL-1 ve tümör nekroz faktörü-α dahil olmak üzere pro-enflamatuar sitokinler yoluyla son derece hassas transkripsiyonel düzenleme altındadır, böylece neredeyse her türlü doku yaralanması, enfeksiyon veya iltihaplanma ve aslında çoğu form olumsuz fizyolojik olmayan 'stres', artan dolaşımdaki CRP değerleri ile ilişkilidir. CRP görünüşte plazmadan temizlenir ve yalnızca hepatositler tarafından katabolize edilir ve insanlarda yaklaşık 19 saatlik plazma yarı ömrü, hastalığın varlığına veya dolaşımdaki CRP konsantrasyonuna bakılmaksızın tüm bireylerde aynıdır. Plazma konsantrasyonunun tek belirleyicisidir bu nedenle sentez hızıdır (Vigushin ve ark., 1993).

1.5. Moleküler Baskı Teknolojisi

Moleküler damgalama, fonksiyonel grupların boyutu, şekli ve uzamsal düzenlemesi ile ilgili olarak şablondan farklı olan polimerik matriste yapay tanıma bölgeleri oluşturmak için kullanılan bir tekniktir. Moleküler damgalama, şablon moleküllerin şeklini, boyutunu ve işlevsel gruplarını hatırlayan özel bağlanma bölgeleri oluşturmaya yönelik bir yöntemdir. Moleküler damgalamayı formüle etmek için iki temel yaklaşım vardır; biri tersinir kovalent bağlara, diğeri damgalanmış moleküller (şablonlar) ve fonksiyonel monomerler arasındaki kovalent olmayan etkileşimlere dayanır. Kovalent baskılamada, şablonlar tipik olarak 4-vinilfenilboronik asit ve 4-vinilbenzilamin gibi ilgili monomerlere kovalent olarak bağlanır (Mosbach, 1994).

Kovalent bağlantı, polimerizasyondan sonra ikiye bölünür ve şablon polimerden çıkarılır. Aynı kovalent bağ, MIP'ler konuk molekülü yeniden bağladığında oluşur. Kovalent baskılama prosedürleri, kovalent bağların daha fazla sürekliliği nedeniyle daha homojen bağlanma bölgesi difüzyonu üretir. Bununla birlikte, eşdeğer yeniden bağlama bağlantıları oluşturmak için şablonlar ve işlevsel monomerler arasında hızla tersine çevrilebilir kovalent etkileşimler gerekliliği nedeniyle kovalent baskılama daha az esnek bir yöntem olarak kabul edilir. Sonuç olarak, kovalent baskılama için uygun şablon sayısı sınırlıdır. Ayrıca, termodinamik dengeye ulaşmak, kovalent bağlantıların güçlü doğası ve aşağıdaki şemada gösterildiği gibi bunun sonucunda ortaya çıkan yavaş bağlanma ve ayrılma nedeniyle son derece zordur (Wulff, 1995).

1.6. Moleküler Baskılamanın Ana Bileşenleri

Bir Moleküler Baskılanmış Polimer şu bileşenlerden oluşur: bir şablon, fonksiyonel bir monomer, bir çapraz bağlayıcı, bir çözücü ve bir başlatıcı. Moleküler Baskılanmış Polimerin başarısını birçok faktör etkiler, ancak en önemlileri Moleküler Baskılı Polimer bileşeni ve şablon monomerler arasındaki etkileşimdir.

1.7. Adsorpsiyon

Adsorpsiyon, bir maddenin bir moleküler türün yüzeyinde daha yüksek konsantrasyonlarda biriktiği süreçtir. Hidrojen, nitrojen ve oksijen gazları aktif kömür üzerinde adsorbe olur. Bu arada, adsorpsiyon ve absorpsiyon arasında ayrım yapmalıyız. İki süreç tamamen farklı mekanizmalar kullanır (Sheta, Elfeky ve Boshra, 2020).

Adsorpsiyon işlemi için iki bileşen gereklidir,

• Adsorbat: Başka bir maddenin yüzeyine bağlanan bir madde. Örneğin, H_2, N_2 ve O_2 gazları.

• Adsorban: Adsorbanın adsorbe olduğu bir maddenin yüzeyi. Örneğin kömür, silika jel ve alümina.

1.8. Adsorpsiyon Kinetiği

Adsorpsiyonun kinetiği anlaşılarak etkili adsorbe edilen madde-adsorbent temas süresi belirlenebileceği gibi adsorpsiyon işleminin hangi aşamasından yapıldığı ve adsorpsiyon işleminin hızının belirlendiği de anlaşılabilir. Adsorpsiyon dört ana adımdan oluşur (Seader ve Herley, 1998; Do, 1998).

1. Birinci aşamada, gaz veya sıvı fazdaki adsorbe edilen madde, adsorbanı kaplayan bir film tabakasının sınırına doğru yayılır. Bu adıma toplu sıvı difüzyonu denir. Adsorpsiyon ortamı genellikle karıştırıldığından, bu adım genellikle hızlıdır ve adsorpsiyonda hız belirleyici değildir. Ancak adsorbanın bulunduğu faz hareketsiz ise bu aşama en yavaş ve adsorpsiyon hızını belirleyen aşama olabilir.
2. Film tabakasına ulaşan adsorbe edilecek madde buradaki durgun kısımdan geçerek adsorbanın gözeneklerine doğru hareket eder. Bu harekete film kütle transferi veya sınır tabakası difüzyonu denir.
3. Adsorbe edilen madde, adsorbanın gözenek boşluklarında hareket eder ve adsorpsiyonun gerçekleşeceği yüzeye doğru hareket eder. Buna parçacık içi difüzyon veya gözenek difüzyonu denir. Sınır tabakası (film difüzyonu) ve partikül içi difüzyon aşamaları genellikle adsorpsiyon hızını birlikte etkiler.

4. Çözünen maddenin malzeme yüzeyi üzerindeki aktif bir bölgede adsorpsiyonu (iyon değişimi, kompleks oluşumu ve/veya şelasyon yoluyla kimyasal reaksiyon). Bu adsorpsiyonun en hızlı adımıdır.

Son adım, denge reaksiyonu olarak kabul edilir. Toplam adsorpsiyon reaksiyon hızı, en yavaş adım tarafından kontrol edilir.

2. LİTERATÜR TARAMASI

Bu araştırmanın yöntemlerine ulaşmak için yapılan literatür taraması, Moleküler imprinting ve bileşenleri ve terapötiklerdeki uygulamaları ve CRP gibi bazı tıbbi parametrelerin belirlenmesi gibi daha önce toplanan çalışmalara dayanmaktadır. Ayrıca, daha önce tanımlandığı gibi moleküler damgalama, belirli bir hedef molekül için sentetik polimerlerin kullanıldığı bir tekniktir. Bu nedenle moleküler olarak damgalanmış polimerler (MIP'ler), biyolojik antikorların en önemli özelliklerinden biri olan spesifik moleküler tanınmaya sahiptir. İmmünolojik testler, afinite ayırma, biyosensörler ve yönlendirilmiş sentez ve kataliz gibi seçici bağlanma olaylarının önemli olduğu uygulamalarda kullanılabilir (Yıldırım, 2020).

3. MATERYAL VE YÖNTEM

Yapılan çalışmada kullanılan; C-Reaktif Protein (CRP), α1-Antitripsin, 1-αAsit glikoprotein, metakrilik asit (MAA), etilen glikol dimetakrilat (EGDMA) 2,2'-azobis(2-metilpropionitril) (AIBN), asetonitril, asetik asit (CH_3COOH), metanol (MeOH) Sigma-Aldrich'ten (ABD) elde edildi. Kullanılan tüm ajanları analitik derecededir.

C-reaktif protein için MIP, batch polimerizasyon prosedürü kullanılarak sentezlenecektir. Bunun için şablon molekül olarak 10 µl CRP, 675 µl fonksiyonel monomer metakrilik asit (MAA) ve 6.04 ml çapraz bağlayıcı EGDMA 20 mL asetonitril çözeltisine ilave edildi ve karışım 10 dakika nitrojenle temizlendi. Daha sonra, çözeltiye 35°C'de 0.05 g başlatıcı (AIBN) eklendi ve polimerizasyon için bir yağ banyosunda 70°C'de 24 saat tutuldu. Polimerizasyon bittiğinde, baskılı polimer çıkarıldı, birkaç kez saf su ile yıkandıktan sonra ve 24 saat boyunca 55°C'de kurutuldu. NIP ise şablon molekülün eklenmesi dışında aynı işlem izlenerek hazırlandı.

Sentezlenen CRP baskılı polimer (MIP), selüloz kartuşlara paketlendi ve soxhlet haznesine yerleştirilerek 48 saat boyunca metanol-asetik asit (4:1) karışımında ekstrakte edildi. MIP'nin son yıkaması birkaç kez metanol ile yapıldı ve elde edilen ürün daha sonra kurutulup ince toz halinde getirildi.

MIP'lerin ve NIP'lerin yeniden bağlanma potansiyelini araştırmak için 25 mg/L konsantrasyondaki CRP çözeltileri 50 mg MIP ve NIP ile 2 saat boyunca oda sıcaklığında karıştırıldı. Daha sonra polimerler filtre kağıdı ile süzülerek ayrıldı ve çözeltide kalan CRP konsantrasyonu UV spektrofotometre kullanılarak 300 nm'de ölçüldü.

MIP ve NIP polimerleri ile CRP adsorpsiyonu koşullarının optimizasyonu için, adsorban miktarı, derişim, adsorbsiyon süresi ve pH parametreleri incelendi. Adsorpsiyon verileri kullanılarak Adsorpsiyon kinetiği

CRP-MIP kolonlarının CRP molekülüne karşı seçiciliğini belirlemek için, CRP gibi pozitif akut faz reaktantları olan ve plazmada bulunan α1-Antitripsin ve α1-asitglikoprotein molekülleri rakip olarak seçildi. CRP, α1-antitripsin ve α1-asitglikoprotein aynı başlangıç konsantrasyonlarında standart çözeltileri hazırlandı ve belirli miktar CRP-MIP ve NIP adsorbanı ile muamele edilerek bağlanma kapasiteleri belirlendi ve MIP'in CRP'ye göre seçiciliği incelendi.

Farklı CRP konsantrasyonlarına sahip 1:10, 1:20 oranında seyreltilmiş insan serumu, optimum adsorpsiyon koşullarında CRP-MIP ile muamele edilerek, CRP'nin baskılı polimere yeniden bağlanma kapasitesi araştırıldı.

4. BULGULAR

4.1. Adsorpsiyon Çalışmaları

Sulu çözeltilerden CRP-MIP ve NIP üzerine CRP adsorpsiyonu kesikli yöntem uygulanarak gerçekleştirildi. Farklı konsantrasyonlarda ve pH'daki CRP çözeltileri, farklı sıcaklıklarda ve değişen sürelerde polimerlerle temas ettirildi. Çalışmalarda pH ayarlaması için 1 M HNO_3 ve 1 M NaOH çözeltileri kullanılmıştır. Adsorpsiyon işlemi sonunda polimerler filtre kağıdı ile süzülerek çözeltiden ayrıldı. Çözelti ortamında kalan CRP miktarı, 300 nm'de UV-spektrofotometre kullanılarak ölçüldü.

Bu çalışmalara ek olarak, CRP'nin sulu çözeltilerden baskılı polimerlere (CRP-MIP) adsorpsiyonu kesikli bir polimerizasyon işlemi ile araştırılmıştır. Adsorpsiyon işleminin kinetik ve izotermal modellere uygulanması ve termodinamik ifadelerin belirlenmesi gerçekleştirilmiş ve sonuçlar baskısız referans polimer (CRP-NIP) ile karşılaştırılmıştır.

Farklı temas süreleriyle elde edilen adsorpsiyon verilerinin adsorpsiyon kinetiğine uygulanmasıyla birinci dereceden yalancı hız denklemi, ikinci dereceden yalancı hız denklemi, Elovich kinetik modeli ve partikül içi difüzyon modelinin CRP-MIP adsorpsiyonu için uygunluğu araştırıldı. Pseudo birinci derece hız denklemi, Elovich kinetiği ve parçacık içi difüzyon modeli, daha düşük korelasyon değerlerine sahip olduklarından, CRP adsorpsiyon mekanizmasına Pseudo ikinci hız denkleminden daha az uyum göstermiştir. Pseudo birinci dereceden hız denkleminin kinetik verilere uymadaki yetersizliği, adsorpsiyon sürecinin başlamasını kontrol eden sınır tabakasından kaynaklanmaktadır. Elovich kinetik modeli ise, sözde birinci ve ikinci derece hız denklemlerinin aksine, sistemde var olan herhangi bir mekanizmayı tahmin edemez. Adsorpsiyon kinetiği genellikle farklı mekanizmalar tarafından kontrol edilir.

Langmuir, Freundlich, Dubinin-Radushkevich (D-R) ve Temkin izoterm modellerine uygulanan CRP adsorpsiyonunun bu dört izoterm modeline göre Freundlich izotermi ile daha uyumlu olduğu belirlendi. Heterojen yüzeylerde adsorpsiyon için Freundlich modeli uygulanmaktadır. Çizilen Freundlich izoterminden hesaplanan korelasyon katsayısı R^2=0,997 olarak bulunmuştur. Adsorpsiyon işleminin favori olduğunu belirleyen bir parametre, Freundlich izoterm denkleminden hesaplanan n değeridir. CRP için 2,13 olarak hesaplanan n değeri $1<n<10$ aralığındadır.

Langmuir denge izotermine göre maksimum tek tabaka adsorpsiyon katsayısı (qmax) 3,63 μmol/g olarak bulundu. Hesaplanan Langmuir parametrelerinden b değeri kullanılarak RL değerleri (boyutsuz ayırma faktörü) 0,44 olarak hesaplanmıştır. Bu değerlerin $0<RL<1$ aralığında olması adsorpsiyon işleminin olumlu olduğunu göstermektedir.

Dubinin-Radushkevich adsorpsiyon izoterminden hesaplanan ortalama adsorpsiyon enerjisi E değeri, adsorpsiyon olayında etkili olan reaksiyon mekanizması hakkında fikir vermektedir. E değeri 8-16 kJ/mol aralığında ise iyon değişimi vardır. $E<8$ kJ/mol ise, fiziksel kuvvetler adsorpsiyonda etkilidir. $E>16$ kJ/mol ise, etkili adsorpsiyon

mekanizması kimyasal sorpsiyondur. CRP-MIP için hesaplanan E değerleri 4,66 kJ/mol olduğundan, CRP adsorpsiyonu fiziksel adsorpsiyon olarak tanımlanabilir.

Tablo 4.3'te verilen adsorpsiyon entalpi değeri dikkate alındığında, CRP adsorpsiyonu için ΔH°'nin pozitif değeri adsorpsiyon işlemlerinin endotermik olduğunu gösterir. ΔH° değeri 40 kJ/mol'den küçük olduğunda, adsorpsiyon türü fiziksel bir süreç olarak kabul edilebilir. Bu çalışmada adsorpsiyon entalpi değerleri 40 kJ/mol'den küçük olarak hesaplandığından adsorpsiyon işleminin fiziksel adsorpsiyon olduğu söylenebilir ve bu sonuç izoterm modellerinden elde edilen sonuç ile uyumludur.

Adsorpsiyona ait Gibbs serbest enerji değerleri -2,59 kJ/mol olarak hesaplanmıştır. Gibbs serbest enerjisinin negatif değerleri, CRP için adsorpsiyon işleminin termodinamik olarak mümkün olduğunu, ΔGº'nin artan sıcaklıkla daha fazla negatif değerlere ulaşması, sıcaklık arttıkça kendi kendine yürüme derecesinin arttığını göstermektedir. Kendiliğinden gerçekleşebilen bu tür olaylarda düzensizlik arttığı için entropi artar. Adsorpsiyon sırasında pozitif entropi değeri (ΔS°), katı-çözelti arayüzünde artan rasgeleliği gösterir. Ayrıca pozitif değere sahip entropi, uranyum ve toryum iyonlarının CRP-MIP adsorbanına afinitesini gösterir.

Tablo 4.4 incelendiğinde CRP-NIP adsorpsiyonu üzerine CRP adsorpsiyonu için en uygun adsorpsiyon kinetik modelinin Pseudo ikinci dereceden hız denklemi olduğu görülmektedir. Bu denklem, düşük konsantrasyonlarda adsorpsiyon davranışını açıklamak için kullanılır. Tabloda, ikinci dereceden hız denkleminin korelasyon katsayısı R^2'nin 1'e (0,9907) çok yakın olduğu ve denklemden hesaplanan qe değerinin (0,65) deneysel qe'ye (0,55) daha yakın bir sonuç verdiği gösterilmektedir. Pseudo birinci dereceden hız denklemi, CRP için Elovich kinetik ve partikül içi difüzyon modeline göre 1'e yakın bir korelasyon katsayısına sahip olmasına rağmen, qe değeri qexp değerinden daha uzak olduğu için adsorpsiyon mekanizmalarıyla daha az uyumludur

Tablo 4.5'te hesaplanan korelasyon katsayıları değerlendirildiğinde, CRP-NIP üzerindeki CRP adsorpsiyonunun, 1'e yakın bir korelasyon katsayısına (R^2=0,9963) sahip olan ve bununla daha uyumlu olan Freundlich izoterm modeli ile açıklanabileceği görülmektedir. modeli. CRP adsorpsiyonları için Freundlich adsorpsiyon izoterm denkleminden hesaplanan n değerleri 1<n<10 aralığında olduğundan adsorpsiyonların uygun olduğu söylenebilir. CRP-NIP için Langmuir modeli ile elde edilen maksimum tek tabaka adsorpsiyon katsayısı (q_{max}) değeri 1,85 μmol/g olarak bulunmuştur. Ayrıca R_L

değerleri 0,85 olarak hesaplanmıştır ve bu değerler $0<R_L<1$ aralığında olduğundan adsorbent ile CRP-NIP adsorpsiyonu gerçekleşebilmekte ve uygun adsorpsiyonlardır.

CRP'nin adsorpsiyonu için Dubinin-Radushkevich adsorpsiyon izoterm denkleminden hesaplanan adsorpsiyon enerjileri (2.89) E<8 kJ/mol olduğundan, CRP'nin NIP'ye adsorpsiyonunun fiziksel adsorpsiyon olduğu sonucuna varıldı

CRP-MIP adsorbanının CRP molekülüne karşı seçiciliğini belirlemek için, CRP gibi pozitif akut faz reaktanları olan ve plazmada bulunan α1-Antitripsin ve α1-asit glikoprotein molekülleri (Şekil 4.17) rakip olarak seçilmiştir. CRP-MIP ve CRP-NIP adsorbanları ile 1 mM başlangıç konsantrasyonlarında hazırlanan CRP, α1-antitripsin ve α1-asit glikoprotein çözeltileri önceden belirlenen optimum koşullarda (45 dk, pH: 4.0, 25 °C ve 500 rpm) gerçekleştirildi. Adsorpsiyon işlemi nedeniyle çözeltide kalan α1-Antitripsin ve α1-asit glikoprotein miktarı sırasıyla 230 ve 250 nm'de UV spektrofotometre ile ölçülerek belirlendi. Elde edilen sonuçlar Şekil 4.18'de gösterilmiştir. Bu çalışma sonucunda CRP-MIP'nin rakip bileşiklere göre oldukça seçici olduğu belirlenmiştir.

İnsan serumundan CRP'nin seçici yeniden bağlanma çalışması için sırasıyla 0,5 mM ve 0,25 mM CRP konsantrasyonları ile 1:10 ve1:20 seyreltilmiş insan serumu kullanılarak yapılan adsorpsiyon işeminde: CRP'nin CRP-MIP ve CRP-NIP'e yeniden bağlanma miktarları %91 ve %37 geri kazanımda, 0,74 μmol/g ve 0,22 μmol/g olarak bulunmuştur. CRP'nin ham insan serumundan %91 gibi yüksek bir oranda CRP-MIP'ye başarılı bir şekilde yeniden bağlanması, sentezlenen baskılanmış molekülün CRP için oldukça seçici özelliklerini göstermiştir.

5- TARTIŞMA VE SONUÇ

C-reaktif protein hem proinflamatuar hem de antiinflamatuar etkilere sahiptir. Bir enfeksiyon veya enflamasyon belirteci olmasının yanı sıra, çok çeşitli biyolojik özellik ve işlevlere sahiptir. CRP genellikle hastalığı tanımlamak ve tedaviye yanıtı izlemek için klinik olarak kullanılır. Bu nedenle CRP düzeyini kolay, hassas ve güvenilir bir şekilde ölçmek önemlidir.

Moleküler baskılı polimerler, üç boyutlu çapraz bağlı polimerik yapıda hedeflenen molekül veya iyon için seçici tanıma bölgelerine sahip yeni nesil akıllı

malzemelerdir. Bu malzemeler, ilgilenilen şablon molekül etrafında fonksiyonel ve çapraz bağlanan monomerlerin polimerizasyonu ile elde edilir. Polimerizasyondan sonra şablon molekülün polimerden çıkarılmasıyla, hedef analitin şekil, boyut ve fonksiyonel gruplar açısından yeniden bağlanabileceği tanıma bölgeleri oluşturulur. Bu teknikle sentezlenen baskılanmış polimerler kararlı ve sağlam malzemeler olmalarının yanı sıra analite karşı yüksek seçicilik gösterirler. Bu tez çalışmasında, önemli bir biyobelirteç olan C-reaktif proteinin insan serumundan seçici adsorpsiyonu için moleküler baskılı polimer (CRP-MIP) sentezlendi. CRP tanıma bölgelerine sahip polimerik yapının karakterizasyon çalışmaları için SEM, FT-IR ve TGA analizleri yapılmıştır.

CRP'nin sulu çözeltilerden sentezlenen baskılı polimere (CRP-MIP) yeniden bağlanma kapasitesi, CRP-MIP polimerinin kuru gramı başına 3,63 mg olarak hesaplanmıştır. Ek olarak, baskılanmış polimerin seçiciliği, benzer moleküler yapıya (α1-antitripsin ve α1-asit glikoprotein) sahip rakip ajanların varlığında yapılmıştır. Çalışmada, baskılanmış polimerin CRP'yi tanıma seçiciliğinin rakip bileşiklere göre daha yüksek olduğu gözlendi. Ek olarak, CRP'nin seyreltilmiş insan serumundan CRP-MIP'ye %91 gibi yüksek bir oranda başarıyla yeniden bağlanması, sentezlenen baskılı polimerin CRP için oldukça seçici olduğunu gösterdi.

CURRICULUM VITAE

He studeid primary and secondary education in 2007, he graduated from the University of Samarra, Salahaddin/Iraq, departments of chemistry in 2017, he was engaged in 2021 at Van Yuzuncu Yıl University, in the Master of Science in Chemistry program.

VAN YÜZÜNCÜ YIL UNIVERSITY
THE INSTITUTE OF NATURAL AND APPLIED SCIENCES
THESIS ORIGINALITY REPORT

Date 30/01/2023

Thesis Title: Determination of C-Reactive Protein with Molecularly Imprinted Polymers"

The title of the mentioned my thesis, above having total 101 (one hundred and one) pages with cover page, introduction, main parts and conclusion, has been checked by me/my supervisor for originality by Turnitin computer program on the date of 30/01/2023 and its detected similary rate was 14% (fourteen) according to the following specified filtering.

The applied filters are given below:

- Excluding the acceptance and approval page,
- Excluding Acknowledgments,
- Excluding table of contents,
- Excluding symbols and abbreviations,
- Excluding materials and methods,
- Excluding references,
- Excluding quotations,
- Excluding publications derived from the thesis
- Excluding the text parts less than 7 words (Limit match size to 7 words)

I read the Thesis Originality Report instruction of Van Yuzuncu Yil University for Obtaining and Using Similarity Rate for the thesis and I declare my thesis does not contain any plagiarism according to the maximum similarity rates specified in this directive; otherwise I accept all kinds of legal responsibility for any dispute arising in situations which are likely to be detected and I declare that the information I have given above is correct.

I submit it to your information.

Date and Signature

Name and Surname: Abdulqader Taher TAWFEEQ
Student ID: 20910001423
Department: Chemistry
Program: Physicalchemistry
Status: (X) M.Sc ( ) Ph.D.

SUPERVISOR	**APPROVAL OF THE INSTITUTE**
SUITABLE	SUITABLE
Asst. Prof. Dr. Çiğdem ÖTER	